COBRA IIIC: A DIGITAL COMPUTER PROGRAM FOR STEADY STATE AND TRANSIENT THERMAL-HYDRAULIC ANALYSIS OF ROD BUNDLE NUCLEAR FUEL ELEMENTS

D. S. Rowe

Battelle

Pacific Northwest Laboratories
Richland, Washington 99352

MARCH 1973

COBRA IIIC: A DIGITAL COMPUTER PROGRAM FOR STEADY STATE AND TRANSIENT THERMAL-HYDRAULIC ANALYSIS OF ROD BUNDLE NUCLEAR FUEL ELEMENTS

By

D. S. Rowe

Fluid and Energy Systems Section
Mechanical Engineering Department

March 1973

COBRA-IIIC may be obtained in either
a UNIVAC-1108 or IBM-360 version from the,
Argonne Code Center
9700 South Cass Avenue
Argonne, Illinois   60439

TABLE OF CONTENTS

FIGURES

COBRA IIIC: A DIGITAL COMPUTER PROGRAM FOR STEADY
STATE AND TRANSIENT THERMAL-HYDRAULIC
ANALYSIS OF ROD BUNDLE NUCLEAR FUEL ELEMENTS

D. S. Rowe

INTRODUCTION

This report presents an expanded version of the COBRA-III computer program for performing both steady-state and transient subchannel analysis of rod bundle nuclear fuel elements. COBRA-III computes the flow and enthalpy in the subchannels of rod bundles during both boiling and non-boiling conditions by including the effects of crossflow mixing.

The subchannel analysis approach has become recognized as a more complete method to analyze the steady-state thermal-hydraulic performance of nuclear fuel bundles. As a result, there has been considerable interest in using a similar analysis method for transients. Much of the safety analysis of nuclear reactors is related to the transient response of the reactor core and fuel following normal operating transients and potential accident situations. The analysis of these transients with one-dimensional analyses method are not entirely complete. More sophisticated multi-dimensional analysis techniques would provide a more detailed understanding of the thermal-hydraulic performance of nuclear fuel bundles during transients.

The previously published interim version of COBRA-III was an extension of the COBRA-II program to consider transients; however, it had limited capability. Several of the more important computational limitations were: (1) lack of a fuel heat transfer model; (2) no provision for forced cross-flow mixing; (3) incomplete transverse momentum equation; (4) inability to consider reverse flow and (5) lack of a pressure drop boundary condition option. The present version, COBRA-IIIC, removes the first three limita-tions. Development work is continuing on Items (4) and (5).

SUMMARY

The COBRA-IIIC computer program computes the flow and enthalpy in rod-bundle nuclear fuel element subchannels during both steady state and transient conditions. It uses a mathematical model that considers both turbulent and diversion crossflow mixing between adjacent subchannels. Each subchannel is assumed to contain one-dimensional, two-phase, separated, slip-flow. The two-phase flow structure is assumed to be fine enough to define the void fraction as function of enthalpy, flow-rate, heat-flux, pressure, position and time. At the present time, steady-state two-phase flow correlations are assumed to apply to transients. The mathematical model neglects sonic velocity propagation; therefore, it is limited to transients where the transient times are greater than the time for a sonic wave to pass through the channel. The equations of the mathematical model are solved by using a semi-explicit finite difference scheme. This scheme also gives a boundary-value flow solution for both steady state and transients where the boundary conditions are the inlet enthalpy, inlet mass velocity, and exit pressure.

The features of COBRA-IIIC can be summarized as follows:

- It contains all the analysis capability of the COBRA-II program.
- It can consider transients of fast-to-intermediate speed--no sonic velocity propagation effects are considered.
- The numerical scheme performs a boundary value solution where the boundary conditions are the inlet flow, inlet crossflow, inlet enthalpy and exit pressure.
- The numerical solution has no stability limitation on space or time steps.
- A more complete transverse momentum equation now includes temporal and spatial acceleration of the diversion crossflow.
- A fuel pin model option allows calculation of fuel and cladding temperatures during transients by specifying power density.
- Forced flow mixing due to diverter vanes or wire wraps is included.
- Improved numerical procedures allow more complete analysis of bundles with partial flow blockages.

The inclusion of the temporal and spatial acceleration of the diversion crossflow provides a more complete physical model with only a small increase in the complexity of the numerical solution. The importance of these additional phenomena are governed by the parameters u*, C, and (s/ℓ). These have only a small-to-moderate affect on subchannel flow solutions for most rod bundle analyses. The effect of the parameters should be evaluated and justified experimentally if they have important influence on the flow solutions.

The use of a fuel rod heat transfer model coupled with the subchannel analysis method provides a more complete way of performing transient thermal-hydraulic analysis of rod bundle nuclear fuel elements. By selecting appropriate heat transfer correlations the fuel temperature response to selected transients can now be analyzed in much greater detail.

While the use of an inlet flow boundary condition may be entirely satisfactory for a wide range of problems, there are many analyses where the pressure at each end of the bundle could be defined with greater ease. This type of boundary condition would allow the inlet flow rate to change as governed by the boundary pressure and the internal driving forces. Work is continuing to provide this type of boundary condition. Numerical methods are concurrently being developed to consider transient flow reversal, coolant expulsion and countercurrent subchannel flow in the presence of a pressure boundary condition.

FLUID TRANSPORT MATHEMATICAL MODEL

To develop a method for predicting the flow and enthalpy in selected regions of a rod bundle, a mathematical model is used that considers lateral mixing processes. The approach used is the same as in earlier versions of the COBRA program[1,2,3] where the cross section of the rod bundle is divided into discrete flow subchannels as shown in Figure 1. By making suitable assumptions concerning the flow and crossflow in these subchannels, the equations of continuity, energy and momentum can be derived for each subchannel. This set of equations can then be solved numerically by using a digital computer.

FUEL ROD

SUBCHANNEL

W'_{ij} W'_{ji}

W_{ij}

(j) (i)

M_j M_j
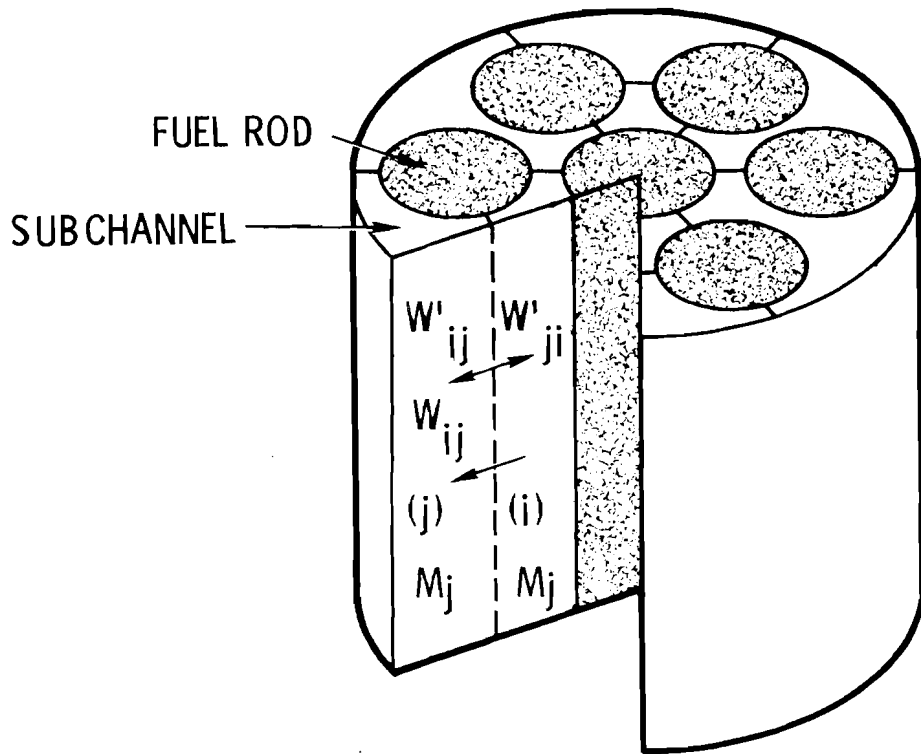
FIGURE 1. Method of Subchannel Selection

BASIC ASSUMPTIONS

- One-dimensional, two-phase, separated, slip-flow exists in each sub-channel during boiling.

- The two-phase flow structure is fine enough to allow specification of void fraction as a function of enthalpy, pressure, flow rate, axial position and time.

- A turbulent crossflow exists between adjacent subchannels that causes no net flow redistribution.

- The turbulent crossflow may be superimposed upon a diversion crossflow between subchannels that results from flow redistribution. This may occur artificially from devices that force diversion crossflow.

- Sonic velocity propagation effects are ignored.

- The diversion crossflow velocity is small compared to the axial velocity within a subchannel.

The first four assumptions are the same as those used in earlier versions of COBRA where Meyer's[4] two-phase flow model is assumed to apply to rod bundle subchannels. The separated slip flow assumption is valid provided that the separated phases have uniform properties and mass flux in the regions they occupy in the channel. This is not always the case, especially for annular flow[22] where the liquid at the wall is at significantly lower velocity than the entrained liquid drops. Although the separated flow assumption allows considerable simplification of the momentum and energy equations, the limitations of the assumption should be realized by users of the COBRA program. More sophisticated two-phase flow modeling is to be performed as part of ongoing work. The last two assumptions greatly simplify the mathematical model and the numerical solution. Neglecting sonic velocity propagation is justified for moderate speed transients. Meyer[4] justifies this assumption for transients with times that are longer than the sonic propagation time through the channel.

The last assumption allows a transverse momentum equation to be derived by only preserving the vector direction between an adjacent pair of subchannels. In other words, the crossflow loses its sense of direction when it enters a subchannel. This assumption also allows the difference between transverse momentum fluxes normal to the gap to be neglected. Calculations to be presented later support this assumption even for severe flow diversions.

EQUATIONS OF THE MATHEMATICAL MODEL

The equations of the mathematical model may be derived by using the previous assumptions and by applying the general equations of continuity, energy and momentum to a segment of an arbitrary subchannel, as shown in Appendix A. The deviations are similar to those presented earlier [1,2,3] and are included here for completeness. For simplicity the equations are presented for an arbitrary Subchannel (i) which is connected to another Subchannel (j). The equations are generalized later to account for an arbitrary subchannel layout.

The right side of the continuity equation

$$A_i \frac{\partial \rho_i}{\partial t} + \frac{\partial m_i}{\partial x} = -w_{ij} \qquad (1)$$

gives the net rate of change of subchannel flow in terms of the diversion cross flow per unit length. By choice, the diversion cross flow is positive when flow is diverted out of Subchannel (i). The turbulent cross flow does not appear because it does not cause a net flow change. The time derivative of density gives the component of flow change caused by the fluid expansion or contraction.

The right side of the energy equation

$$\frac{1}{u''} \frac{\partial h_i}{\partial t} + \frac{\partial h_i}{\partial x} = \frac{q_i'}{m_i} - (h_i - h_j) \frac{w_{ij}'}{m_i} - (t_i - t_j) \frac{c_{ij}}{m_i} + (h_i - h^\star) \frac{w_{ij}}{m_i} \qquad (2)$$

contains three terms for thermal energy transport in a rod bundle fuel element. The first term is the power-to-flow ratio of a subchannel and gives the rate of enthalpy change if no thermal mixing occurs. The second term accounts for the turbulent enthalpy transport between all interconnected subchannels. The turbulent thermal mixing w' is analogous to eddy diffusion and is defined through empirical correlations.[2] The third term accounts for the thermal conduction mixing. The fourth term accounts for thermal energy carried by the diversion crossflow. This is a convective term that requires a selection of the enthalpy h* to be carried by the diversion crossflow. The first term on the left side of Equation (2) gives the transient contribution to the spatial rate of enthalpy change. These are convective terms with a transport velocity u". Since u" represents the effective velocity for energy transport, the time duration of a transient is related to this velocity. Note that sonic velocity propagation effects are ignored by the absence of a $\partial \rho / \partial t$ term.

The right side of the axial momentum equation

$$\frac{1}{A_i}\frac{\partial m_i}{\partial t} - 2u_i\frac{\partial \rho_i}{\partial t} + \frac{\partial p_i}{\partial x} = -\left(\frac{m_i}{A_i}\right)^2\left[\frac{v_i f_i \phi}{2D_i} + \frac{k_i}{2\Delta x} + A_i\frac{\partial(v_i'/A_i)}{\partial x}\right] - \rho_i g\cos\theta \tag{3}$$

$$- \frac{f_t}{A_i}(u_i - u_j)w_{ij}' + \frac{1}{A_i}(2u_i - u^*)w_{ij}$$

contains several terms that govern the axial pressure gradient in a sub-channel. Without the crossflow terms, these are the frictional, spatial acceleration and elevation components of pressure gradient. The turbulent crossflow term tends to equalize the velocities of adjacent sub-channels. This is analogous to turbulent stresses in turbulent flow. The factor f_T is included to help account for the imperfect analogy between the turbulent transport of enthalpy and momentum. The diversion crossflow term accounts for the momentum changes due to changes in subchannel velocity. The first two terms on the left side of Equation (3) are the transient components of the axial pressure gradient.

Appendix A presents a derivation of a more complete transverse momentume that more properly accounts for the crossflow momentum coupling. For two adjacent subchannels this equation can be written as

$$\frac{\partial w_{ij}}{\partial t} + \frac{\partial(u_{ij}^* w_{ij})}{\partial x} + \left(\frac{s}{\ell}\right)C_{ij}w_{ij} = \left(\frac{s}{\ell}\right)(P_i - P_j) \tag{4}$$

The first two terms are new to the momentum equation used in the previous COBRA program flow models. They represent the temporal and spatial acceleration* of the crossflow. The remaining two terms are the friction and pressure terms used in an earlier transverse momentum equation.[1,2,3]

---

* A term analogous to $\partial(\rho v^2)/\partial y$ has been ignored in relation to a term analogous to $\partial(\rho uv)/\partial x$ by the assumption of small crossflow velocity. This can be justified by an order of magnitude analysis

$$\underset{\delta}{v\frac{\partial u}{\partial x}} + \underset{\delta}{u\frac{\partial v}{\partial x}} + \underset{\delta}{2v\frac{\partial v}{\partial y}} \underset{}{\sim} u\frac{\partial v}{\partial x}$$

The new parameter (s/ℓ) represents the importance of friction and pressure terms versus the inertial terms. These inertial terms also represent the transport of the crossflow at axial velocity u^*_{ij}. These terms cause the crossflows to persist as they move down the channel. This is the "axial inertia" effect often included in crossflow resistance correlations.[2,6] The friction term is linearized representation of fluid friction; however, COBRA presently considers C_{ij} to be a nonlinear function that depends on the absolute value of the diversion crossflow.

The primary assumptions used to derive Equation (4) is that the crossflow through a rod gap loses its sense of direction upon entering or leaving a subchannel and that the difference in lateral momentum flux is small. The direction of the crossflow is only considered between the two interconnecting subchannels of interest. This assumption is valid if the crossflow velocities are small compared to the axial velocities. This is usually the case for most computations in nuclear reactor rod bundles.

An equation of state of the form

$$\rho_i = \rho(h_i, p^*, m_i, x, t) \tag{5}$$

is used to define the two-phase fluid density. This equation can be obtained by using an appropriate correlation for void fraction.

For a large rod bundle the previous equations become unwieldy; therefore, a more compact form is very desirable. Reference 3 presents a vector form of the equations by using a matrix transformation $[S]$ and its transpose $[S]^T$. Using the $[S]$ transformation the previous equations may be written as follows:

Continuity

$$\left\{A\frac{\partial \rho}{\partial t}\right\} + \left\{\frac{\partial m}{\partial x}\right\} = -[S]^T\{w\} \tag{6}$$

Energy

$$\left\{\frac{m}{u'''}\frac{\partial h}{\partial t}\right\} + \left\{m\frac{\partial h}{\partial x}\right\} = \{q'\} - [S]^T[\Delta h]\{w'\} - [S]^T[\Delta t]\{c\}$$
$$+ [h][S]^T\{w\} - [S]^T[h^*]\{w\} \tag{7}$$

Axial Momentum

$$\left\{\frac{1}{A}\frac{\partial m}{\partial t}\right\} - \left\{2u\frac{\partial\rho}{\partial t}\right\} + \left\{\frac{\partial p}{\partial x}\right\} = \{a'\} + [A]^{-1}\left[[2u][S]^T - [s]^T[u*]\right]\{w\} \qquad (8)$$

Transverse Momentum

$$\left\{\frac{\partial w}{\partial t}\right\} + \left\{\frac{\partial(u*w)}{\partial x}\right\} + \left(\frac{s}{\ell}\right)\{Cw\} = \left(\frac{s}{\ell}\right)[S]\{p\} \qquad (9)$$

where

$$\{a'\} = -\left\{\left(\frac{m}{A}\right)^2\left(\frac{vf\phi}{2D} + \frac{Kv'}{2\Delta x} + A\frac{\partial(v'/A)}{\partial x}\right) + \rho\cos\theta\right\}$$
$$ - f_T[A]^{-1}[S]^T[\Delta u]\{w'\} \qquad (10)$$

The elements of the matrix [S] are defined through two column vectors i(k) and j(k) where, for each pair of connected subchannels (i, j), a unique connection number k is assigned. The connections numbers are assigned in ascending order by considering Subchannel (i) and then assigning a unique connection number for each successively connected Subchannel (j) where j is greater than i. By using this identification procedure the crossflows can be written as w_k where k implies the subchannel pair i(k), j(k). For $w_k > 0$ the crossflow is chosen to be from Subchannel (i) to Subchannel (j) where i is less than j. The elements of the matrix [S] are defined as: $S_{ki} = 0$; except, $S_{ki} = 1$, if i=i(k); and $S_{ki} = -1$, if i=j(k).

METHOD OF SOLUTION

The previous equations are solved as a boundary-value problem by using a semiexplicit finite difference scheme. The boundary conditions selected for the problem are the inlet enthalpy, inlet flow, inlet crossflow, and exit pressure. Initial conditions for enthalpy, flow, and crossflow distribution are established from an initial steady-state calculation. No inlet condition for pressure is required as it is determined from the other boundary conditions and resulting solution. Solving the problem this way is an improvement over the initial-value solutions that are used in many subchannel analysis computer programs. While the use of the

9

initial value solution can be justified as an approximation to the boundary-value solution if the crossflow resistance is small, it restricts the solutions to a limited class of problems.

Equation (6) through (9) are solved by using a finite difference procedure. Finite difference node interfaces are numbered starting at the inlet end of each node. The location at end of the last node is N+1 where N is the number of nodes. Enthalpy, flow, pressure and crossflow are defined at the node interfaces. Boundary conditions for enthalpy, flow and crossflow are set at the channel inlet (J=1) and the exit pressure boundary condition set at the channel outlet (J=N+1). The distance x=o corresponds to J=1 and x=L corresponds to J=N+1. The finite difference scheme is written for an interval J-1 to J corresponding to x_{J-1} and x_J respectively.

The finite difference analogs to Equation (6) through (9) are:

Continuity

$$\left\{ A_J \; \frac{\rho_J - \bar{\rho}_J}{\Delta t} \right\} + \left\{ \frac{m_J - m_{J-1}}{\Delta x} \right\} = -[S] \left\{ w_J \right\} \tag{11}$$

Energy

$$\left\{ \frac{1}{u''_J} \; \frac{h_J - \bar{h}_J}{\Delta t} \right\} + \left\{ \frac{h_J - h_{J-1}}{\Delta x} \right\} = [m_{J-1}]^{-1} \left\{ q_{J-1/2} - [S]^T [\Delta h_{J-1}] \right.$$

$$\left. \{ w_{J-1} \} \; -[S]^T [\; t_{J-1}] \{ c_{J-1} \} + \left[[h_{J-1}] [S]^T - [S]^T [h^*_{J-1}] \right] \{ w_{J-1} \} \right\} \tag{12}$$

---

*The overscore bar ($^-$) indicates previous time.

Axial Momentum

$$\left\{\frac{1}{A_J} \frac{m_J - \bar{m}_J}{\Delta t}\right\} - \left\{2 u_J \frac{\rho_J - \bar{\rho}_J}{\Delta t}\right\} + \left\{\frac{p_J - p_{J-1}}{\Delta x}\right\} =$$

$$\left\{a'_J\right\} + [A_J]^{-1} \left[[2u_J][S]^T - [S]^T [u^*_J]\right]\left\{w_J\right\} \qquad (13)$$

Transverse Momentum

$$\left\{\frac{w_J - \bar{w}_J}{\Delta t}\right\} + \left\{\frac{u^*_J w_J - u^*_{J-1} w_{J-1}}{\Delta x}\right\} + \left(\frac{s}{\ell}\right) \left\{C_J w_J\right\} = \left(\frac{s}{\ell}\right) [S] \left\{p_{J-1}\right\} \qquad (14)$$

Equation (11), (13) and (14) can be combined to eliminate $\{p_{J-1}\}$ and $\{m_J\}$. Let $\{a'_J\}$ in equation (13) be written as

$$\left\{a'_J\right\} = \left\{K_J m_J^2\right\} - \left\{f_J\right\} \qquad (15)$$

where K_J represents coefficient of the flow-squared terms and $\{f_J\}$ are the remaining terms of $\{a'_j\}$. Now let

$$\left\{m_J\right\} = \left\{m_{J-1} + \Delta m\right\} \qquad (16)$$

where $\Delta m = -[S]^T \left\{w_J\right\} \Delta x - A_J(\rho_J - \bar{\rho}_J)\Delta x/\Delta t \qquad (17)$

Squaring m_j gives

$$\left\{m_J^2\right\} = \left\{m_{J-1}^2 + \left(2m_{J-1} + \Delta m\right) + \Delta m^2\right\} \qquad (18)$$

Normally Δm^2 would be discarded as being small, however, for flow blockage analysis Δm can be as large as m. It can be retained by using the following form for Equation (18)

$$\left\{ m_J^2 \right\} = \left\{ m_{J-1}^2 + (2m_{J-1} + \Delta m)\ \Delta m \right\}$$

and upon substituting Equation (16) it becomes

$$\left\{ m_J^2 \right\} = \left\{ m_{J-1}^2 + (m_{J-1} + m_J)\ \Delta m \right\} \tag{19}$$

The value of m_J on the right side is unknown but it can be initially estimated and updated through iteration. By using Equations (13), (15), and (19) the pressure at J-1 can be written as

$$\left\{ p_{J-1} \right\} = \left\{ p_J \right\} - \left\{ F_J \right\} \Delta x - [R_J] \left\{ w_J \right\} \Delta x \tag{20}$$

where

$$[R_J] = [A_J]^{-1} \left[[2u_J + \frac{\Delta x}{\Delta t}]\ [S]^T - [S]^T [u_J^*] \right]$$

$$\Delta x\ [K_J(m_{J-1} + m_J)]\ [S]^T \tag{21}$$

and

$$\left\{ F_J \right\} = -\left\{ K_J m_{J-1}^2 \right\} - \left\{ f_J \right\} + \left\{ \frac{\bar{m}_J - m_{J-1}}{A_J \Delta t} \right\}$$

$$+ \left\{ \left(\frac{p_J - \bar{p}_J}{\Delta t} \right) \left(2u_J + \frac{\Delta x}{\Delta t} + \Delta x K_J A_J (m_{J-1} + m_J) \right) \right\} \tag{22}$$

12

The pressure difference between subchannels can now be written as

$$[S] \left\{ p_{J-1} \right\} = [S] \left\{ p_J \right\} - [S] \left\{ F_J \right\} \Delta x - [S] [R_J] \left\{ w_J \right\} \Delta x \tag{23}$$

Substituting this result into Equation (14) to eliminate $[S] \{ p_{J-1} \}$ gives a set of simultaneous equations of the form

$$[M_J] \left\{ w_J \right\} = \left\{ b_J \right\} \tag{24}$$

where

$$[M_J] = \left[\frac{1}{\Delta t} \right] + \left[\frac{u_J^*}{\Delta x} \right] + \left(\frac{s}{\ell} \right) [C_J] + \left(\frac{s}{\ell} \right) [S] [R_J] \Delta x \tag{25}$$

and

$$\left\{ b_J \right\} = \left\{ \frac{\bar{w}_J}{\Delta t} \right\} + \left\{ \frac{(u^* w)_{J-1}}{\Delta x} \right\} + \left(\frac{s}{\ell} \right) [S] \left\{ p_J \right\} - \left(\frac{s}{\ell} \right) [S] \left\{ F_J \right\} \Delta x \tag{26}$$

The first three items on the right side of Equation (25) are diagonal matrices. The first two of these come from the added temporal and spatial acceleration terms in the transverse momentum equation. They are also very important as they provide additional numerical stability. Reducing Δx and Δt adds more diagonal dominance and thus more stability to the numerical solution. As in earlier difference schemes[1,2,3] the last term on the right side of Equation (25) includes a matrix which is singular for any rod bundle problem with a lateral transverse flow loop. The additional terms in Equation (25) remove the singularity thus allow a unique solution for the crossflow. This last term also includes some new terms as compared to the previous COBRA-III model. As shown in Equation (21) one is a term to account for the axial friction pressure loss at x_j. This is a very important term

for flow blockage analysis because it allows the calculation to look downstream and account for a sudden large change in the friction pressure gradient. Previously, COBRA-III could not consider large local pressure loss coefficients for very nonuniform lateral placement of blockages. The other new term $\Delta x/\Delta t$ in Equation (21) accounts for rapid changes in the flow m_j. The previous [16] version of COBRA-III could not consider transients with time steps less than the transit time through a node.

The matrix [M] controls the distribution of crossflow; however, the vector {b} contains the crossflow forcing terms. The first two terms on the right side of Equation (26) try to maintain the crossflow that existed at previous time or space. If other forces did not exist, crossflow would tend to persist. The third term is the pressure difference affecting the crossflow. This is also the term that feeds downstream information into the crossflow solution. The fourth term provides the basic driving force for crossflow. If the pressure gradients due to friction, acceleration and gravity are unbalanced, crossflows occur in an attempt to equalize them.

DISCUSSION OF PARAMETERS

Solutions to the previous set of equations require a certain amount of empirical information. Because of the incomplete knowledge of steady state and transient two-phase flow in bundles some of this information must be supplied by assumption. For example, h* and u* are commonly assumed to be their respective values from the donor subchannels. Other selections of u* and h* may be made[8] to account for the nonuniform enthalpy distribution in a subchannel. This usually requires information about the liquid-and-vapor-phase distribution. The factor f_T used to account for the imperfect analogy between eddy diffusivity of heat and momentum is also unknown but its effect is weak. For many problems f_T can be safely set equal to zero.[1] The correlations required for calculating the pressure gradient are of major importance. This includes the correlations for friction factor, subcooled void fraction, bulk void fraction and two-phase friction multiplier. Fortunately, correlations of these effects developed for simple channels[9-12] may be applied to rod bundle subchannels for steady state with reasonably good results.[13-15] Since their

14

accuracy is questionable for high speed transients, additional experimental work is needed in this area. Turbulent mixing must also be specified from empirical correlations or data. At the present time a definitive correlation for mixing does not exist for all bundle geometries and all flow conditions. Some progress has been made to describe mixing for single[5,16,17] and two-phase flow;[8,14,15] however, very little is known about two-phase mixing processes during transients.

The transverse momentum equation and fuel heat transfer model add still more parameters to the subchannel analysis method. These parameters and their effect on typical rod bundle calculations are discussed in the succeeding sections.

Transverse Momentum Equation Parameters

The more complete transverse momentum equation introduces a new parameter (s/ℓ) and also suggests possible new importance for the terms u^* and C. Some insight concerning the importance of these parameters can be found by inspecting the finite difference form of the combined transverse momentum equation, Equation (24). For discussion purposes, consider the matrix [M] for two interconnected subchannels of equal area.* The matrix has only one element given by

$$m = \frac{1}{\Delta t} + \frac{u^*}{\Delta x} + \left(\frac{s}{\ell}\right) C + \left(\frac{s}{\ell}\right) \frac{2u^*}{A} \Delta x \tag{27}$$

where u^* is the average of the two subchannel velocities. The relative importance of the terms can be controlled by arbitrarily selecting Δx. The second and fourth terms can be made of comparable magnitude by selecting $s/\ell = 1/2$ and $\Delta x^2 = A$ which usually requires $\Delta x < 0.5$ inch for typical nuclear reactor rod bundle problems. A larger value of Δx is normally used as it reduces computation time for long bundles. In those cases the last term is the largest one. The smallest term is usually the transverse friction term, C. It contains the friction coefficient K_{ij} which could

---

* A similar equation for unequal areas shows that a sign change leading to instabilities can occur depending upon the subchannel velocities and flow areas. This is a source of computation failure of COBRA when subchannel areas are highly nonuniform.

be expected to be on the order of unity or less. This friction coefficient does not include an "axial inertia" term contained in some previous crossflow resistance correlations.[5,6] It is improper to use those correlations here because the "axial inertia" effect is contained in the transverse momentum term $u*/\Delta x$. This can be seen by writing the pressure difference $p_i-p_j =$ $u*dw/dx$. If dw is approximated by w and if dx is approximated by an appropriate length, then, $p_i-p_j \propto (u*/v) v^2$ and the resistance coefficient due to axial inertia is proportional to $u*/v$. This ratio is large for small crossflow velocity. The same result is reported in a combined momentum and friction crossflow correlation by Khan[6] at large values of $u*/v$. At small values of $u*/v$ Khan's correlation, et.al, reduces to $K_{ij} \approx 0.25$ which would presumably be an estimate of the friction coefficient for pure crossflow. This discussion points out the usual dominance of $u*/\Delta x$ over $(s/\ell)C$. The values of C are therefore relatively unimportant for most problems. This conclusion may not be true, however, for very closely spaced rod bundles since C is believed to be nearly inversely proportional to the square of the gap spacing.

The (s/ℓ) parameter appears in all but the transverse momentum terms; therefore, as long as $u*/\Delta x$ and $1/\Delta t$ are small components of [M], (s/ℓ) is a weak parameter. Since this is usually the case for the value of Δx used in rod bundle analysis (s/ℓ) need not be specified to high accuracy. For core-wide analysis of pressurized water reactors this conclusion may not be valid because Δx^2 may be small compared to A.

The velocity $u*$ appears in the transverse and axial momentum terms. Since these are usually the largest components of [M], $u*$ could have a stronger effect on crossflow solutions than the previously discussed parameters. The choice of $u*$ must presently be made by assumption because of insufficient data to define it accurately. Fortunately, a variety of assumptions can be made that give comparable values of $u*$. This is because most bundles have rather uniform subchannel velocity distributions. The most serious errors in $u*$ could occur where large subchannel velocity differences occur. In those cases the effect of the $u*$ assumption should be checked.

The previous comments concerning the usually small magnitude of u*/Δx and C does not mean that they can be dropped from the calculations. They play a vital role in the numerical stability. As discussed previously, part of the matrix [M] is a singular matrix for any problem where one or more transverse flow loops exist such as around a fuel rod. In those cases the crossflow around the loop is not unique. Including u*/Δx and C remove the singularity by imposing the friction and momentum constraint that the sum of the pressure drop around may transverse loop is equal to zero. Mathematically these terms add diagonal dominance to [M], thus, improve the condition of [M]. The diagonal dominance can be improved by decreasing Δx.

FORCED CROSS FLOW MIXING

The previous finite difference scheme allows forced diversion cross-flows to be specified. This feature allows the effects of forced flow diverter vanes and forced crossflow mixing from wire wrapped bundles to be considered.

COBRA-IIIC includes a forced crossflow mixing model which was originally developed for the COBRA-II program[2] but not published. Initial calculations with COBRA-II were not entirely satisfactory because the numerical solution was not a boundary-value flow solution. The absence of the boundary-value solution allowed crossflows to increase fictitiously around the periphery of a bundle as the bundle size was increased. The method of solution did not allow the forced flow diversions to redistribute flow axially. The boundary-value solution used in COBRA-IIIC allows these calculations to be included on a more realistic basis. The following tentative model is the one contained in COBRA-IIIC. Consider the wire wrap as it passes from one subchannel to another as shown in the sketch.
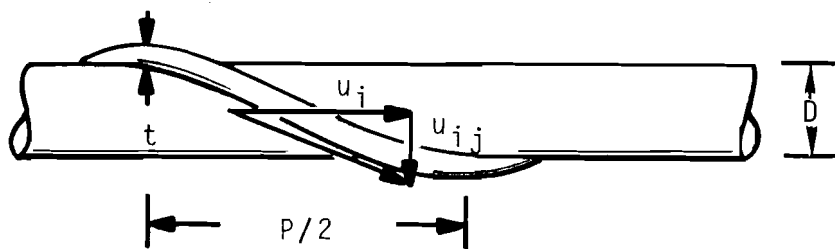
Where the wrap crosses the minimum part of the gap the slope of the wrap imposes a transverse velocity given by

$$u_{ij} = \pi \; \frac{D+t}{P} \; u_i \tag{28}$$

If this is multiplied by the fluid density and gap spacing the crossflow per unit length becomes

$$w_{ij} = \rho_i s_{ij} u_{ij} = \pi \left(\frac{D+t}{P}\right) \left(\frac{s_{ij}}{A_i}\right) m_i \tag{29}$$

This equation applied at the gap only. When the wrap is sufficiently far away from the gap it probably has little or no effect on forcing flow through the gap in question. It is now postulated that there is some function $f(x/P)$ that periodically defines the importance of Equation (29) for defining the forced crossflow through a chosen gap. This function may look something like the one in the following sketch
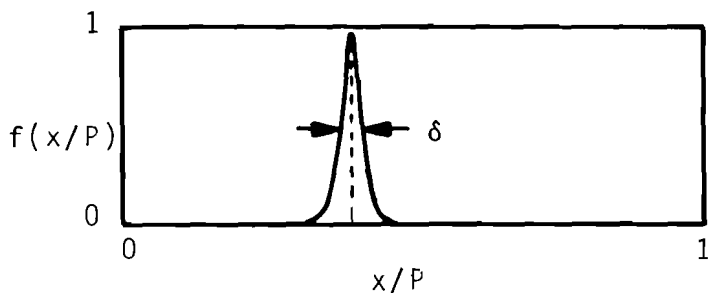
The rise in the function represents the approach of the wire toward the gap. The function peaks at 1.0 according to Equation (29) and then decays as the wrap moves away from the gap. The area under the curve represents the fraction of flow diverted through the gap as compared to the total possible flow that could be carried by a wrap over an entire pitch length. Since the shape of this function is not known, the pulse is assumed to be a rectangular pulse with width δ. The forcing function is then $f(x/p) = 0$, except for

$$f(x/p) = 1 \; ; \; (x_c/P - \delta/2) \leq x \leq (x_c/P + \delta/2) \tag{30}$$

For computations in COBRA it is presently assumed that the flow carried through a gap by a wrap occurs over one node length, Δx. The total flow diverted is; therefore,

$$w\delta p = \pi \left(\frac{D+t}{p}\right) \left(\frac{S_{ij}}{A_i}\right) m_i \delta P \tag{31}$$

Dividing this by Δx gives the crossflow per unit length over one node length

$$w_{forced} = \frac{w\delta p}{\Delta x} = \pi (D+t) \left(\frac{S_{ij}}{A_i}\right) \left(\frac{\delta}{\Delta x}\right) m_i \; ; \; x-\Delta x < x_c < x \tag{32}$$

This equation shows that a fraction of the subchannel flow m_i is diverted from one subchannel to another when a wrap crosses a gap at axial position x_c when $x-\Delta x \leq x_c < x$.

The calculations also correct the subchannel flow area and wetted perimeter for the number a wraps in a subchannel at each axial position.

The specified value of forced crossflow is included by simply modifying Equation (24). Suppose the crossflow in gap ℓ is to be specified. First the right side {b} must be modified. For each $k \neq \ell$

$$b_{k_{mod}} = b_k - M_{k\ell} \, w_{\ell_{forced}} \tag{33}$$

and for $k = \ell$

$$b_{k_{mod}} = w_{\ell_{forced}} \tag{34}$$

The matrix [M] is modified by setting row ℓ and column ℓ equal to zero except $M_{\ell\ell} = 1$. As an example if $\ell = 3$ the matrix modification would be

$$
\begin{bmatrix}
M_{11} & M_{12} & 0 & M_{14} & \text{---} & M_{1n} \\
M_{21} & M_{22} & 0 & M_{24} & \text{---} & M_{2n} \\
0 & 0 & 1 & 0 & \text{---} & 0 \\
M_{41} & M_{42} & 0 & M_{44} & \text{---} & M_{4n} \\
- & - & 1 & - & & - \\
- & & 1 & - & & - \\
- & & 1 & - & & - \\
M_{n1} & & & & & M_{nn}
\end{bmatrix}
\begin{Bmatrix}
w_1 \\ w_2 \\ w_3 \\ w_4 \\ - \\ - \\ - \\ w_n
\end{Bmatrix}
=
\begin{Bmatrix}
b_1 - M_{13}\, w_{3_{forced}} \\
b_2 - M_{23}\, w_{3_{forced}} \\
w_{3_{forced}} \\
b_4 - M_{43}\, w_{3_{forced}} \\
- \\ - \\ - \\
b_n - M_{n3}\, w_{3_{forced}}
\end{Bmatrix}
\qquad (35)
$$

The same procedure applies if more than one crossflow is being forced.

Forced crossflow mixing due to diverter vanes is considered in much the same way. When subchannel grid spacer losses are specified for input to COBRA-IIIC, a flow diversion fraction is specified where the fraction is defined by the ratio $w_{ij}\,\Delta x/m_i$ if $w_{ij} > 0$ and $w_{ij}\,\Delta x/m_j$ if $w_{ij} < 0$.

The previous method of considering forced crossflow should be considered tentative until experimental data are available to check the validity.

COMPUTATION PROCEDURE

Steady-state computations are performed first to obtain initial conditions for the transient. Since the previously presented finite difference equations are stable for large time steps, those same equations are used for the steady state calculations by setting Δt equal to some arbitrarily large value. An iteration is performed until convergence of the flow solution is obtained. Convergence is achieved when the change in any subchannel flow is less than a user selected fraction of the flow from the previous iteration.

For each iteration the computation sweeps from the inlet to the exit of the channel. With inlet boundary information on flow, crossflow and enthalpy given, the enthalpy can be advanced one space step by using Equation (11). For the first iteration the flow $\{m_J\}$ is set equal to $\{m_{J-1}\}$ otherwise the previous iterate is used. The crossflow solution is performed by solving Equation (24) where the previous iterate value of the subchannel pressure difference $[S]\{p_J\}$. After the crossflow $\{w_J\}$ is calculated $\{m_J\}$ is calculated from Equation (11) and $[S]\{p_{J-1}\}$ is calculated from Equation (23) and saved for use during the next iteration. Note that $[S]\{p_J\}$ is downstream of $[S]\{p_{J-1}\}$; therefore, iteration allows the downstream pressure differences to be felt at upstream locations. At the end of the channel the boundary condition is $[S]\{p\} = 0$. In this way a boundary value solution is obtained. Only a few iterations are sufficient for convergence because the pressure difference $[S]\{p\}$ only propagates a few nodes most problems.

The above equations do not require actual pressure since pressure difference is only used in the combined momentum equation. The calculation of pressure is, therefore, only a back calculation. It is calculated from Equation (13) in a forward direction. When the exit is reached the pressures are set equal to the exit pressure.

Transient calculations are performed in the same way but for a selected time step Δt. Boundary conditions and other forcing functions are set to their desired values at new time; then, the calculation sweeps through the channel for the number of iterations required to achieve convergence on the crossflow. The converged solution is used for the new initial condition and the procedure continues for all time steps.

FUEL ROD HEAT TRANSPORT

In a previously published version of COBRA-III the fuel heat flux was assumed to be known from input data. This was rather unsatisfactory for some computations since it required a prior knowledge of the fuel heat

21

transfer. A more satisfactory approach is to let the heat flux occur naturally by changing the heat generation, heat transfer coefficient or fluid temperature.

The fuel heat transfer model included in COBRA-IIIC considers radial conduction within the fuel by dividing the fuel into equally spaced concentric rings as shown in Figure 2. Axial and circumferential heat conduction are presently ignored. Axial heat conduction can be ignored because axial temperature gradients are usually small. Circumferential heat conduction is ignored to maintain a reasonable limit on the number of fuel nodes. This assumption can be justified if the heat transfer coefficients and fluid temperatures are rather uniform around a fuel rod. For boiling flow the fluid temperature is usually quite uniform. The validity of assuming a uniform heat transfer coefficient must be evaluated for each problem.

Figure 2 shows the node layout used to construct the conduction model. The fuel is divided into equal radial nodes plus a node for the cladding. For N nodes this gives N+1 temperatures where the temperature at i = N+1
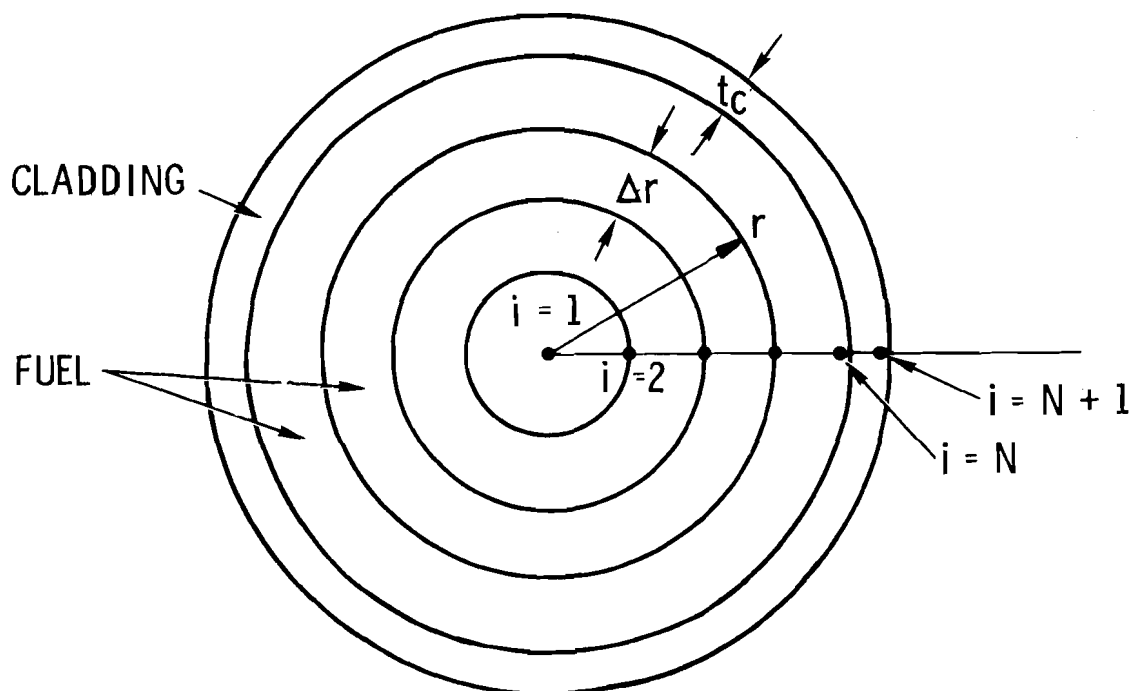
FIGURE 2. Fuel Model Node Designation

is at the outer surface of the cladding. An effective gap conductance coefficient is used at the fuel-clad interface to combine the conductance of the cladding and the gap. The surface heat transfer coefficient is arbitrarily specified through heat transfer correlations. An average heat transfer coefficient is determined from a circumferentially weighted average of the heat transfer coefficients in the subchannels surrounding a fuel rod. A similar calculation is performed to obtain an average fluid temperature.

The numerical solution developed in Appendix B uses an implicit finite difference scheme[18,19] that is stable for all time steps. The equations used for the numerical solution are as follows:

i = 1, temperature at fuel center

$$\left(\frac{\rho c}{\Delta t} + \frac{4k}{\Delta r^2} \right) T_1 - \frac{4k}{\Delta r^2} T_2 = q_1''' + \frac{\rho c \bar{T}_1}{\Delta t} \tag{36}$$

1 < i ≤ N-1, temperature in fuel region

$$\left(-\frac{k}{\Delta r^2} + \frac{k}{2(i-1)\Delta r^2} \right) T_{i-1} + \left(\frac{\rho c}{\Delta t} + \frac{2k}{\Delta r^2} \right) T_i + \left(-\frac{k}{\Delta r^2} \quad \frac{k}{2(i-1)\Delta r^2} \right) T_{i+1}$$

$$= q_i''' + \frac{\rho c \bar{T}_i}{\Delta t} \tag{37}$$

i = N, fuel temperature at fuel-clad interface

$$\left(-\frac{2k}{\Delta r^2} \right) T_{N-1} + \left(-\frac{\rho c}{\Delta t} + \frac{2k}{\Delta r^2} + \frac{2h_{gap}}{\Delta r} + \frac{h_{gap}}{(i-1)\Delta r} \right) T_N + \left(-\frac{2h_{gap}}{r} - \frac{h_{gap}}{(i-1)\Delta r} \right) T_{N+1}$$

$$= q_N''' + \frac{\rho c \bar{T}_N}{\Delta t} \tag{38}$$

i = N +1, cladding temperature

$$-\left(\frac{h_{gap}}{t_c} \frac{r_N}{r_{N+1}} \right) T_N + \left(\frac{\rho c}{\Delta t} + \frac{h_{gap}}{t_c} \frac{r_N}{r_{N+1}} + \frac{h_{surf}}{t_c} \right) T_{N+1} = q_{N+1}''' + \frac{\rho c \bar{T}_{N+1}}{\Delta t} + \frac{h_{surf}}{t_c} T_c \tag{39}$$

23

These equations are arranged as a set of simultaneous equations where the temperature coefficient matrix is tridiagonal. This system of equations is solved by using a compact Gaussian elimination routine for tridiagonal matrices.

The fuel heat transfer model is used only once per time step to calculate the fuel rod heat flux. By using data at time t the fuel temperature is advanced to t + Δt during the first flow solution iteration. That temperature and resulting heat flux calculation is held constant during the flow solution iteration.

COMPUTER PROGRAM DESCRIPTION

COBRA-III should be thought of as an automated solution to the basic set of differential equations of the mathematical model. To actually perform this solution, the user must provide input. This input not only includes the geometric parameters and operating conditions, but also the various required empirical or semiempirical correlations. Any set of correlations can give a solution, but some correlations will give better solutions. At the present time, guidelines have not been established for complete selection of these correlations; therefore, the COBRA-III program does not contain a pre-selected set of input correlations. Several correlations are provided for examples, but the final selection must be made by the user. Considerable work is required to define correlations and flow modelling applicable to rod bundle transients. The applicability of the two-phase flow model should always be evaluated by the user. Users should also justify use of COBRA for any analysis outside the range experimental verification. Experiments may be required in some cases to verify application of COBRA.

The following sections present the general features of the COBRA-III program, an illustrated description of the program organization and a description of the program's subroutines.

GENERAL FEATURES

The significant features of COBRA-III include the following:

- It considers both steady-state and transient flow in rod bundle fuel elements.
- It performs a boundary-value flow solution that permits the influence of downstream flow disturbances to be felt upstream.
- It can consider both single- and two-phase flow.
- It considers the effects of turbulent and thermal conduction mixing throughout the bundle by using empirically determined mixing coefficients.
- It includes mixing which results from the convective transport of enthalpy by diversion crossflow.
- It includes the momentum transport between adjacent subchannels which results from both turbulent and diversion crossflow.
- It includes the effect of temporal and spatial acceleration in the transverse momentum equation.
- It includes the effect of transverse resistance to diversion crossflow.
- It can consider an arbitrary layout of fuel rods and flow sub-channels for analysis of most any rod bundle configuration. A single subchannel may interact with up to four adjacent subchannels, and a fuel rod may transfer heat to a maximum of six adjacent subchannels.
- It can include arbitrary heat flux distribution by specifying the axial flux distribution, relative rod power, and the fraction of rod power to each of the six adjacent subchannels. (The latter feature allows variation in circumferential rod heat flux.)
- It can consider time varying fuel rod temperatures.
- It can consider variable subchannel area and gap spacing.
- It can consider nonuniform hydraulic behavior by assigning differ-ent single-phase friction factors to selected subchannels.
- Its subroutines are designed to allow the user to set up empirical correlations of his choice and then select these correlations through input options.

25

- It includes options to select arbitrary subchannel inlet flow and enthalpy.
- It can consider forced crossflow mixing due to diverter vanes or wire wrap spacers.
- The numerical solution allows analysis of partial flow blockages in rod bundles.

PROGRAM ORGANIZATION

The organization of the COBRA-IIIC program is similar to that of the COBRA-III program; however, several new subroutines have been added and the old subroutines have been reorganized to permit the expanded program capability. The calculational procedure has been revised to use the previously described numerical solutions for both steady state and transient conditions.

The organization of the main COBRA-IIIC program can best be described by following the flow chart of Figure 3. The first function of the program is to read in the input data. This is accomplished by successively reading in the 12 groups of input data that are required for the calculations. Some of these groups are optional and are not needed for certain problems. New cases, after the first, require input of only the card groups that will change the input of the previous case. The new input data for each case may be printed out prior to starting the calculations. The user can also omit this or can print out the entire set of input for each case.

Boundary conditions are established for the steady-state solution by recalling previously stored values of inlet flow rate and enthalpy established from the input data. Subroutine SPLIT is used to calculate subchannel flows to give equal subchannel pressure gradients, if it is requested by an input option. All crossflows and the matrix $[S]$ $\{p\}$ are set equal to zero to establish the inlet crossflow and exit pressure boundary condition and to provide an initial estimate for starting the iteration procedure.
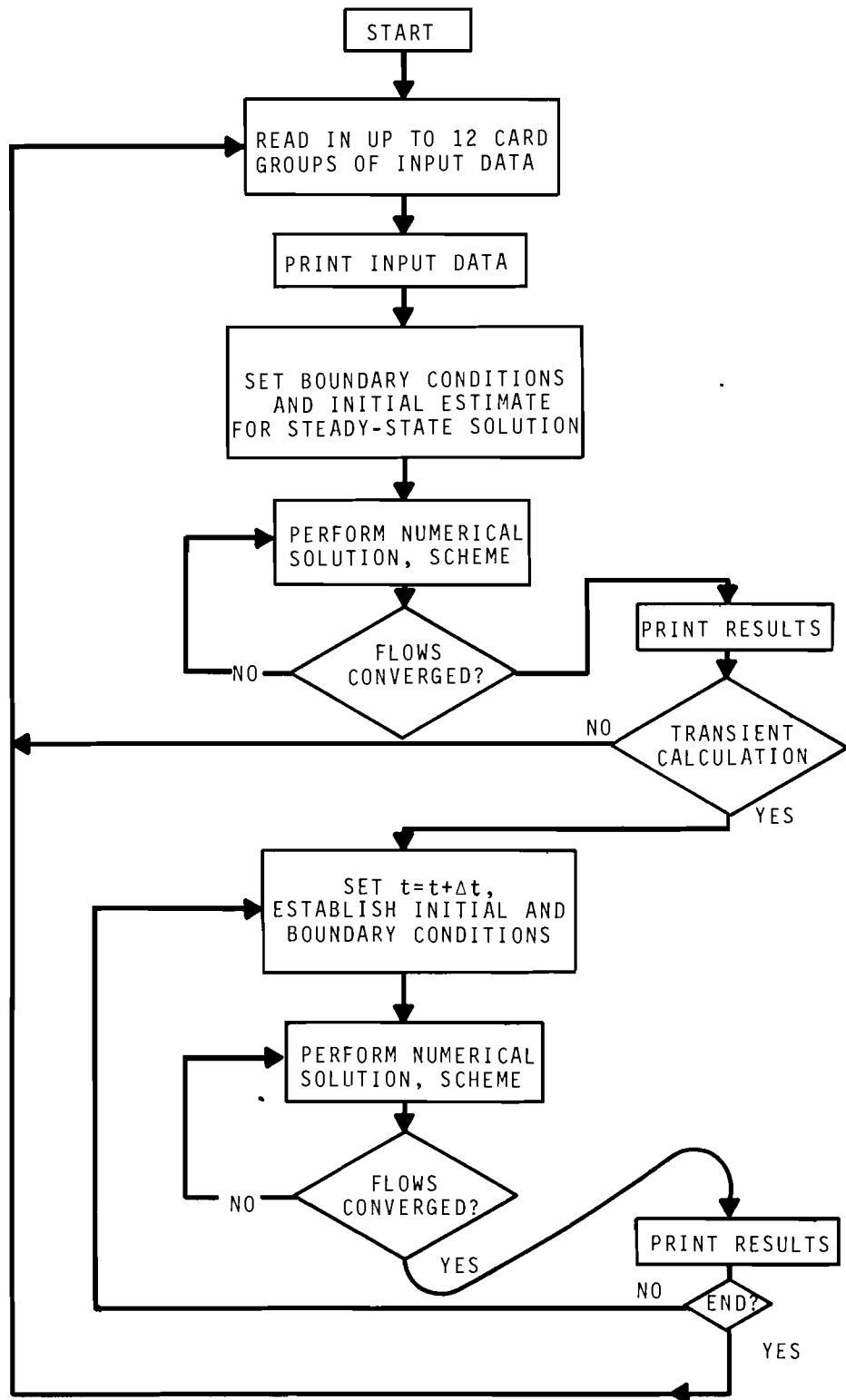
FIGURE 3. Main COBRA-IIIC Program Flow Chart

An iteration loop is now entered which sweeps the calculation through the bundle. Within this loop is a call to Subroutine SCHEME that carries the solution through the bundle at steps of Δx. The iteration continues until the flow converges to within a selected tolerance.

The transient calculation is performed in much the same way as the steady state solution. A time loop is entered that carries the solution through successive time steps of Δt. At the beginning of each time step, the channel boundary conditions and forcing functions are set at t + Δt. During each time step iteration is performed as described above to obtain a converged flow solution. This calculation procedure repeats for each time step until the end of the transient is reached. The calculation then moves on to a new case if there is one.

SUBROUTINES

The organization of the COBRA-IIIC program puts most of the calculational effort into subroutines. The more important ones are discussed here to describe their use.

Subroutine SCHEME (JUMP)

This subroutine performs the previously outlined numerical solution. Given a set of boundary and initial conditions it carries the calculations once through the bundle in a stepwise manner. Upon completion of calculation it returns to the main program with an indication of whether (JUMP = 2) or not (JUMP = 1) the flow solution has converged. Special provision is included in SCHEME to preserve the flow and crossflow solution for suc-ceeding cases. After convergence of the first case an option is provided to set JUMP = 3. This flag bypasses the tedious crossflow solution and instead uses the crossflow solution residing in core.*

The flow chart shown in Figure 4 outlines the calculation procedure in SCHEME. The calculations start by checking the value of JUMP to determine if the previous crossflow solution is to be used.

---

* The code also includes an option to read from tape a previously written crossflow solution.
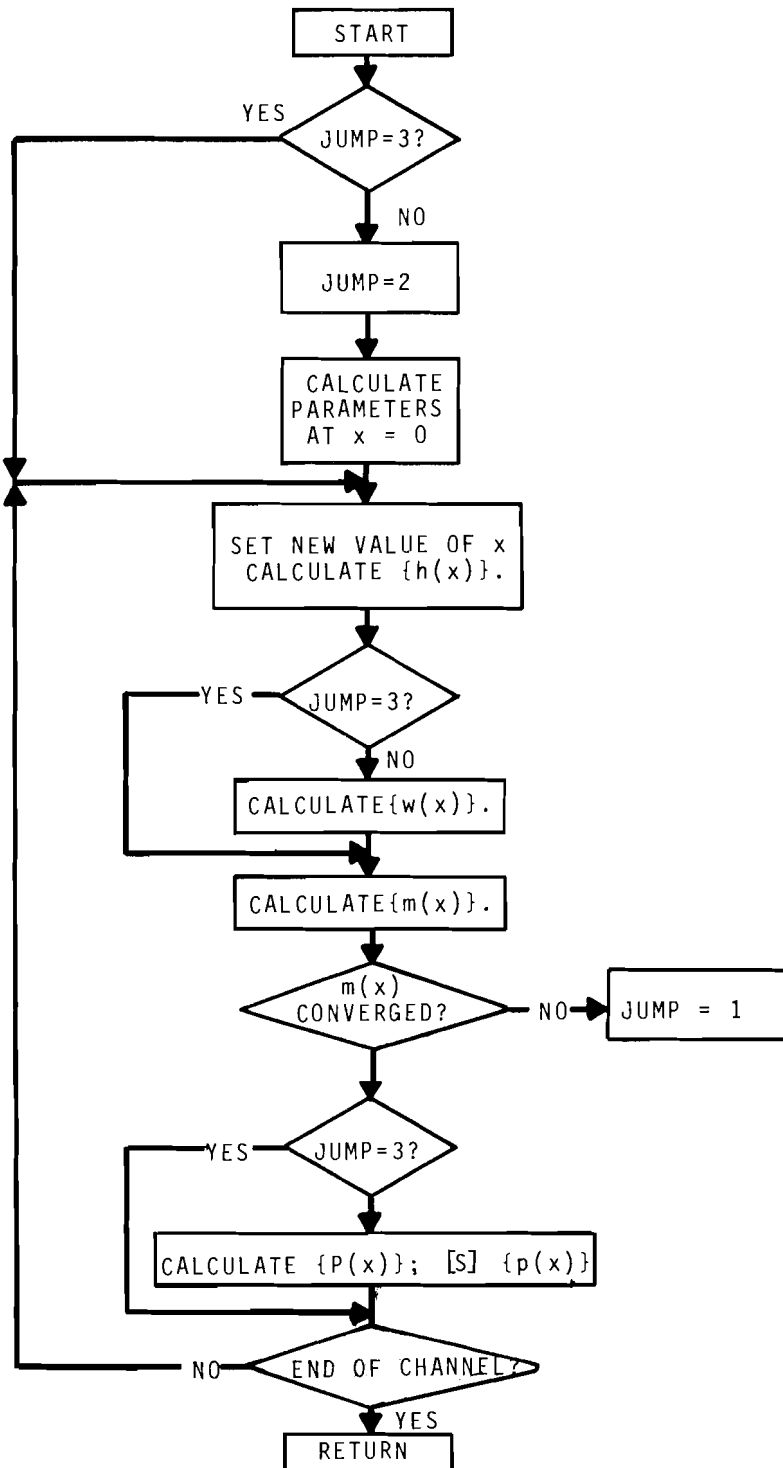
FIGURE 4. Flow Chart of the Calculation Procedure in SCHEME

Subchannel flow and heat transfer parameters are calculated at the beginning of the channel to start the calculations. A loop is now entered to take the calculation through the channel.

First, the enthalpy {h(x)} is calculated and an estimate is made for {m(x)} for the first iteration only. If JUMP ≠ 3, the crossflow {w(x)} is calculated. The flows are calculated next followed by the pressures {p(x)} and pressure difference [S] {p(x)} provided JUMP ≠ 3. Any value of flow not converged to within a selected tolerance is sufficient to set JUMP = 1 which is the nonconvergence signal. The calculation continues until the end of the channel is reached and then returns to the main program.

Function S(K, I)

This function subprogram calculates the elements of [S] according to the subchannel connection logic described in Appendix B. This calculation first assumes that

$$S(K, I) = 0$$

and then checks to see if I corresponds to either of the subchannel pair that defines K. If I corresponds to Subchannel i of the pair ij where i < j then

$$S(K, I) = 1.$$

If I corresponds to Subchannel j of the pair ij then

$$S(K, I) = -1$$

On some cases the [S] transformation is performed directly without using this function by noting that the kth element of [S] {p} is just $p_i(k) - p_j(k)$.

Subroutine DIFFER (IPART,J)

Subroutine DIFFER is divided into four parts as indicated by the variable IPART.

Part 1 calculates the right hand side of Equation (12) which is designated DHDX(I). This quantity is the steady state value of the enthalpy gradient {dh/dx}. Part 1 contains the calculation of the enthalpy carried by the crossflow h* which is presently assumed to be the enthalpy of the donor subchannel.

Part 2 calculates the right hand side of Equation (11) which is designated DFDX(I). This is the steady-state value of the flow gradient {dm/dx}.

Part 3 calculates the pressure gradient coefficient $\{K_j\}$ used in Equation (15) and designates it DPK(I). It also calculates the other components of the pressure gradient $\{F_j\}$ without the division crossflow terms as defined by Equation (22) and designates it as DPDX(I).

Part 4 calculates the complete pressure gradient {dp/dx} including the crossflow terms and designates it DPDX(I).

Subroutine DIVERT

This subroutine calculates the diversion crossflows $\{w_x\}$ by setting up and solving the set of simultaneous Equations (24). The matrix [M] is designated by AAA(K,L) and the vector {b} by B(K) in DIVERT. The simultaneous solution is performed by a call to DECOMP and SOLVE. The value of the axial velocity u* carried by the crossflow is calculated in DIVERT. Presently, u* is assumed to be the average velocity of the two adjacent subchannels or

$$u^*_k = \frac{1}{2}(u_{i(k)} + u_{j(k)}) \tag{40}$$

If forced flow diversion between subchannels is specified by FORCE, the simultaneous equations are modified prior to solving for {w(x)}.

Subroutine MIX

Subroutine MIX calculates the thermal mixing parameters w' and c which are designated by WP(k) and COND(K), respectively. Since completely general correlations for mixing have not been developed for single and two

phase mixing, this subroutine is set up so that improved correlation functions can be included when they become available. The approach used for now is to separate the mixing into boiling and nonboiling regions. For nonboiling conditions, several correlation forms are included as shown in Appendix C. For two-phase flow, the single-phase correlations may be assumed to apply or the mixing rate may be specified as a function of quality.

The thermal conduction coefficient is assumed to be a function of the subchannel geometry and the average fluid thermal conductivity as discussed in Appendix C.

Subroutine PROP (IPART)

This subroutine consists of two parts. The first part calculates the saturated fluid properties as a function of the system reference pressure. The second part calculates all the liquid fluid properties as a function of temperature and limits these to saturated values during boiling. The second part also calculates the convection heat transfer coefficient used in Levy's subcooled void model.

Subroutine VOID

Subroutine VOID calculates the subcooled void fraction, bulk void fraction, density, effective specific volume for momentum, two-phase friction gradient multiplier velocity and energy transport velocity. Several correlations are included in this subroutine that the user can select by option. These are provided as an example with the thought that the users will set up correlations that are most applicable to their particular problems.

Subroutine AREA

This subroutine calculates subchannel area and gap spacings by using the tabular list of area and gap variations supplied as input. A linear interpolation is used to select values from these tables. When wire wrap mixing is included AREA corrects the subchannel flow area and hydraulic diameter according to the wire wrap inventory provided by FORCE.

Subroutine FORCE

Subroutine FORCE is provided to specify forced diversion crossflow at selected gaps and at selected axial positions. If a forced crossflow is specified, the logical variable FDIV = .TRUE.; otherwise, FDIV = .FALSE. Subroutine FORCE includes two options for forced crossflow mixing in COBRA-IIIC. One option is the wire wrap mixing model described previously. FORCE identifies when a wire wrap crosses a gap, computes the forced crossflow and corrects the wire wrap inventory for the adjacent subchannels. The other option is for a specified flow fraction diverted from one subchannel to an adjacent subchannel.

Subroutine HEAT

This subroutine calculates the heat input {q} to each of the subchannels and designates it as QPRIM(I). Two options are included in HEAT. One option is to specify heat flux without using the fuel heat transfer model. The heat input contribution from the adjacent rods are simply added as defined by the input data. This is the same procedure used in previous versions of COBRA. The other option uses a similar procedure but instead obtains the heat flux from the fuel heat transfer model. The power transient is input to the fuel and the heat flux responds as governed by the fuel thermal properties, fluid temperature and surface heat transfer coefficients.

Subroutine TEMP

This subroutine calculates the fuel temperatures by using the previously described heat transfer model. Both cylinderical and plate type fuel can be considered. The plate fuel option can be used to account for heat transfer to a flow housing. TEMP obtains heat transfer correlations from Function HCOOL.

Function HCOOL

This function computes the surface heat transfer coefficient designated by HCOOL(N,I,J) where N is the rod number, I is the adjacent subchannel and J is the axial position. No correlations are presently included in this

function. Only a dummy value of 5000 Btu/hr-ft^2-°F is used at the present time. Users are expected to select and program correlations applicable to the problem being analyzed.

Subroutine CHF (JSTART, JEND)

At the completion of the subchannel flow and enthalpy calculation an optional call to subroutine CHF is provided to calculate critical heat flux ratios over the portion of the channel denoted by J = JSTART through J = JEND. The critical heat flux ratio CHFR(N,J) and critical channel CCHANL(N,J) are calculated for each rod N at position J. CHFR(N,J) is also searched to determine the minimum critical heat flux ratio MCHFR(J), critical rod MCHFRR(J) and critical channel MCHFRC(J) at each axial location J. The data is printed as part of the fuel temperature and heat flux output.

Other Subroutines

Several other subroutines are required for operation of the COBRA-II program. Subroutine CURVE performs a linear interpolation of tabulated data. Subroutine DECOMP and SOLVE perform the solution to the simultaneous equations. Subroutine GAUSS performs a solution of the tridiagonal system of equations used for the dual heat transfer model. Subroutine SPLIT divides the subchannel flow rates at the inlet of the bundle to give equal pressure gradients by assuming that there is no spatial acceleration component of pressure drop.

USE OF COBRA

This section presents some general comments on the use of COBRA and then illustrates its capabilities by showing the results of some sample calculations.

The COBRA-III program is written for the UNIVAC-1108. Except for the round-off problems that are encountered on computers with a short word length, there should be no difficulty in setting up and operating this program for other computers capable of compiling FORTRAN IV or V. Adjustable dimensions are included so that the program can be easily contracted or expanded to accommodate the users' computer or problem size. For computers

that do not allow adjustable dimensions as permitted by the UNIVAC-1108 INCLUDE Statement, fixed dimension COMMON must be prepared and inserted in the main program and in each designated subroutine. An initialization is provided in COBRA-IIIC to start computation; however, this may not be complete enough for computers that do not preset the core to zero as done in the UNIVAC-1108 at the start of a job. The UNIVAC-1108 also does not provide divide checks, underflow or overflow messages. Division by zero is assigned a value zero on the 1108.

Complete input instructions are included in the program listing. The input is set up with options by which the user may select correlations for input to a problem. This has been done to make it clear that the user should treat these correlations as input since none of these correlations have universal validity. By forcing the user to make this selection, the correlations are given the status of input. In particular, the user must select or provide for:
- Friction factor correlation
- Subcooled void fraction correlation
- Two-phase friction multiplier correlation
- Two-phase void fraction correlation
- Single-phase mixing correlation
- Two-phase mixing correlation
- Pressure loss coefficients for spacers
- Flow diversion from spacing devices
- Diversion crossflow resistance factor
- Crossflow momentum factors
- Heat transfer correlations

COBRA-IIIC uses steady-state correlations for transients. This approximation must be evaluated for applicability to any transient analysis.

SAMPLE PROBLEMS

To illustrate the new features contained in COBRA-IIIC the results of several sample calculations are presented. These include results for both

a 49-rod bundle with and without the fuel heat transfer model and flow
blockage. A sample problem for forced crossflow mixing in a wire-wrapped
bundle is also presented.

49-Rod Bundle

A 1/8 section of symmetry is used for this bundle. The subchannel
layout is shown in Figure 5 and the input parameters are in Table 1.

Several sets of calculations are presented to show the effect of the
crossflow resistance factor K_{ij}, transverse momentum factor (s/ℓ) and
velocity u*.

Figure 6 presents the distribution of flow[†] in Subchannel 8 both
with and without a blockage with an assumed loss coefficient of K_8 = 10.
The calculated flow distribution without blockage is rather uniform
except for periodic perturbation caused by the grid spacers. The flow
distribution with the blockage decreases rather abruptly at the blockage
and gradually recovers downstream where a grid spacer aids the flow

ROD DIAMETER   0.562"
ROD-ROD SPACING   0.177"
ROD-WALL SPACING   0.140"
LENGTH   120"

ROD POWER PEAKING AS SHOWN
NOMINAL OPERATING CONDITIONS,

1000 psia	SYSTEM
505 °F	INLET TEMPERATURE
1.0×10^6 LB/HR/FT^2	AVERAGE MASS VELOCITY
0.3×10^6 BTU/HR/FT^2	HEAT FLUX
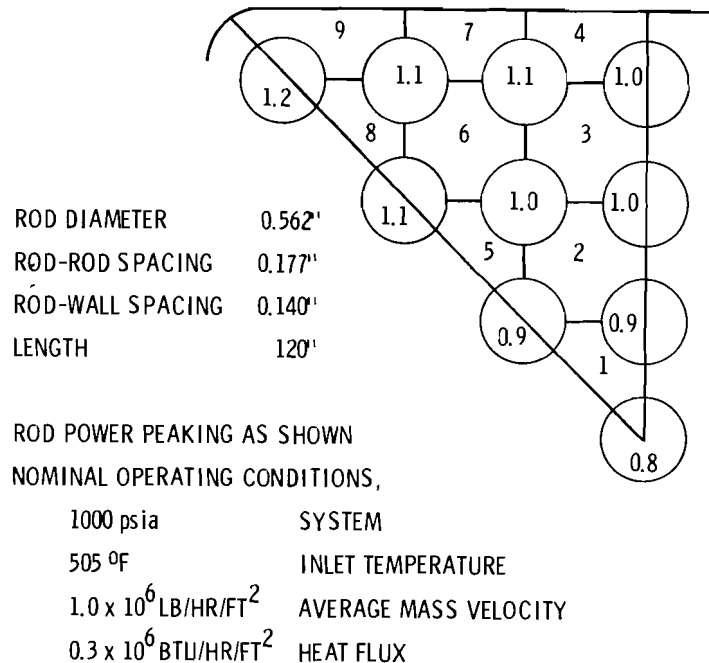
FIGURE 5. Subchannel Layout for a 1/8 Section
of Symmetry from a 49-Rod Bundle

---

† Earlier flow solutions reported in ASME paper 72-WA/HT-49 are somewhat
different because of the improved numerical solution for blockage.

TABLE 1. Input Parameters for BWR Sample Problems

Water Thermodynamic Properties	1967 ASME Tables
Subchannel Friction Factor	$f = 0.186 \ R_e^{-0.2}$
Subcooled Voids	Not Included
Void Fraction*	$\alpha = Xv_g/[(1-X)v_f+Xv_g]$
Two-phase Mutiplier*	$\phi = \rho_f/\rho$
Two-phase Density*	$\rho = \rho'' = \alpha\rho_g+(1-\alpha)\rho_f$
Two phase Specific Volume*	$v' = 1/\rho$
Enthalpy Carried by Crossflow (h*)	h* = h from donor subchannel
Axial Velocity of Crossflow (u*)	Average velocity of adjacent subchannels
Axial Heat Flux	Chopped Cosine, peak/avg = 1.26
Momentum Turbulent Factor	0
Transverse Momentum Parameter (s/ℓ)	0.5
Crossflow Resistance (K_{ij})	0.5
Bundle Length	120 inches
Number of Axial Nodes	60
Turbulent Mixing Parameter, β	0.02
Fuel Thermal Properties:	
k	2.0 Btu/hr ft °F
ρ	640 lb/ft^3
C	0.08 Btu/lb °F
Diameter	0.502 inches
Cladding Thermal Properties:	
k	8.8 Btu/hr ft °F
ρ	405 lb/ft^3
C	0.076 Btu/lb °F
Thickness	0.030 inches
Gap Conductance	1000 Btu/hr ft^2 °F
Surface Heat Transfer Coefficient	5000 Btu/hr ft^2 °F
Grid Spacer Location	x/L = 0.2, 0.4, 0.6, 0.8
Spacer Pressure Loss Coefficient	k = 1.0

---

* Homogeneous two-phase flow correlations.
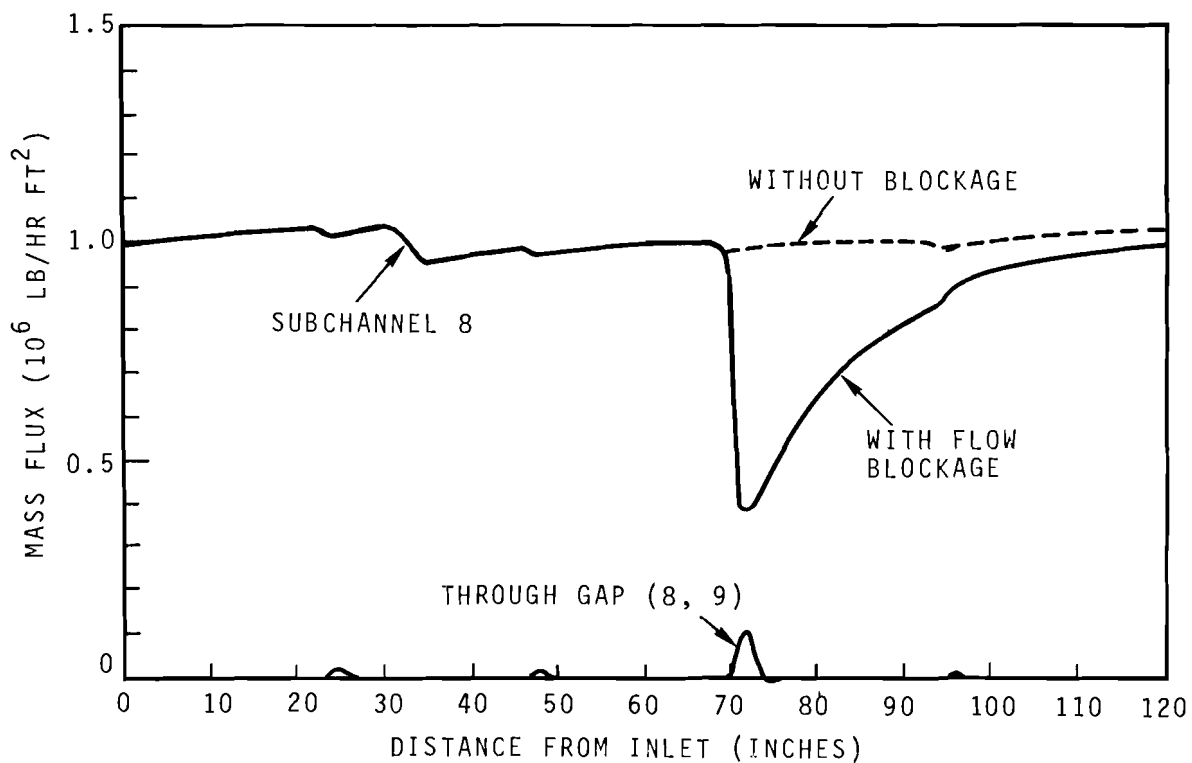
FIGURE 6. Subchannel 8 Flow Distribution
With and Without Flow Blockage

recovery at x/L = 0.8. The influence of the blockage is slightly evident
at the first node before the blockage. The enthalpy increase downstream
of the blockage is less than 10 Btu/lb for the chosen value of crossflow
mixing. The diversion crossflow mass flux also shown in Figure 6 is very
small compared to the axial mass flux except at the blockage. There it is
still less than 10% of the average. This shows that the assumption of
small transverse velocity compared to axial velocity is well satisfied for
this problem even in the presence of a large subchannel flow diversion.
Although this result would apply to most rod bundle problems the assumption
should be checked, especially for problems where gross flow redistributions
occur.

Changing the crossflow resistance factor K_{ij} from 0.5 to 1.0 and 0.25
had no significant effect on the flow solution as shown in Table 2. This
could be expected based on the previous discussion concerning the magnitude

TABLE 2. Parameter Sensitivity Evaluation for BWR Bundle Sample Problem

Parameter	Pressure Ahead of Blockage (psia)	G_8 Minimum $(10^6\ lb/hr\ ft^2)$	Enthalpy 1 ft Downstream of Blockage (Btu/lb)
No Blockage	3.50	.958	657.72
Base Case Blockage	3.97	.380	667.70
$K_{ij} = 1.0$	3.98	.381	667.67
$K_{ij} = 0.25$	3.97	.380	667.74
$s/\ell = 1.0$	3.96	.373	667.38
$s/\ell = 0.25$	3.99	.390	668.31
$\Delta x = 4$ inches	--	.384	669.92
$u^* = \left\{ \begin{matrix} u_{ij};\ w_{ij} > 0 \\ u_{ij};\ w_{ij} \le 0 \end{matrix} \right\}$	3.97	.423	665.90
$u^* = \min(u_i, u_j)$	3.98	.423	668.76

of C. Increasing K_{ij} had the larger effect by increasing the subchannel pressure difference near the blockage and by moving the start flow diversion slightly upstream. The maximum lateral Δp_{ij} near the blockage was 0.05 psi. The values of crossflow resistance used in the example probably bracket those that could be expected for rod bundles. These calculations indicate that crossflow resistance does not have to be known precisely as its effect on the computed flow is small. This should be checked for particular problems to determine the importance of crossflow resistance.

Changing the value of (s/ℓ) from 0.5 to 0.25 and 1.0 also had no significant effect on the flow solution. Increasing it increases the importance of the friction and pressure terms. This has the effect of allowing more rapid flow diversions by reducing the importance of the "axial inertia." The reduced importance of axial inertia tends to reduce the pressure ahead of the blockage and allows more flow reduction as show in Table 2. This range of (s/ℓ) would seem to be reasonable from geometric considerations.

Figure 7 presents the results of calculations using various assumptions for u*. The reference assumption is that u* is the average velocity of the adjacent subchannels. Another assumption is that u* is the velocity of the donor subchannel. This gives a discontinuity in u* when the crossflow changes direction. The other assumption is that u* is the smaller of the two adjacent subchannel velocities. While this may not be realistic, it can help stablize flow solutions near regions of severe flow maldistribution when subchannel areas are not uniform. All of these assumptions are seen to cause only moderate changes in the flow solution. This is fortunate because it would be difficult to provide a meaningful generalized correlation for u*. The data in Table 2 indicate only small changes in enthalpy due to changing the u* assumption.
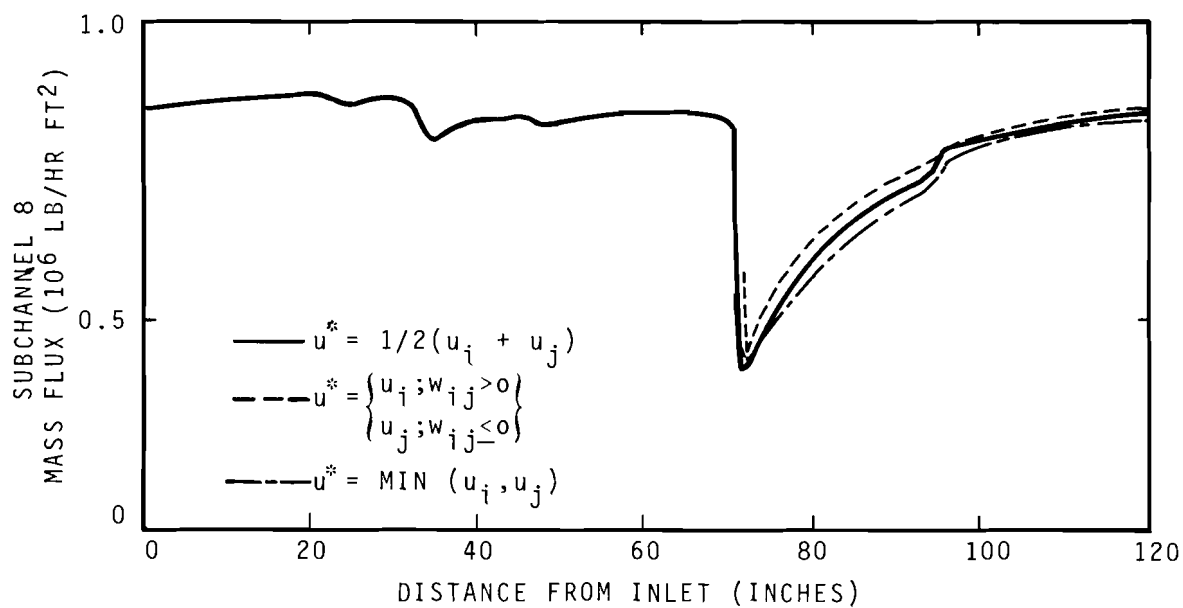
FIGURE 7. Effect of u* Assumption on Sub-
channel 8 Flow Distribution

The previous parameter evaluation indicates that rather large changes in the parameters C, (s/ℓ) and u* cause only small-to-moderate changes in the subchannel flow solution. Similar results have been found for calculations with large inlet flow imbalances for core-wide flow analysis in pressurized water reactors. For more typical design analysis problems, where flow

imbalances are not large, changes in the above parameters are weak. For most problems the reference values of the three parameters should provide reasonable results; however, computational experiments should be performed to check this. For cases where the parameters have a meaningful effect on flow solutions laboratory experiments may be necessary to define them more accurately.

Fuel Temperature and Flow Transients

The use of the fuel temperature model introduces some additional considerations for transient analysis of rod bundles. The fuel heat transfer and flow are coupled by their respective time responses. The time response of the fuel is its time constant and the time response for the flow is the transit time through the bundle. Depending upon the nature of the transient being considered the time responses may or may not be comparable.

If the time response of the fuel is much longer than the transit time through the bundle, the flow solution can be treated as a series of quasi steady-state solutions during the duration of the fuel temperature transient. If, for these conditions a flow related transient occurs over a short period of time the fuel may not have time to respond. Conversely, if the time response of the fuel is much faster than the transit time through the bundle, then the flow is significantly affected by fuel temperature transient.

As an example, consider the power transient show in Figure 8 which might occur after a turbine trip for a boiling water reactor. The flow and enthalpy solutions[+] are shown in Figures 9 and 10 as a function of time. Note that the flow is only slightly perturbed by the power transient and that the enthalpy decays rather slowly when the fuel heat transfer model is used. The transit time through the bundle is approximately 1.5 seconds which is about a factor of 10 less than the fuel time constant. For the 0.05 second time step used for this problem, each time step

---

[+] Slightly different results from an earlier calculation are reported in ASME paper 72 WA/HT-49. The difference is due to a different axial flux profile.
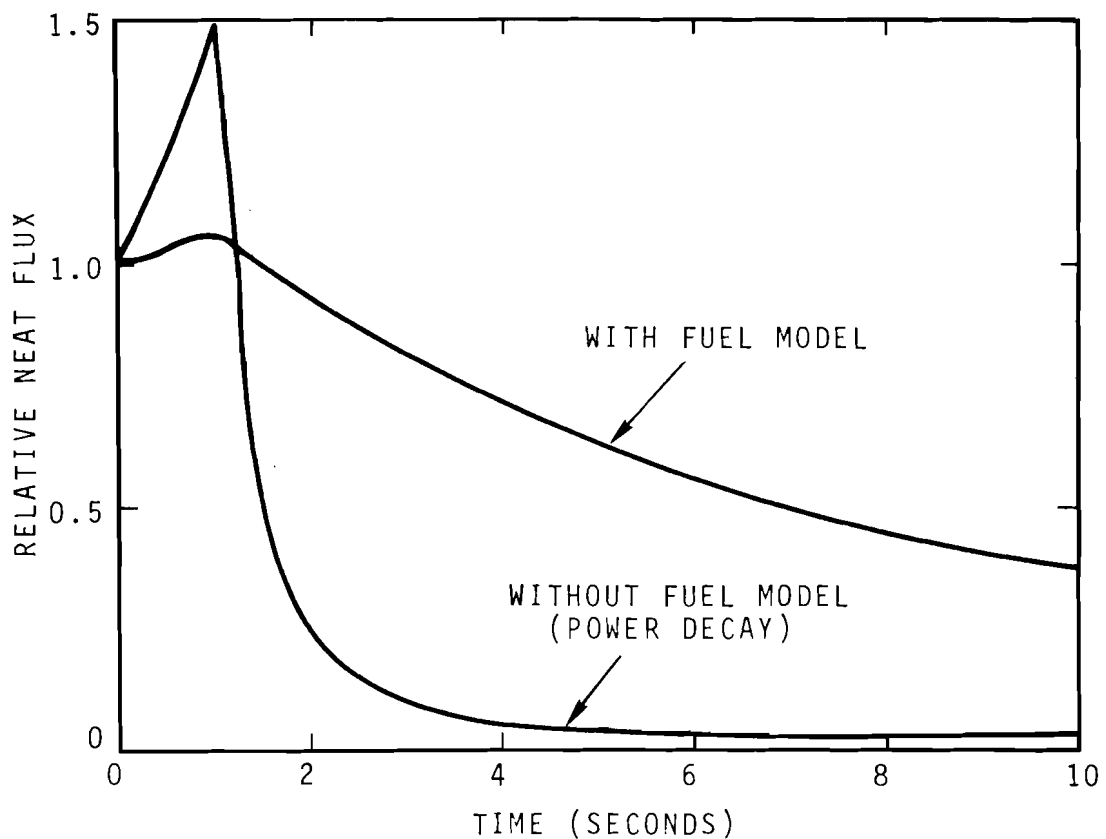
FIGURE 8. Fuel Heat Flux Versus Time With and
Without the Fuel Heat Transfer Model

solution is nearly a quasi-steady flow solution that is following a fuel
temperature transient. As a contrast to this, the same calculation was
performed but without the fuel heat transfer model. Here the heat flux has
an infinitely fast response and decays with the power. In this case the
transient has a very dramatic effect on the flow and enthalpy solution.
The exit flow first increases due to the void growth in the bundle. Then
as the power and enthalpy decay, the flow decreases rapidly as the voids
begin to collapse. At the end of 10 seconds the entire bundle has all
liquid flow. While this is a fictitious case it does show how the fuel ther-
mal response can have an important effect on the flow depending upon the
relative time response of the fuel and flow channel.
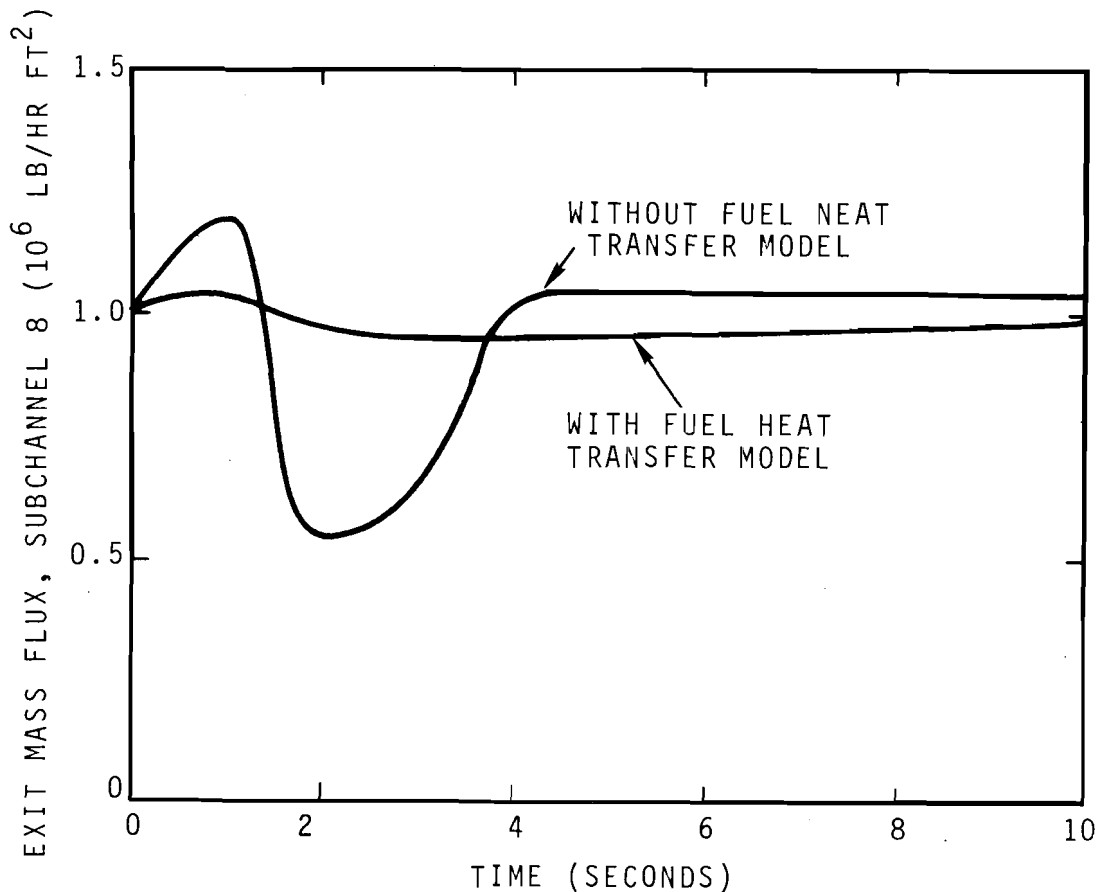
FIGURE 9. Subchannel 8 Flow Distribution With
and Without Fuel Heat Transfer Model

7-Pin Wire Wrapped Bundle

To illustrate the use of the wire wrap forced flow mixing capability
in COBRA-IIIC, consider the 7-pin bundle in Figure 11. This 7-pin bundle
has 0.230 inch diameter fuel pins on a 0.286 inch pitch (0.056 inch gap
spacing). The wire wraps are assumed to start at the top and move clock-
wise with one rotation every 12 inches. The bundle is 36 inches long to
allow flow through three pitch lengths. Uniform radial and axial power
is assumed with a heat flux of 0.5×10^6 Btu/hr ft^2. The inlet temperature
is 800°F and the mass flux is 3.0×10^6 lb/hr ft^2. A complete input list-
ing and computer output for this problem is contained in Appendix D.
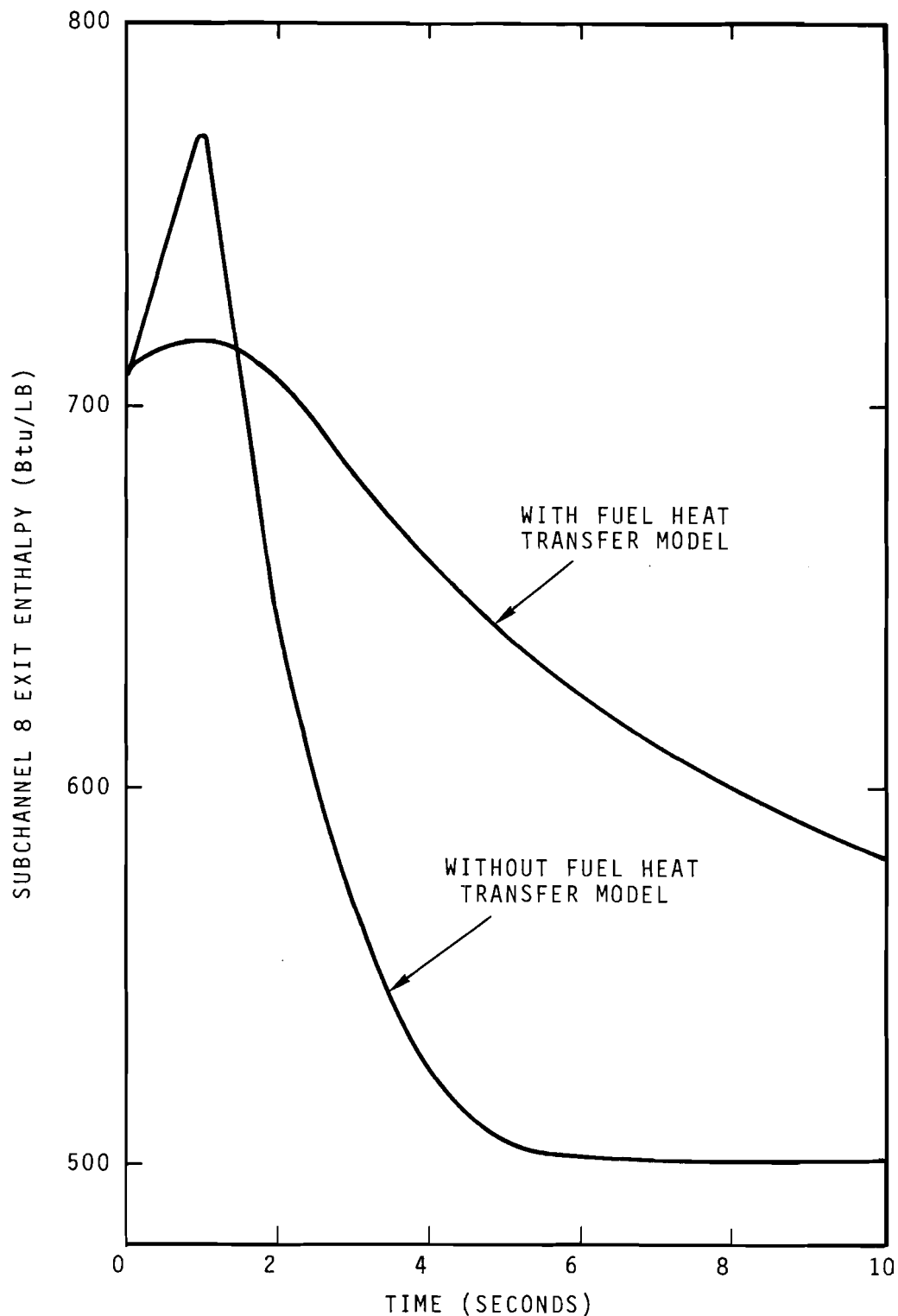
FIGURE 10. Subchannel 8 Exit Enthalpy With and Without Fuel Heat Transfer Model
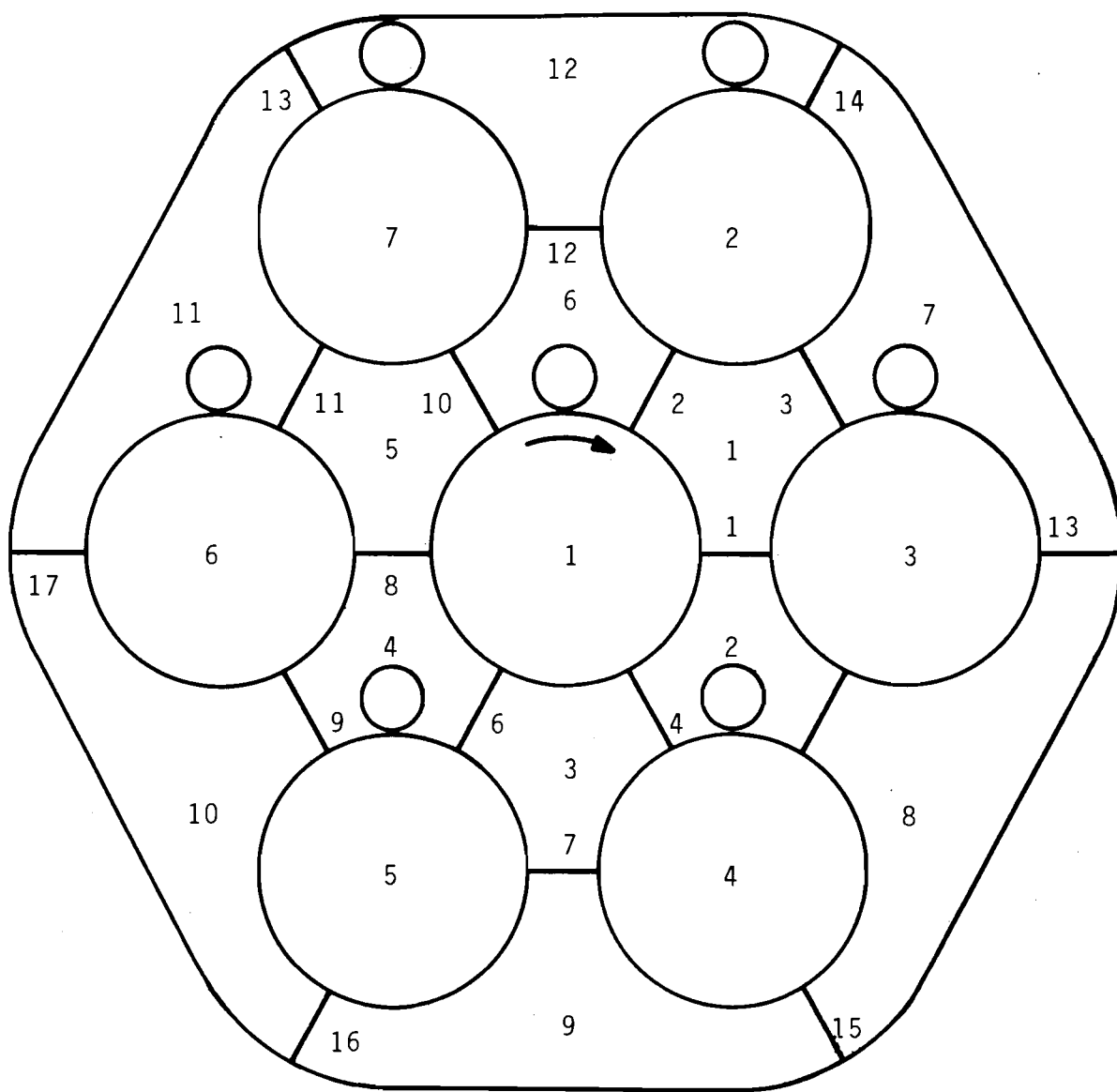
FIGURE 11. Subchannel Layout and Wire Wrap Positions Looking in the Direction of Flow at the Inlet

Figure 12 shows the computed temperature profile in Subchannel 1 (interior) and Subchannel 7 (wall) for two mixing assumptions: (1) no mixing; (2) turbulent mixing (β = .02) plus forced wire wrap mixing (δ = .06). Over half of the temperature difference reduction is due to the turbulent mixing alone. Presently it is uncertain how turbulent and wire wrap mixing should be combined. The problem presented here should only be interpreted as a sample. Experimental data comparisons are needed to verify the wire model and to determine the values of the mixing parameters.
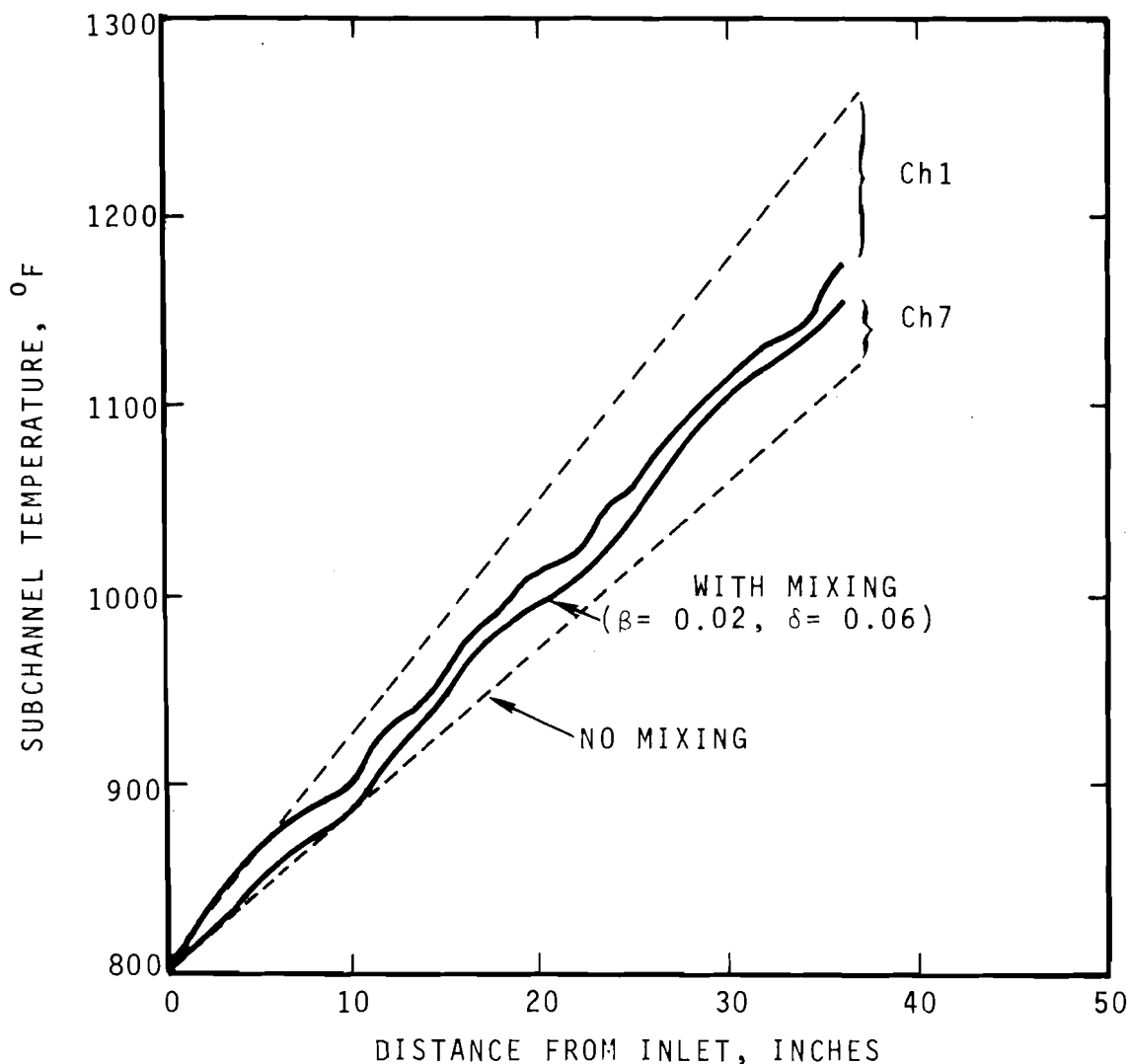
FIGURE 12. Subchannel Enthalpy Distribution With and Without Forced Crossflow Mixing

Figure 13 shows the computed subchannel flow distribution along the length of the bundle. The periodic changes in flow were caused by the periodic entry and exit of wraps from the subchannels and by the forced flow mixing.
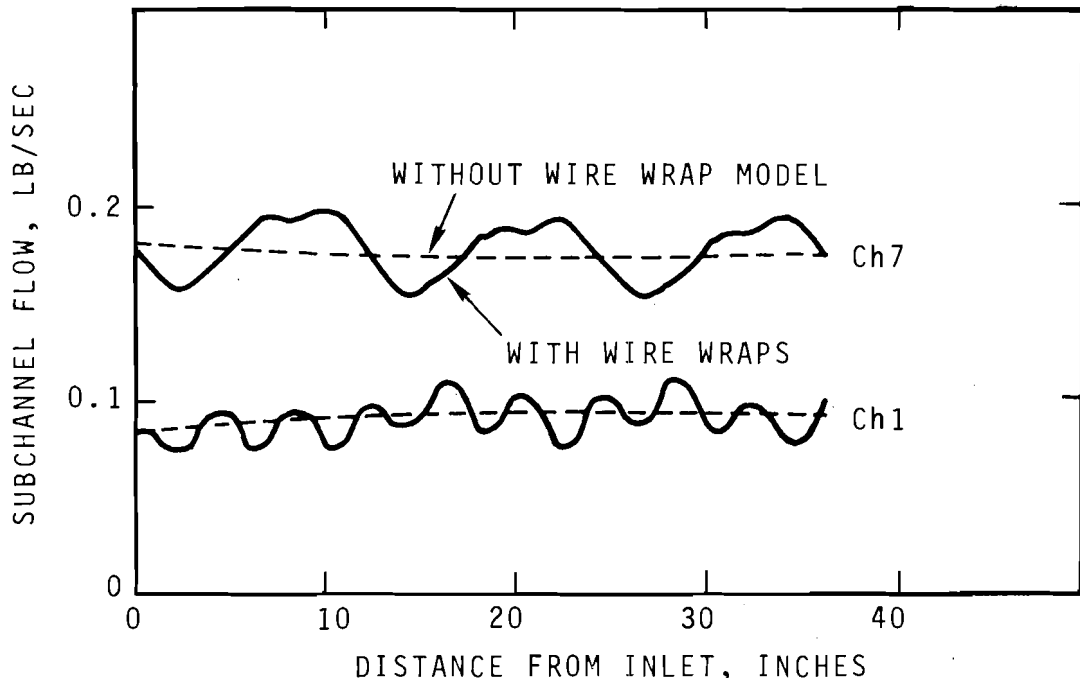
FIGURE 13. Subchannel Flow Distribution with Wire Wrap Spacers

Figure 14 shows the computed crossflow between selected subchannels. the exterior "rod-wall" gap always has a positive value indicating lateral flow in the direction of wire wrap rotation. It is interesting that the maximum crossflow occurs on the opposite side from where the wire wrap is forcing flow. This is caused by the accumulation of crossflows from the other gaps forcing crossflow. The other gaps show periodic behavior but with positive and negative values of crossflow. The crossflow through the radial gap tends to average to zero; however, the crossflow through circumferential rod gap does not. It shows a small net crossflow in the direction of wire wrap rotation.
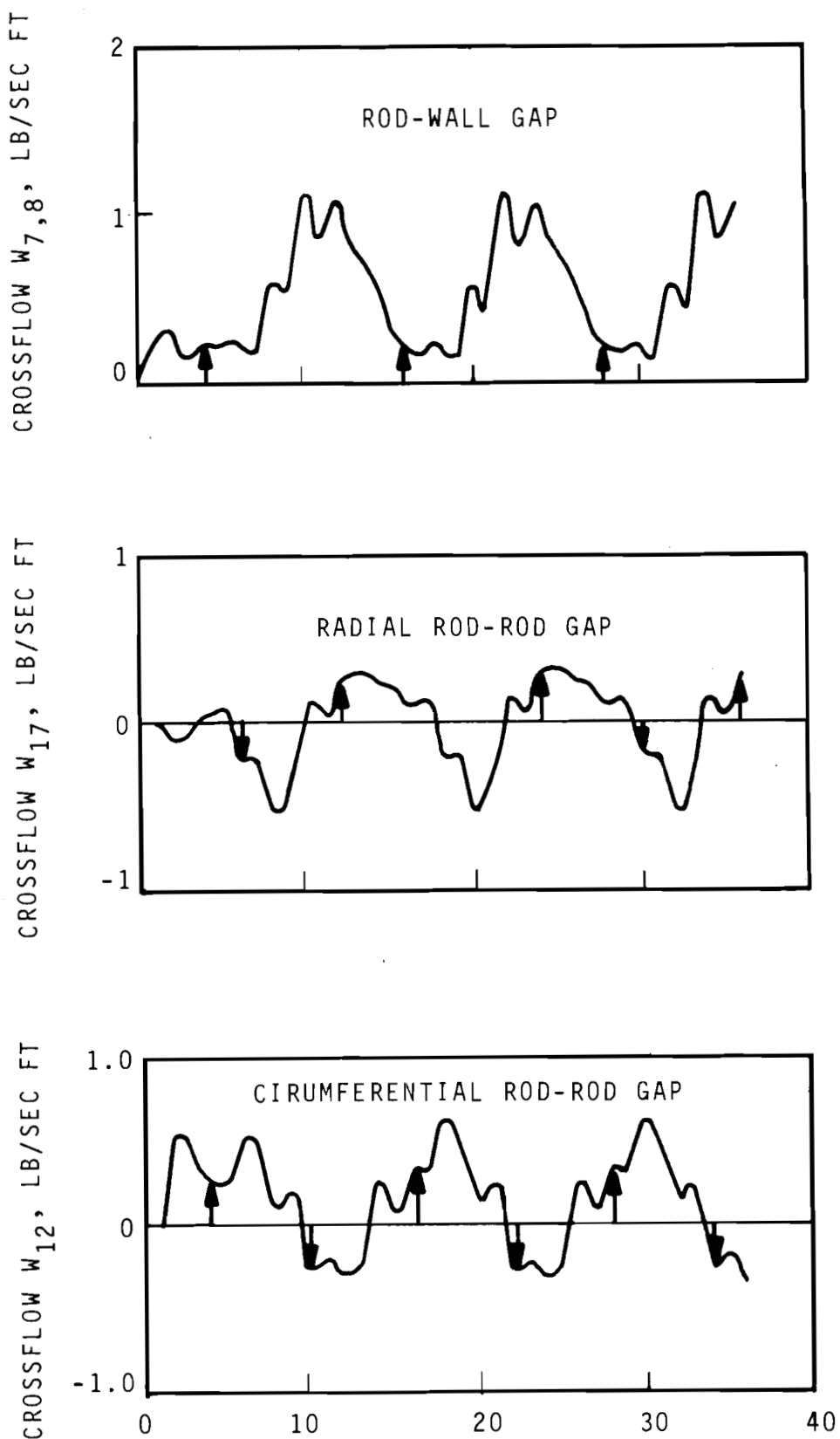
FIGURE 14. Crossflow Distribution with Wire Wrap Forced Mixing

FUTURE DEVELOPMENT

Further development of COBRA is continuing to improve its computational capability. Major emphasis is being directed toward developing reverse flow analyses capability and a pressure drop boundary condition option.

The present program is only capable of considering flow in one direction. The ability to consider flow reversals is required for analysis of many problems; therefore, significant effort is being directed to develop this computational capability in COBRA-III.

For the analysis of many problems, the inlet flow boundary condition is not very convenient because it is not known except through the results of a system analysis. A more convenient boundary condition may be the pressure drop. This boundary condition permits the inlet flow to respond as changes occur within the bundle or in the connecting piping. The complete success of using this type of boundary condition for a wide range of transient analyses will depend, in part, on the ability to consider flow reversals.

The subchannel analysis programs such as COBRA, and others, are experiencing rather widespread use in the nuclear industry. In some cases these computer programs are being used for analyses where they have little (or no) experimental verification and input data. It is recommehded that expanded experimental studies be performed:

- To provide a more definitive range of application of the subchannel analysis methods. This should include the full spectrum flows and enthalpies anticipated for normal reactor operating conditions as well as for accident situations.
- To provide more complete experimental data for two-phase crossflow mixing.
- To provide experimental verification of the flow models for transient analysis.

REFERENCES

1. D. S. Rowe, Crossflow Mixing Between Parallel Flow Channels During Boiling, Part 1. COBRA--Computer Program for Coolant Boiling in Rod Arrays, BNWL-371, Pt 1. Pacific Northwest Laboratory, Richland, Washington (March 1967).

2. D. S. Rowe, COBRA-II: A Digital Computer Program for Thermal Hydraulic Subchannel Analysis of Rod Bundle Nuclear Fuel Elements, BNWL-1229. Pacific Northwest Laboratory, Richland, Washington (February 1970).

3. D. S. Rowe, Interim Report. COBRA-III: A Digital Computer Program for Steady State and Transient Thermal-Hydraulic Analysis of Rod Bundle Nuclear Fuel Elements, BNWL-B-82. Pacific Northwest Laboratory, Richland, Washington (1971).

4. J. E. Meyer. Conservation Laws in One-Dimensional Hydrodynamics, WAPD-BT-20, pp. 61-72. Westinghouse Electric Corporation, Bettis Atomic Power Laboratory, Pittsburgh, Pennsylvania (September 1960).

5. J. T. Rogers and N. E. Todreas. "Coolant Mixing in Reactor Fuel Rod Bundles--Single-Phase Coolants," Heat Transfer in Rod Bundles, ASME, pp. 1-56 (1968).

6. E. U. Khan, K. Kim, G. E. Lindstrom, "Crossflow Resistance and Diversion Crossflow Mixing Between Rod Bundles," ANS Transactions, Vol. 14, No. 1, pp. 249-250 (1971).

7. D. S. Rowe, "Initial-and Boundary-Value Flow Solutions During Boiling in Two Interconnected Parallel Channels," American Nuclear Society Transactions, Vol. 12, No. 2 pp. 834-835 (November 1969).

8. R. T. Lahey, Jr., B. S. Shiralkar, D. W. Radcliffe, "Mass Flux and Enthalpy Distribution in a Rod Bundle for Single- and Two-Phase Flow Conditions," ASME Paper 70-WA/HT-8 91970).

9. J. P. Waggener. "Friction Factors for Pressure Drop Calculations," Nucleonics, Vol. 19, p. 145 (1961).

10. A. A. Armand. "The Resistance During the Movement of a Two-Phase System in Horizontal Pipes," Translated by V. Beak, AERE Trans. 828. Izvestiya Vsesojuznogo Teplotekhnicheskogo Instituta (1), pp. 16-23 (1946).

11. W. A. Massena. Steam-Water Pressure Drop and Critical Discharge Flow - A Digital Computer Program, HW-65706. Hanford Atomic Products Operation, Richland, Washington (June 17, 1960).

12. S. Levy. Forced Convection Subcooled Boiling--Prediction of Vapor Volumetric Fraction, GEAP-5157. General Electric Co., Atomic Power Equipment Dept., San Jose, California (April 1966).

13. L. S. Tong. "Pressure Drop Performance of a Rod Bundle," Heat Transfer in Rod Bundles, ASME, pp. 57-69 (1968).

14. J. E. Casterline, F. S. Castellana, Flow and Enthalpy Redistribution in a Simulated Nuclear Fuel Assembly, CU-187-2 (February 1969).

15. D. S. Rowe, "A Thermal-Hydraulic Subchannel Analysis for Rod Bundle Nuclear Fuel Elements," Paper No. FC-13, 4th International Heat Transfer Conference, Versailles, France (1970).

16. L. Ingesson and S. Hedberg, "Heat Transfer Between Subchannels in a Rod Bundle," Paper No. FC 7.11, 4th International Heat Transfer Conference, Versailles, France (1970).

17. J. T. Rogers and R. G. Rosehart, "Mixing by Turbulent Interchange in Fuel Bundles. Correlations and Inferences," ASME Paper No. 72-HT-53 (1972).

18. G. E. Forsythe and W. R. Wasow, Finite-Difference Methods for Partial Differential Equations, John Wiley and Sons, New York (1960).

19. B. Carnahan, H. A. Luther, and J. O. Wilkes, Applied Numerical Methods, Wiley (1969).

20. L. S. Tong, Boiling Heat Transfer and Two-Phase Flow, Wiley (1966).

21. S. Y. Ahmad, "Axial Distribution of Bulk Temperature and Void Fraction in a Heated Channel with Inlet Subcooling," Journal of Heat Transfer, pp. 595-609, (November 1970).

22. G. F. Hewitt and N. S. Hall-Taylor, Annular Two-Phase Flow, Pergammon Press (1970).

23. L. S. Tong, Boiling Crisis and Critical Heat Flux, TID-25887 (1972).

NOMENCLATURE*

Equations	Computer Program	
a	DPDX	Single channel pressure gradient, (F/L^3)
a'	DPDX	Pressure gradient without crossflow in Equation (8), (F/L^3)
A	A	Cross-sectional area, (L^2)
[b]	B	Column vector defined by Equation (26)
c	COND	Thermal conduction coefficient $(H/\theta L)$
C	CIJ	Loss function for transverse crossflow in Equation (4), (FT/ML)
C_p	CP	Specific heat $(H/M\theta)$
dh/dx	DHDX	Enthalpy derivative, (H/TL)
dm/dx	DFDX	Flow rate derivative, (M/TL)
dp/dx	DPDX	Pressure gradient, (F/L^3)
D	DHYD	Hydraulic diameter, $4A/P_w$, (L)
D_r	D	Rod Diameter (L)
f	FSP	Friction factor based on all-liquid flow, (Dimensionless)
f_A	AXIAL	Local-to-average axial power distribution
f_c	PWRF	Fraction of rod power transferred to an adjacent subchannel (Dimensionless)
f_R	RADIAL	Relative rod power distribution (Dimensionless)
f_T	FTM	Turbulent momentum factor (Dimensionless)
F		Force (F)
g_c	GC	Gravitational constant, (ML/FT^2)
G		Mass velocity, (M/TL^2)
h	HFILM	Heat transfer coefficient, $(H/TL^2\theta)$
h	H	Enthalpy, $Xh_g + (1-X)h_f$, (H/M)
h*	HSTAR	Enthalpy carried by diversion crossflow, (H/M)
h_g, h_f	HG, HF	Saturated vapor and liquid enthalpy (H/M)
$[\Delta h]$		Enthalpy matrix (H/M)
k	CON	Thermal conductivity, $(H/TL\theta)$

---

* Dimensions are denoted by: L = length, T = time, M = mass, θ = temperature
  F = ML/T^2 = force and H = ML^2/T^2 = energy

NOMENCLATURE* (Cont.)

Equations	Computer Program	
K	NK	Number of connections between adjacent subchannels, (Dimensionless)
K	CDRAG,CD	Spacer loss coefficient
K_g	GK	Geometry factor for conduction (Dimensionless)
K	KIJ	Crossflow resistance coefficient
L	Z	Channel length, (L)
[M]	AAA	Matrix of coefficients defined by Equation (25)
m	F	Flow rate (M/T)
p	PEXIT, PREF	Pressure (F/L^2)
P_H	HPERIM	Heated perimeter, (L)
P_w	PERIM	Wetted perimeter, (L)
P_r	PR	Prandtl number (Dimensionless)
q'	QPRIM	Heat addition per unit length, (H/L)
$\bar{q}''$	AFLUX	Average heat flux, (H/TL^2)
Q		Specific power-to-flow ratio, q'_i/m_i, (H/ML)
Q	Q	Parameter given by Equation (C-17)
Re	RE	Reynolds number, (Dimensionless)
s	GAP	Rod spacing (L)
[S]	S	Matrix transformation defining adjacent subchannels, (Dimensionless)
t		Time (T)
[ΔT]		Temperature matrix (θ)
T	T	Temperature (θ)
u		Internal energy (H/M)
u	U	Effective momentum velocity (L/T)
u''	UH	Effective enthalpy transport velocity defined by Equation (A-9) (L/T)
u*	USTAR, USAVE	Effective velocity carried by diversion crossflow (L/T)
[Δu]		Velocity matrix (T/L^2)

NOMENCLATURE* (Cont.)

Equations	Computer Program	
v	V	Liquid specific volume, $1/\rho$, (L^3/M)
v'	VP	Effective specific volume for momentum, $(1-X)^2/\rho_f(1-\alpha) + X^2/\rho_g\alpha$, (L^3/M)
w	W	Diversion crossflow between adjacent sub-channels (M/TL)
w'	WP	Turbulent (fluctuating) crossflow between adjacent subchannels, (M/TL)
x	X	Distance (L)
X	QUAL	Quality, $m_g/(m_g + m_f)$, (Dimensionless)
X_d	XD	Parameter given by Equation (C-15)
z_{ij}	LENGTH	Effective centroid distance (L)
α	ALPHA	Void fraction, $A_g/A_g + A_f)$, (Dimensionless)
β		Turbulent mixing parameter, (Dimensionless)
γ	AV(1)	Slip ratio, u_g/u_f, (Dimensionless)
θ	THETA	Orientation of channel with respect to vertical, (Radians)
ρ	RHO	Two-phase density, $\rho_g\alpha + \rho_f(1-\alpha)$, (M/L^3)
ρ''		Effective density for enthalpy transport, $(\rho_g h_g\alpha + \rho_f h_f(1-\alpha))/h$, (M/L^3)
ρ_g, ρ_f	RHOG,RHOF	Saturated vapor and liquid density, (M/L^3)
σ	SIGMA	Surface tension, (F/L)
τ_w	TAUW	Wall shear stress (F/L^2)
ϕ	PHI,FMULT	Two-phase friction multiplier, (Dimensionless)
μ	VISC	Viscosity, (F/LT)
μ_w	VISCW	Wall viscosity, (F/LT)
Ψ		Slip correction function for energy transport, $\rho_f X(1-\alpha) - \rho_g\alpha(1-X)$, (M/L^3)

Subscripts

f,g		Saturated conditions for liquid and vapor, respectively
i	I	Fuel node number
i,j	I,J	Subchannel identification number

NOMENCLATURE* (Cont.)

Subscripts

ij,ji		Double subscripts imply subchannel connection i to j and j to i, respectively
i(k),j(k)	IK,JK	Subchannel pair for connection number (k)
k	K,L	Subchannel connection number
J	J	Axial node number

APPENDIX A

DERIVATION OF EQUATIONS FOR FLUID TRANSPORT MODEL

APPENDIX A

DERIVATION OF EQUATIONS FOR FLUID TRANSPORT MODEL

The equations of continuity, energy and momentum for each Subchannel are derived by applying the conservation equations to a control volume that consists of a segment of Subchannel (i) connected to an arbitrary Subchannel (j). The primary assumptions given in the description of the mathematical model are used together with a few additional assumptions that are required to formulate complete equations.

Continuity Equation

Apply the continuity equation for a control volume to Subchannel (i) which is adjacent to Subchannel (j).
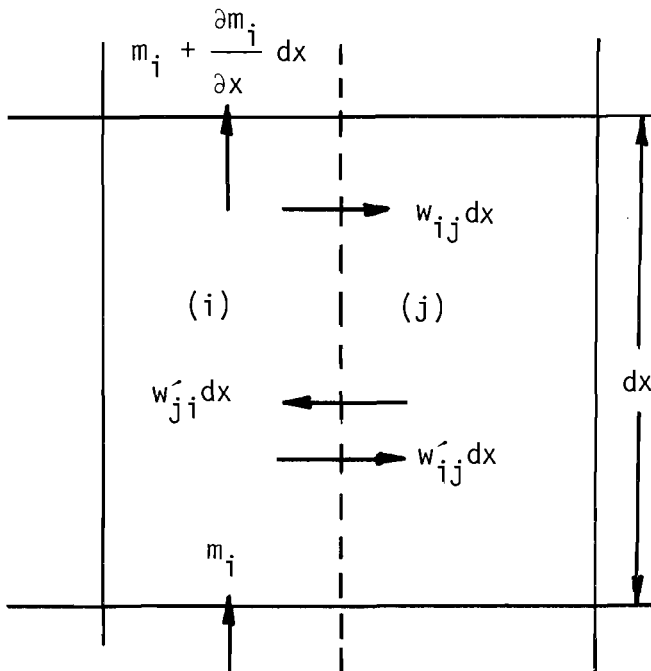
$$\frac{\partial}{\partial t} \rho_i A_i dx - m_i + m_i + \frac{\partial m_i}{\partial x} dx - w'_{ji} dx + w'_{ij} dx + w_{ij} dx = 0. \tag{A-1}$$

By assuming $w'_{ij} = w'_{ji}$ and $\partial A/\partial t = 0$

$$A_i \frac{\partial \rho_i}{\partial t} + \frac{\partial m_i}{\partial x} = -w_{ij} \tag{A-2}$$

By considering all adjacent subchannels and taking w_{ij} to be positive for flow from i to j, Equation (A-2) can be written as

$$A_i \frac{\partial \rho_i}{\partial t} + \frac{\partial m_i}{\partial x} = -\sum_{j=1}^{N} w_{ij} \; ; \; i = 1,2,3,---N. \tag{A-3}$$

Energy Equation

Apply the energy equation for a control volume to Subchannel (i) which is adjacent to Subchannel (j).
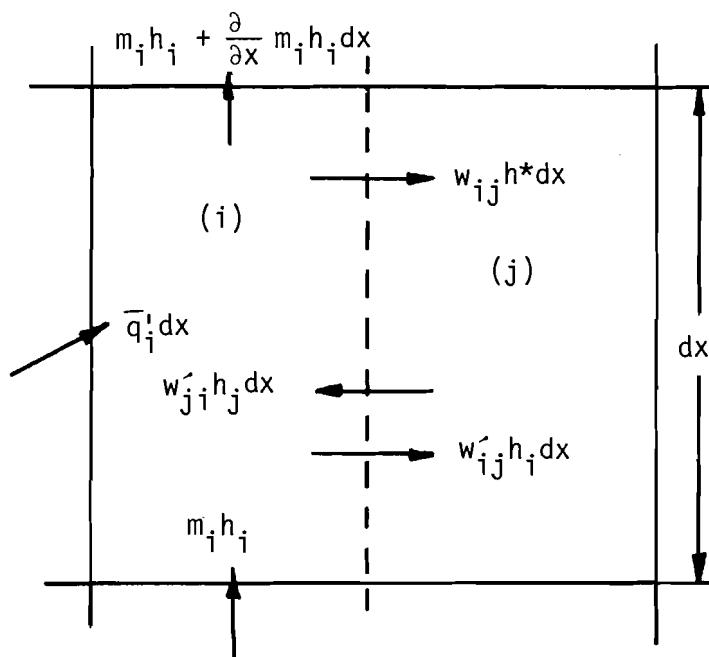
$$\frac{\partial}{\partial t} \rho_i'' u_i A_i h_i dx - m_i h_i + m_i h_i + \frac{\partial}{\partial x} m_i h_i dx - \bar{q}_i' dx$$

$$- w_{ji}' h_j dx + w_{ij}' h_i dx + w_{ij} h^* dx = 0 \tag{A-4}$$

The internal energy is defined by the relationship

$$\rho_i'' u_i = \rho_i'' h_i - \rho_i \tag{A-5}$$

A-2

By assuming $\partial A/\partial t = 0$ and using Equation (A-5), this reduces to

$$A_i \frac{\partial}{\partial t} \rho_i'' h_i + \frac{\partial}{\partial x} m_i h_i = \overline{q}_i' + (h_j - h_i) w_{ij}'$$
$$- w_{ij} h^* + A_i \frac{\partial p_i}{\partial t} \qquad (A-6)$$

where h^* is the enthalpy carried by the diversion crossflow and ρ_i'' is the effective density for heat capacity.[15] By using the function Ψ as presented by Tong, pg. 208, Equation (A-2) and neglecting $\partial p_i/\partial t$ this may be reduced to

$$A_i \left[\rho_i - h_{fg} \frac{\partial \Psi}{\partial h} \right] \frac{\partial h_i}{\partial t} + m_i \frac{\partial h_i}{\partial x} = \overline{q}_i'$$
$$- (h_i - h_j) w_{ij} + (h_i - h^*) w_{ij}' \qquad (A-7)$$

By neglecting $\partial p_i/\partial t$, sonic velocity progagation is omitted from this mathematical model.

The heat transfer term $\overline{q}_i$ may be divided into two terms. The first is the heat transfer rate from the fuel surface q_i'. For steady state this term can be specified quite easily; however, for transients it depends upon the fluid temperature, fuel surface temperature and surface heat transfer coefficient. At the present time the transient heat transfer effect on the fuel is ignored in this interim description of COBRA-III. As an alternate, the value of q_i' is specified as a function of time. The second term of q_i' is the thermal conduction between adjacent subchannels. It is assumed to be proportional to the subchannel temperature difference and constant of proportionality is assumed to depend upon the subchannel geometry and fluid thermal conductivity.

By considering the thermal conduction term and all the adjacent subchannels, the energy equation can be written as

$$\frac{1}{u_i''} \frac{\partial h_i}{\partial t} + \frac{\partial h_i}{\partial x} = \frac{q_i'}{m_i} - \sum_{j=1}^{N} (t_i - t_j) \frac{c_{ij}}{m_i}$$

$$- \sum_{j=1}^{N} (h_i - h_j) \frac{w_{ij}'}{m_i} + \sum_{j=1}^{N} (h_i - h^*) \frac{w_{ij}}{m_i} \qquad \text{(A-8)}$$

where an effective enthalpy transport velocity may be defined as

$$u_i'' = \frac{m}{A\left(\rho - h_{fg} \dfrac{\partial \Psi}{\partial h}\right)} \qquad \text{(A-9)}$$

For homogeneous two-phase flow or for single-phase flow, the quantity in brackets reduces to 1 and $u_i'' = u_i$.

Axial Momentum Equation

Apply the momentum equation for a control volume to Subchannel (i) which is adjacent to Subchannel (j).
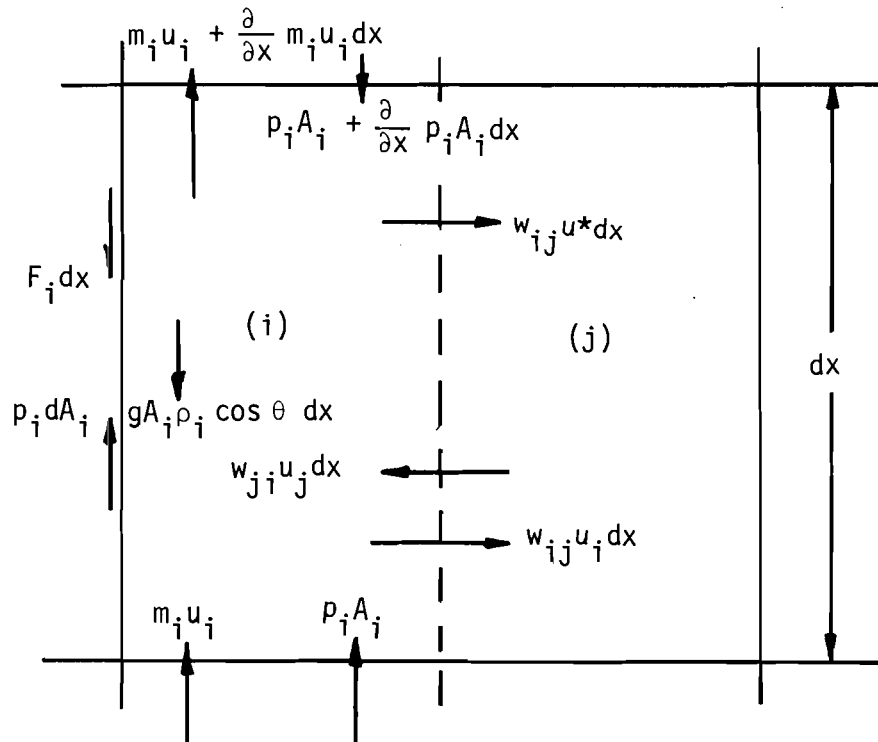
$$- F_i dx + p_i dA_i - gA_i \rho_i \cos \theta \, dx + p_i A_i - p_i A_i - \frac{\partial}{\partial x} p_i A_i dx =$$

$$\frac{\partial}{\partial t} m_i dx - m_i u_i + m_i u_i + \frac{\partial}{\partial x} m_i u_i dx$$

$$- w_{ji}' u_j dx + w_{ij}' u_i dx + w_{ij} u^* dx \ . \tag{A-10}$$

Since $w_{ij}' = w_{ji}'$, this reduces to

$$- F_i - gA_i \rho_i \cos \theta - A_i \frac{\partial p_i}{\partial x} = \frac{\partial m_i}{\partial t} + \frac{\partial}{\partial x} m_i u_i \tag{A-11}$$

$$+ (u_i - u_j) w_{ij}' + u^* w_{ij} \ .$$

By using the equations

$$u_i = \frac{m_i v_i'}{A_i} \ ; \qquad F_i = \left[\frac{A_i v_i f_i \phi_i}{2D_i} + \frac{A_i K_i v_i'}{2\Delta x} \right] \left(\frac{m_i}{A_i} \right)^2 \tag{A-12,13}$$

and Equation (A-2); Equation (A-11) may be written as

$$\frac{\partial m_i}{\partial t} - 2u_i \frac{\partial}{\partial t} \rho_i A_i + A_i \frac{\partial p_i}{\partial x} = - A_i \left(\frac{m_i}{A_i} \right)^2 \left[\frac{v_i f_i \phi_i}{2D_i} + \frac{K_i v_i'}{2\Delta x} + A_i \frac{\partial}{\partial x} \left(\frac{v_i'}{A_i} \right) \right]$$

$$- gA_i \rho_i \cos \theta - (u_i - u_j) w_{ij}'$$

$$+ (2u_i - u^*) w_{ij} \tag{A-14}$$

By considering all adjacent subchannels and assuming $\partial A / \partial t = 0$, this can be written as

$$\frac{1}{A_i} \frac{\partial}{\partial t} m_i - 2u_i \frac{\partial p_i}{\partial t} + \frac{\partial p_i}{\partial x} = - \left(\frac{m_i}{A_i} \right)^2 \left[\frac{v_i f_i \phi_i}{2D_i} + \frac{K_i v_i'}{2\Delta x} + A_i \frac{\partial}{\partial x} \left(\frac{v_i'}{A_i} \right) \right]$$

$$- g\rho_i \cos \theta - f_T \sum_{j=1}^{N} (u_i - u_j) \frac{w_{ij}'}{A_i}$$

$$+ \sum_{j=1}^{N} (2u_i - u^*) \frac{w_{ij}}{A_i} \ . \tag{A-15}$$

The factor f_T is included to help account for the imperfect analogy between the eddy diffusivity of heat and momentum.

TRANSVERSE MOMENTUM EQUATION

Consider a rectangular control volume placed in the gap between two subchannels.
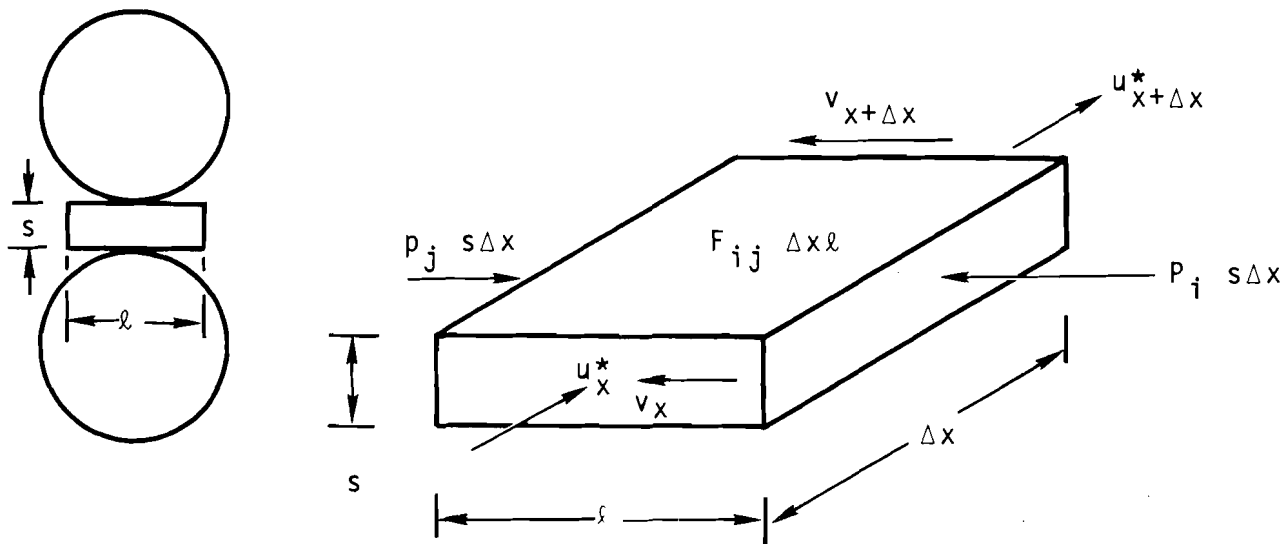
Assume that difference between crossflow momentum flux entering and leaving the control volume through the transverse surfaces is negligibly small. Applying the conservation of momentum equation to this control volume in the transverse direction gives

$$-F_{ij} \Delta x \ell - p_j s \Delta x + p_i s \Delta x = \frac{\partial \rho^*}{\partial t} s \ell \Delta x v - (\rho^* s \ell u^* v)_x$$
$$+ (\rho^* s \ell u^* v)_{x + \Delta x}. \tag{A-16}$$

By rearranging this equation and taking the limit at $\Delta x \to 0$, the following equation is obtained

$$\frac{\partial w_{ij}}{\partial t} + \frac{\partial (u^* w_{ij})}{\partial x} = \frac{s}{\ell} (p_i - p_j) - F_{ij} \tag{A-17}$$

where $w_{ij} = p*sv$. F_{ij} represents the friction and form pressure loss due to crossflow. For steady flow let

$$p_i - p_j = K \frac{p*v^2}{2} .$$ (A-18)

Therefore,

$$F = \frac{K|w|w}{2s^2 p*} \left(\frac{s}{\ell}\right)$$ (A-19)

To put this in the form used previously in COBRA-III, let

$$F = Cw \left(\frac{s}{\ell}\right)$$ (A-20)

where $C = K|w|/2s^2 p*$ and $p*$ is the density of the diversion crossflow. Presently $p*$ is assumed to be the density of the donor subchannel defined by

$$p* = \begin{Bmatrix} p_i & ; & w_{ij} > 0 \\ p_j & ; & w_{ij} < 0 \end{Bmatrix}$$ (A-21)

The loss coefficient K_{ij} consists of both the friction and the form loss components of the transverse pressure drop. The K_{ij} replaces the factor $f\ell$ in the earlier versions of COBRA. The relationship between them is given by

$$K_{ij} = \frac{f\ell}{2s_{ij}}$$ (A-22)

In the present version of COBRA-III the quantity K_{ij} is input as the constant cross flow resistance factor K. Other forms can be used by changing the function subprogram CIJ.

APPENDIX B
DERIVATION OF EQUATIONS FOR FUEL HEAT TRANSFER MODEL

APPENDIX B

DERIVATION OF EQUATIONS FOR FUEL HEAT TRANSFER MODEL

The equations of the heat transfer model were derived by using a Taylor's series approximation to the heat conduction equation

$$\rho c \frac{\partial T}{\partial t} = k \left(\frac{\partial T}{\partial r^2} + \frac{1}{r} \frac{\partial T}{\partial r} \right) + q''' \tag{B-1}$$

at each location i designated in Figure 2.

i=1

By using L' Hospital's rule and the boundary condition $\partial T/\partial r = 0$, the differential equation at $r = 0$ is[19]

$$\rho c \frac{\partial T}{\partial t} = 2k \frac{\partial^2 T}{\partial r^2} + q''' \tag{B-2}$$

From Taylor's series

$$T_2 = T_1 + \Delta r \frac{\partial T^0}{\partial r} \bigg| r = 0 + \frac{\Delta r^2}{\partial 2!} \frac{\partial T}{\partial r^2} + \cdots \tag{B-3}$$

and

$$T_1 = \bar{T}_1 + \Delta t \frac{\partial T}{\partial t} + \cdots \tag{B-4}$$

Substituting these into the differential equation gives the finite difference equation

$$\rho c \left(\frac{T_1 - \bar{T}_1}{\Delta t} \right) = 4k \left(\frac{T_2 - T_1}{\Delta r^2} \right) + q'''_1 \tag{B-5}$$

Where the overscore bar (⁻) denotes previous time.

<u>1<i<N</u>

By using the above procedure the finite difference equation can be written as

$$\rho c \; \frac{T_i - \bar{T}_i}{\Delta t} = k \left[\frac{T_{i-1} - 2T_i + 2T_{i+1}}{\Delta r^2} + \frac{T_{i+1} - T_{i-1}}{2(i-1) \Delta r^2} \right] + q_i''' \tag{B-6}$$

<u>i=N</u>

The fuel-clad interface condition is

$$-k \frac{\partial T}{\partial r} \Big|_{i=N} = h_{gap} \left(T_N - T_{N+1} \right) \tag{B-7}$$

By using Taylor's series

$$T_{N-1} = T_N - \Delta r \; \frac{\partial T}{\partial r} \Big|_{i=N} + \frac{\Delta r^2}{2} \; \frac{\partial^2 T}{\partial r^2} \Big|_{i=N} \tag{B-8}$$

and substituting this and Equation (B-7) into Equation (B-1) gives the finite difference equation

$$\rho c \left(\frac{T_N - \bar{T}_N}{\Delta t} \right) = 2k \left(\frac{T_{N-1} - T_N}{\Delta r^2} \right) + \left(\frac{2}{\Delta r} + \frac{1}{(N-1) \Delta r} \right) h_{gap} \left(T_{N-1} - T_N \right) + q_N''' \tag{B-9}$$

<u>i=N+1</u>

The cladding is treated as lumped parameter node. The conductance through the cladding is lumped with the gap heat transfer coefficient to give an effective coefficient.

$$\frac{1}{h_{gap}} = \frac{1}{h_{gap_{cond}}} + \frac{t_{clad}}{k_{clad}} \tag{B-10}$$

By performing a transient heat balance on the cladding the finite difference equation can be written as

$$(\rho c)_{clad}\left(\frac{T_{N+1} - \overline{T}_{N+1}}{\Delta t}\right) = \frac{h_{gap}}{t_{clad}} \quad \frac{r_N}{r_{N+1}} (T_N - T_{N+1})$$

$$- \frac{h_{surf}}{t_{clad}} (T_{N+1} - T_{fluid}) + q'''_{N+1} \qquad \text{(B-11)}$$

The previous set of equations are arranged into a tridiagonal system of equations and are solved by using a compact Gauss elimination routine. The same set of equations, except for the radial coordinate term $(1/r)(\partial T/\partial r)$, are used for the plate fuel model.

The fuel power density is defined in terms of the equivalent impressed flux as if there is no fuel model. The total power is

$$q = \pi D \Delta x q'' \qquad \text{(B-12)}$$

and dividing by the fuel volume gives

$$q''' = q'' \frac{\pi D \Delta x}{\frac{\pi D^2_f}{4} \Delta x} = q'' \frac{4D}{D^2_f} \qquad \text{(B-13)}$$

where D_f is the fuel pellet diameter.

The plate fuel is considered to be an equivalent unwrapped rod with its thickness equal to the radius of the fuel rod. The thickness in this case being the distance from the outer surface of the cladding to the adiabatic centerline of the plate as shown in Figure C-1. The power density is defined as for the rod where

$$q = q'' \pi D \Delta x \qquad \text{(B-14)}$$

or

$$q''' = q'' \frac{\pi D \Delta x}{\pi D \frac{D_f}{2}} = q'' \frac{2}{D_f} \qquad \text{(B-15)}$$

When using the equivalent rod as a flat plate the plate width is assumed to be the circumference πD. To account for the actual width facing a given subchannel, use the factor in COBRA (card group 8) for specifying the fraction of power from a rod to a subchannel. This fraction is defined as

$$\frac{\text{Actual width facing Subchannel}}{\pi D}$$

As an example, if the plate is used to model the wall shown in the sketch
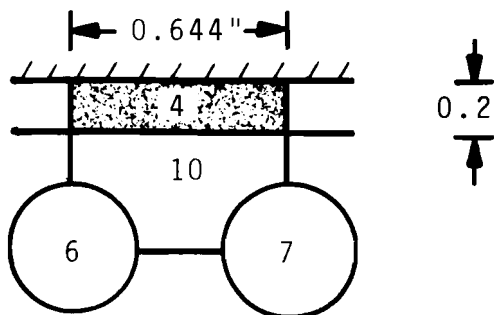
The wall is modeled as rod 4 and it is designated fuel type 2 for the code input. The diameter is $(2)(0.2) = 0.4$ inches. The fraction of power from Rod 4 to Channel 10 is $0.644/10.4.\pi) = 0.513$.

ROD   PLATE EQUIVALENT
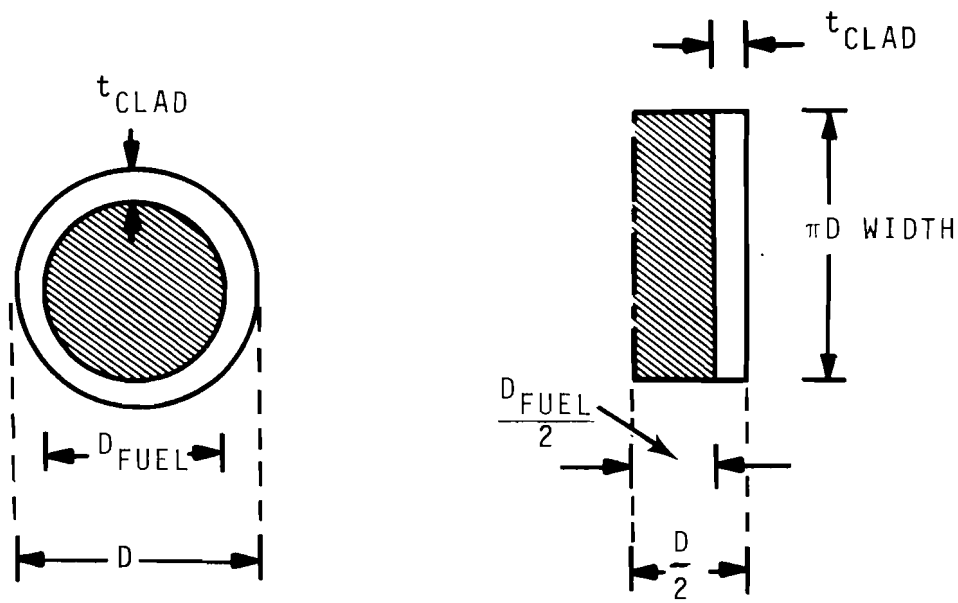
FIGURE B-1.   Rod and Plate Fuel Dimension Equivalents.

APPENDIX C
COMPUTER PROGRAM CORRELATIONS

APPENDIX C

COMPUTER PROGRAM CORRELATIONS

To carry out a solution, empirical and semiempirical correlations must be selected for input to the computer program.

Friction Factor

The friction factor correlation is assumed to be of the form[9]

$$f_i = a(R_{e_i})^b + c \tag{C-1}$$

where a, b, and c are specified constants that depend upon the subchannel roughness and geometry. Since these constants can be influenced by different subchannel roughnesses and the pitch-to-diameter ratio,[13] the program can accept up to four sets of constants that correspond to four subchannel types which may be assigned to the subchannels of the bundle. For example, subchannels next to a flow housing may be given a different friction factor from those subchannels within the bundle.

The friction factor is also corrected for wall viscosity by using the relationship[13]

$$\frac{f}{f_{iso}} = 1 + \frac{P_h}{P_w}\left[\left(\frac{\mu_{wall}}{\mu_{bulk}}\right)^{.6} - 1\right] \tag{C-2}$$

where μ_{wall} is evaluated at the wall temperature which is calculated from

$$t_{wall} = t_{bulk} + \frac{q'}{P_h h}. \tag{C-3}$$

This correction is based on the assumption of the total perimeter consisting of two regions--one heated and the other unheated and also that the heated portion has uniform heat flux. The heat transfer coefficient is calculated from

$$\frac{hD}{k} = 0.023 \left(\frac{GD}{\mu}\right)^{0.8} \left(\frac{C_p\mu}{k}\right)^{0.4} \tag{C-4}$$

where bulk fluid properties are used.

Two-Phase Friction Multiplier

Several correlations are available for the two-phase friction multiplier. Three are presently included in the program.

Homogeneous Model

$$\phi = 1.0 \quad X < 0.$$

$$\phi = \frac{\rho_f}{\rho} \quad X > 0. \tag{C-5}$$

Armand[10]

$$\phi = 1.0 \qquad\qquad\qquad\qquad \alpha \leq 0$$

$$\phi = \frac{(1-X)}{(1-\alpha)^{1.42}} \qquad\qquad 0.39 < (1-\alpha) \leq 1.0$$

$$\phi = 0.478 \, \frac{(1-X)^2}{(1-\alpha)^{2.2}} \qquad 0.1 \ < (1-\alpha) \leq 0.39$$

$$\phi = 1.730 \, \frac{(1-X)^2}{(1-\alpha)^{1.64}} \qquad 0. \ \ < (1-\alpha) \leq 0.1 \tag{C-6}$$

Polynomial Function

$$\phi = 1.0 \qquad\qquad\qquad\qquad\qquad X < 0$$

$$\phi = a_0 + a_1 X + a_2 X^2 + \ldots a_n X^n \qquad X > 0 \tag{C-7}$$

where the coefficients are supplied as input.

Spacer Loss Coefficient

The pressure drop from spacers is lumped into an effective loss coefficient which may be defined[13] in terms of all liquid flow as

$$\Delta P = \frac{K}{2\rho} \left(\frac{m}{A}\right)^2 \tag{C-8}$$

For two-phase flow, the same coefficient is used but it is modified by the two-phase specific volume for momentum. This pressure drop loss coefficient is converted to a pressure gradient loss coefficient at the location of the spacer by dividing by the calculation increment Δx; therefore,

$$K_i = \frac{K}{\Delta x} \qquad \text{(C-9)}$$

This is the coefficient used in Equation (A-12).

Void Fraction

Four ways of specifying void fraction are presently included in the program:

Homogeneous Model

$$\alpha = 0. \qquad\qquad X \leq 0.$$

$$\alpha = \frac{Xv_g}{(1-X)v_f + Xv_g} \qquad\qquad X > 0. \qquad \text{(C-10)}$$

Slip Model

$$\alpha = 0. \qquad\qquad X \leq 0.$$

$$\alpha = \frac{Xv_g}{(1-X)v_f \gamma + Xv_g} \qquad\qquad X > 0. \qquad \text{(C-11)}$$

where γ is a specified slip ratio.

Modified Armand[11]

$$\alpha = 0. \qquad\qquad X \leq 0$$

$$\alpha = \frac{(0.833+0.167X)Xv_g}{(1-X)v_f + Xv_g +} \qquad\qquad X > 0. \qquad \text{(C-12)}$$

Polynomial Function

$$\alpha = 0. \qquad\qquad X < 0.$$

$$\alpha = a_0 + a_1X + a_2X^2 + \ldots a_nX_x \qquad\qquad X > 0. \qquad \text{(C-13)}$$

Subcooled Void Fraction

Two options are presently included. Subcooled void formation may be ignored or it may be included by using Levy's subcooled void model.[12] Levy's model calculates the true quality in terms of the equilibrium quality and the quality at which bubble departure starts. It is given by

$$X = 0. \qquad\qquad X_e < X_d$$

$$X = X_e = X_d \exp\left(\frac{X_e}{X_d} - 1\right) \qquad\qquad X_e/X_d < 1 \qquad (C\text{-}14)$$

where X_e is the equilibrium quality and

$$X_d = -\frac{C_p \Delta T}{h_{fg}} \qquad (C\text{-}15)$$

$$\Delta T = \frac{q'}{P_h h} - Q P_r Y_B \qquad\qquad 0 < Y_B \le 5$$

$$\Delta T = \frac{q'}{P_h h} - 5Q\left(P_r + \log\left(1 + P_r\left(\frac{Y_B}{5} - 1\right)\right)\right) \qquad 5 < Y_B \le 30$$

$$\Delta T = \frac{q'}{P_h h} = 5Q\left(P_r + \log(1 + 5P_r) + \frac{1}{2}\log\left(\frac{Y_B}{30}\right)\right) \qquad 30 < Y_B \qquad (C\text{-}16)$$

$$Q = \frac{q'}{P_h v} C_p \sqrt{\tau_w v} \qquad (C\text{-}17)$$

$$\tau_w = \frac{fv}{8}\left(\frac{m}{A}\right)^2 \qquad (C\text{-}18)$$

$$Y_B = \frac{0.015}{\mu}\sqrt{\frac{\sigma D}{v}} \qquad (C\text{-}19)$$

The heat transfer coefficient h is calculated from Equation (C-4). The use of Levy's model may not apply universally since the use of a single phase heat transfer coefficient is not always compatible with experimental measurements.[21]

Single-Phase Turbulent Mixing

Several forms of equations for specifying the turbulent crossflow are included. The presently available forms in COBRA-III for calculating w' include:

$$w'_k = \beta s_k \bar{G} \qquad (C\text{-}20)$$

$$w'_k = a \, Re^b s_k \bar{G} \qquad (C\text{-}21)$$

$$w'_k = a \, Re^b \bar{D} \bar{G} \qquad (C\text{-}22)$$

$$w'_k = a\ Re^b\ \frac{s_k}{z_k}\ \bar{D}\ \bar{G} \tag{C-23}$$

where $Re = \dfrac{\bar{G}\ \bar{D}}{\bar{\mu}}$ (C-24)

$$\bar{D} = 4\ (A_{i(k)} + A_{j(k)})/(Pw_{i(k)} + Pw_{j(k)}) \tag{C-25}$$

$$\bar{G} = (m_{i(k)} + m_{j(k)})/(A_{i(k)}) + A_{j(k)}) \tag{C-26}$$

$$\bar{\mu} = \frac{1}{2}\ (\mu_{i(k)} + \mu_{j(k)}) \tag{C-27}$$

and a and b are input constants. Since a definitive mixing correlation does not exist and other forms are available,[5,16,17] the user should set up correlations of his choice.

Also included in the subcooled mixing is the thermal conduction. When it is included, the conduction coefficient is given by

$$c_k = \left(\frac{k_{i(k)} + k_{j(k)}}{2}\right)\ \frac{s_k}{z_k}\ K_g \tag{C-28}$$

where K_g is a geometric correction factor. Note that the distance z_k is used in both Equations (C-23) and (C-28). This is the centroid-to-centroid distance between subchannels. Care should be taken to select this value for its intended use. For example, z_k could be selected as the effective mixing distance.

Two-Phase Turbulent Mixing

Complete information concerning mixing during boiling is not available. It is known, however, that mixing is strongly dependent on quality; therefore, COBRA-III is set up to accept β as tabular function of quality. When the quality of two adjacent subchannels is different, the calculations use a quality calculated from the mean mixed enthalpy of the two subchannels.

Transient Correlations

In the present version of COBRA-III, steady state correlations are assumed to apply to transients. This assumption should be thoroughly evaluated for transient analyses.

Critical Heat Flux Correlations

Subroutine CHF presently contains two internal functions denoted CHF1 and CHF2 which calculate the critical heat flux by using the B&W-2 and W-3 heat flux correlations,[23] respectively. An input option is provided to allow the user to select either of these correlations. Reference 23 summarizes the details of these two correlations. Other correlation options can be easily set up the same way.

To implement the nonuniform axial flux factor into COBRA a finite increment integration scheme is used. Given the axial flux factor at location X_j of the form

$$F = \frac{C}{q'(X_j)(1-e^{-CX_j})} \int_{X_o}^{X_j} q''(X)e^{-(X_j-X)}dX \tag{C-29}$$

where C is a constant, consider the integral to be a summation of finite integrals each taken over the calculation increment ΔX. Over each ΔX assume a constant value of the heat flux $q''(X)$. The integral from $X - \Delta X$ to X is

$$q'(X) \int_{X-\Delta X}^{X} e^{-C(X_j-X)}dX = \frac{q''(X)}{C} e^{-CX_j}\left[e^{CX}-e^{C(X-\Delta X)}\right] \tag{C-30}$$

and the entire integral taken as a summation over the increments of ΔX from X_o to X_j is

$$F = \frac{e^{-CX_j} \displaystyle\sum_{j=J_o+1}^{J} q''(X_j)(e^{CX_j}-e^{CX_{j-1}})}{q''(X_j)[1-e^{-C(X_j-X_{J_o})}]} \tag{C-31}$$

where $X_{J_o} = 0$ is the axial location of the start of integration. For B&W-2 it is the channel inlet and for W-3 it is the start of local boiling defined by the Jens-Lottes correlation.[23]

APPENDIX D
SAMPLE PROBLEM INPUT AND OUTPUT

SAMPLE PROBLEM INPUT

```
'N XQT TCOBRA
2000
   1      SAMPLE PROBLEM FOR COBRA-IIIC WITH FUEL PIN MODEL
   1   30
  50.281.0   0.017274   8.5140    250.2    1174.1    0.491    0.3959   0.003012
 100.327.8   0.017740   4.4310    298.5    1187.2    0.410    0.3936   0.002606
 150.358.4   0.01809    3.0139    330.6    1194.1    0.369    0.3893   0.002350
 200.381.8   0.01839    2.2873    355.5    1198.3    0.345    0.3852   0.00209
 250.401.0   0.01865    1.8432    376.1    1201.1    0.326    0.3806   0.00193
 300.417.4   0.01889    1.5427    394.0    1202.9    0.313    0.3760   0.00180
 350.431.7   0.01912    1.3255    409.8    1204.0    0.301    0.3718   0.00168
 400.444.6   0.01934    1.1610    424.2    1204.6    0.290    0.3682   0.00158
 440.454.0   0.01950    1.0554    434.8    1204.8    0.283    0.3658   0.00150
 480.462.8   0.01967    0.9668    444.7    1204.8    0.278    0.3631   0.00144
 520.471.1   0.01982    0.89137   454.2    1204.5    0.273    0.3604   0.00138
 560.478.8   0.01988    0.82637   463.1    1204.2    0.269    0.3580   0.00132
 600.486.2   0.02013    0.76975   471.7    1203.7    0.264    0.3550   0.00127
 640.493.2   0.02028    0.71995   479.9    1203.0    0.260    0.3552   0.00122
 680.499.9   0.02043    0.67581   487.7    1202.3    0.255    0.3494   0.00117
 720.506.2   0.02058    0.63639   495.4    1201.4    0.252    0.3462   0.00113
 760.512.3   0.02072    0.60097   502.7    1200.4    0.248    0.3435   0.00108
 800.518.2   0.02087    0.56896   509.8    1199.4    0.245    0.3405   0.00104
 840.523.9   0.02101    0.53988   516.7    1198.2    0.242    0.3377   0.00100
 880.529.3   0.02116    0.51333   523.4    1197.0    0.240    0.3350   0.00096
 920.534.6   0.02130    0.48901   530.0    1195.7    0.237    0.3325   0.00092
 960.539.7   0.02145    0.46662   536.3    1194.4    0.234    0.3299   0.00089
1000.544.6   0.02159    0.44596   542.4    1192.9    0.232    0.3275   0.00086
1040.549.4   0.02174    0.42681   548.6    1191.4    0.229    0.3243   0.00082
1080.554.0   0.02188    0.40902   554.6    1189.9    0.227    0.3224   0.00079
1120.558.5   0.02203    0.39244   560.5    1188.2    0.225    0.3198   0.00076
1160.562.9   0.02217    0.37695   566.2    1186.6    0.223    0.3174   0.00073
1200.567.2   0.02232    0.36245   571.9    1184.8    0.221    0.3140   0.00070
1240.571.4   0.02247    0.34884   577.4    1183.0    0.219    0.3113   0.00068
1280.575.4   0.02262    0.33603   582.9    1181.2    0.217    0.3086   0.00065
   2    0      0     0    1
 .186   -.2
   3   11
   0.   .40     .1  .78     .2 1.03    .3 1.14    .4 1.22    .5 1.26
   .6 1.22     .7 1.14    .8 1.03    .9  .78    1.  .40
   4    9      9
   1.1489.8823.8823       2 .177
   2.29971.7651.765       3 .177          5 .177
   3.29971.7651.765       4 .177          6 .177
   4.18761.622.8823       7 .140
   5.1489.8823.8823       6 .177
   6.29971.7651.765       7 .177          8 .177
   7.18761.622.8823       9 .140
   8.1489.8823.8823       9 .177
   9.23092.1991.103
   7    2      4     2
 .199     1  .399    1  .599    2  .799     1
   1   1.
   2   1.
   3   1.
   4   1.
   5   1.
   6   1.
   7   1.
   8   1.
   9   1.
   1   1.
   2   1.
   3   1.
   4   1.
   5   1.
   6   1.
   7   1.
   8   1.
   9   1.
   8   10    10     7    1
   1  .562   .8     1 .125
   2  .562   .9     1 .250     2 .250
   3  .562   .95    2 .250     3 .250
   4  .562  1.      3 .250     4 .250
   5  .562   .9     1 .125     2 .250     5 .125
   6  .562   .95    2 .250     3 .250     5 .250    6 .250
   7  .562  1.0     3 .250     4 .250     6 .250    7 .250
   8  .562  1.      5 .125     6 .250     8 .125
   9  .562  1.1     6 .250     7 .250     8 .250    9 .250
  10  .562  1.2     8 .125     9 .375
 2.0   .08 640. .502  8.8 .076 405. .0301000.
   9    2      2
 .5   0. 120.          60    4   2.   30
  10
 .02
  11    1                        8
    1000.           505.        1.0        .3
 0.0  1.0   0.5   1.2  1.0  1.5  1.5  0.5  2.0  .23  3.0  .08
 4.0   .04  50.   .02
  12    2      1     1
   8
  10
     0
```

```
    2          7-PIN WIRE WRAP SAMPLE PROBLEM FOR COBRA-IIIC
  1   30
52E-4500.0      .01801    999999.      303.76    2204.83      .9235      45.43    .01238
17E-4550.0      .01801    999998.      319.44    2212.94      .8591      44.60    .01219
48E-3600.0      .01828    999997.      335.01    2220.52      .8038      43.79    .01200
12E-2650.0      .01842    409866.      350.49    2227.58      .7558      42.98    .011813
30E-2700.0      .01856    178122.      365.88    2234.13      .7138      42.18    .011623
66E-2750.0      .01870     83102.      381.19    2240.18      .6767      41.39    .011432
14E-1800.0      .01885     41266.      396.43    2245.77      .6437      40.62    .011242
24E-1840.0      .01897     24533.      408.58    2249.94      .6198      40.00    .011089
40E-1880.0      .01909     15060.      420.69    2253.87      .5980      39.39    .010937
65E-1920.0      .01921      9519.      432.77    2257.57      .5778      38.79    .010784
82E-1940.0      .01927      7645.      438.80    2259.35      .5683      38.50    .010708
10E+0960.0      .01933      6180.      444.83    2261.09      .5592      38.20    .010632
13E+0980.0      .01940      5026.      450.85    2262.78      .5504      37.91    .010556
16E+01000.      .01946      4111.      456.86    2264.44      .5419      37.61    .010480
20E+01020.      .01952      3382.      462.87    2266.06      .5338      37.42    .010403
24E+01040.      .01959      2798.      468.88    2267.65      .5259      37.03    .010327
29E+01060.      .01965      2326.      474.88    2269.22      .5183      36.74    .010251
35E+01080.      .01971      1944.      480.88    2270.75      .5110      36.46    .010175
47E+01100.      .01978      1632.      486.88    2272.27      .5004      36.03    .010060
54E+01120.      .01985      1376.      492.87    2273.76      .4970      35.89    .010022
61E+01140.      .01991      1166.      498.87    2275.24      .4904      35.61    .009946
72E+01160.      .01998       992.0     504.86    2276.70      .4840      35.33    .009870
85E+01180.      .02005       847.5     510.86    2278.15      .4778      35.05    .009794
10E+11200.      .02011       726.9     516.85    2279.60      .4717      34.78    .009718
21E+11300.      .02046       356.3     546.85    2286.72      .4442      33.42    .009337
42E+11400.      .02082       189.1     576.95    2293.86      .4204      32.11    .008956
78E+11500.      .02119       107.4     607.21    2301.10      .3995      30.84    .008575
14E+21600.      .02157        64.63    637.70    2308.47      .3811      29.61    .008194
15E+21619.      .02165        59.34    643.40    2310.19      .3779      29.38    .008123
12E+32145.      .02388     8.52153     810.92    2351.67      .3094      23.64    .006119
    2    0      0    0     1
 .316 -.25
    3    2
    0   1.    1.   1.
    4   12   12
    1.0146.3613.3613      2 .056          6 .056          7 .056
    2.0146.3613.3613      3 .056          8 .056
    3.0146.3613.3613      4 .056          9 .056
    4.0146.3613.3613      5 .056         10 .056
    5.0146.3613.3613      6 .056         11 .056
    6.0146.3613.3613     12 .056
    7.0312.9499.4813      8 .056         12 .056
    8.0312.9499.4813      9 .056
    9.0312.9499.4813     10 .056
   10.0312.9499.4813     11 .056
   11.0312.9499.4813     12 .056
   12.0312.9499.4813
    7    1   18      2    0
   12.        .230        .056
    1  .06 .250-.750
    2  .06-.084 .584
    3  .06-.417 .917
    4  .06 .417-.917
    5  .06-.584 .084
    6  .06 .584-.084
    7  .06-.750 .250
    8  .06 .750-.250
    9  .06 .417-.917
   10  .06-.417 .917
   11  .06 .584-.084
   12  .06 .750-.250
   13  .06 .250
   14  .06-.084
   15  .06 .417
   16  .06 .584
   17  .06 .750
   18  .06 .917
    0    1    0    0    1    1    0    0    0
    1    2
    8    7    7
    1  .23   1.    1 .167    2 .167    3 .167    4 .167    5 .167    6 .167
    2  .23   1.    1 .167    6 .167    7 .333   12 .333
    3  .23   1.    1 .167    2 .167    7 .333    8 .333
    4  .23   1.    2 .167    3 .167    8 .333    9 .333
    5  .23   1.    3 .167    4 .167    9 .333   10 .333
    6  .23   1.    4 .167    5 .167   10 .333   11 .333
    7  .23   1.    5 .167    6 .167   11 .333   12 .333
    9
  .5       36.   0.   36    0    0   30
   10    0    0    0
  .02
   11    1    1
          60.       800.       3.        .5
   12    1    2
  1 7

  ' FIN                                                    X
```

FLUID PROPERTY TABLE

P	T	VF	VG	HF	HG	VISC.	KF	SIGMA
50.0	281.00	.01727	8.51400	250.20	1174.10	.49100	.39590	.00301
100.0	327.80	.01774	4.43100	298.50	1187.20	.41000	.39360	.00261
150.0	358.40	.01809	3.01390	330.60	1194.10	.36900	.38930	.00235
200.0	381.80	.01839	2.28730	355.50	1198.30	.34500	.38520	.00209
250.0	401.00	.01865	1.84320	376.10	1201.10	.32600	.38060	.00193
300.0	417.40	.01889	1.54270	394.00	1202.90	.31300	.37600	.00180
350.0	431.70	.01912	1.32550	409.80	1204.00	.30100	.37180	.00168
400.0	444.60	.01934	1.16100	424.20	1204.60	.29000	.36820	.00158
440.0	454.00	.01950	1.05540	434.80	1204.80	.28300	.36580	.00150
480.0	462.80	.01967	.96680	444.70	1204.80	.27800	.36310	.00144
520.0	471.10	.01982	.89137	454.20	1204.50	.27300	.36040	.00138
560.0	478.80	.01988	.82637	463.10	1204.20	.26900	.35800	.00132
600.0	486.20	.02013	.76975	471.70	1203.70	.26400	.35500	.00127
640.0	493.20	.02028	.71995	479.90	1203.00	.26000	.35520	.00122
680.0	499.90	.02043	.67581	487.70	1202.30	.25500	.34940	.00117
720.0	506.20	.02058	.63639	495.40	1201.40	.25200	.34620	.00113
760.0	512.30	.02072	.60097	502.70	1200.40	.24800	.34350	.00108
800.0	518.20	.02087	.56896	509.80	1199.40	.24500	.34050	.00104
840.0	523.90	.02101	.53988	516.70	1198.20	.24200	.33770	.00100
880.0	529.30	.02116	.51333	523.40	1197.00	.24000	.33500	.00096
920.0	534.60	.02130	.48901	530.00	1195.70	.23700	.33250	.00092
960.0	539.70	.02145	.46662	536.30	1194.40	.23400	.32990	.00089
1000.0	544.60	.02159	.44596	542.40	1192.90	.23200	.32750	.00086
1040.0	549.40	.02174	.42681	548.60	1191.40	.22900	.32430	.00082
1080.0	554.00	.02188	.40902	554.60	1189.90	.22700	.32240	.00079
1120.0	558.50	.02203	.39244	560.50	1188.20	.22500	.31980	.00076
1160.0	562.90	.02217	.37695	566.20	1186.60	.22300	.31740	.00073
1200.0	567.20	.02232	.36245	571.90	1184.80	.22100	.31400	.00070
1240.0	571.40	.02247	.34884	577.40	1183.00	.21900	.31130	.00068
1280.0	575.40	.02262	.33603	582.90	1181.20	.21700	.30860	.00065

FRICTION FACTOR CORRELATION
    CHANNEL TYPE 1   FRICT = .186*RE**(-.200) + -.0000
    WALL VISCOSITY CORRECTION TO FRICTION FACTOR IS INCLUDED

TWO-PHASE FLOW CORRELATIONS
    NO SUBCOOLED VOID CORRELATION
    HOMOGENEOUS BULK VOID MODEL
    HOMOGENEOUS MODEL FRICTION MULTIPLIER

HEAT FLUX DISTRIBUTION
  X/L   RELATIVE FLUX
  .000   .400
  .100   .780
  .200   1.030

D-3

```
.300   1.140
.400   1.220
.500   1.260
.600   1.220
.700   1.140
.800   1.030
.900    .730
1.000   .400
```

SUBCHANNEL INPUT DATA

CHANNEL NO.	TYPE	AREA (SQ-IN)	WETTE PERIM. (IN)	HEATED PERIM. (IN)	HYDRAULIC DIAMETER (IN)	(ADJACENT CHANNEL NO., SPACING, CENTROID DISTANCE)			
1	1	.148900	.862300	.882300	.675054	(2, .177,-.000)	(-0,-.000,-.000)	(-0,-.000,-.000)	(-0,-.000,-.000)
2	1	.299700	1.765000	1.765000	.679207	(3, .177,-.000)	(5, .177,-.000)	(-0,-.000,-.000)	(-0,-.000,-.000)
3	1	.299700	1.765000	1.765000	.679207	(4, .177,-.000)	(6, .177,-.000)	(-0,-.000,-.000)	(-0,-.000,-.000)
4	1	.187600	1.622000	.882300	.462639	(7, .140,-.000)	(-0,-.000,-.000)	(-0,-.000,-.000)	(-0,-.000,-.000)
5	1	.148900	.862300	.882300	.675054	(6, .177,-.000)	(8, .177,-.000)	(-0,-.000,-.000)	(-0,-.000,-.000)
6	1	.299700	1.765000	1.765000	.679207	(7, .140,-.000)	(-0,-.000,-.000)	(-0,-.000,-.000)	(-0,-.000,-.000)
7	1	.187600	1.622000	.982300	.462639	(9, .177,-.000)	(-0,-.000,-.000)	(-0,-.000,-.000)	(-0,-.000,-.000)
8	1	.148900	.862300	.882300	.675054	(9, .177,-.000)	(-0,-.000,-.000)	(-0,-.000,-.000)	(-0,-.000,-.000)
9	1	.230900	2.199000	1.103000	.420009	(-0,-.000,-.000)	(-0,-.000,-.000)	(-0,-.000,-.000)	(-0,-.000,-.000)

SPACER DATA

SPACER TYPE NO.   1   1   2   1
LOCATION (X/L)   .199   .199   .599   .799

SPACER TYPE 1

CHANNEL NO.	DRAG COEFF.	CHANNEL NO.	DRAG COEFF.	CHANNEL NO.	DRAG COEFF.	CHANNEL NO.	DRAG COEFF.
1	1.000	2	1.000	3	1.000	4	1.000
5	1.000	6	1.000	7	1.000	8	1.000
9	1.000						

SPACER TYPE 2

CHANNEL NO.	DRAG COEFF.	CHANNEL NO.	DRAG COEFF.	CHANNEL NO.	DRAG COEFF.	CHANNEL NO.	DRAG COEFF.
1	1.000	2	1.000	3	1.000	4	1.000
5	1.000	6	1.000	7	1.000	8	1.000
9	1.000						

ROD INPUT DATA

ROD NO.	TYPE NO.	DIA (IN)	RADIAL POWER FACTOR	FRACTION OF POWER TO ADJACENT CHANNELS (ADJ. CHANNEL NO.)				
1	1	.5620	.3000	.1250(1)	-.0000(-0)	-.0000(-0)	-.0000(-0)	-.0000(-0)
2	1	.5620	.9000	.2500(1)	.2500(2)	-.0000(-0)	-.0000(-0)	-.0000(-0)
3	1	.5620	.9500	.2500(2)	.2500(3)	-.0000(-0)	-.0000(-0)	-.0000(-0)
4	1	.5620	1.0000	.2500(3)	.2500(4)	-.0000(-0)	-.0000(-0)	-.0000(-0)
5	1	.5620	.9000	.1250(1)	.2500(2)	.1250(5)	-.0000(-0)	-.0000(-0)

```
  6   1   .5620    .9500       .2500( 2)     .2500( 3)     .2500( 5)     .2500( 6)    -.0000(-0)    -.0000(-0)
  7   1   .5620   1.0000       .2500( 3)     .2500( 4)     .2500( 6)     .2500( 7)    -.0000(-0)    -.0000(-0)
  8   1   .5620   1.0000       .1250( 5)     .2500( 6)     .1250( 8)    -.0000(-0)    -.0000(-0)    -.0000(-0)
  9   1   .5620   1.1000       .2500( 6)     .2500( 7)     .2500( 8)     .2500( 9)    -.0000(-0)    -.0000(-0)
 10   1   .5620   1.2000       .1250( 8)     .3750( 9)    -.0000(-0)    -.0000(-0)    -.0000(-0)    -.0000(-0)
```

THERMAL PROPERTIES FOR FUEL MATERIAL   7 RADIAL FUEL NODES

		FUEL PROPERTIES				CLAD PROPERTIES			
TYPE	COND.	SP. HEAT	DENSITY	DIA.	COND.	SP. HEAT	DENSITY	THICK.	GAP COND.
NO.	(B/HR-FT-F)	(B/LB-F)	(LB/FT3)	(IN.)	(B/HR-FT-F)	(B/LB-F)	(LB/FT3)	(IN.)	(B/HR-FT2-F)
1	2.00	.0800	640.0	.5020	8.80	.0760	405.0	.0300	1000.00

```
CALCULATION PARAMETERS
  CROSSFLOW RESISTANCE,KIJ       .500
  MOMENTUM TURBULENT FACTOR      .0000
  PARAMETER, (S/L)               .500
  CHANNEL LENGTH              120.00 INCHES
  CHANNEL ORIENTATION           -.0 DEGREES
  NUMBER OF AXIAL NODES          60
  NODE LENGTH                  2.000 INCHES
  NUMBER OF TIME STEPS            4
  TOTAL TRANSIENT TIME         2.000 SECONDS
  TIME STEP                     .5000 SECONDS
  ALLOWABLE ITERATIONS           30
  FLOW CONVERGENCE FACTOR      .10000-02


MIXING CORRELATIONS
  SUBCOOLED MIXING,   BETA =  .0200
  BOILING MIXING, BETA IS ASSUMMED SAME AS SUBCOOLED


OPERATING CONDITIONS
  SYSTEM PRESSURE     =    1000.0 PSIA
  INLET ENTHALPY      =     493.9 BTU/LB
  AVG. MASS VELOCITY =      1.000 MILLION LB/(HR-SQFT)
  INLET TEMPERATURE   =     505.0 DEGREES F
  AVG. HEAT FLUX      =    .300000 MILLION BTU/(HR-SQFT)
   UNIFORM INLET TEMPERATURE
   UNIFORM INLET MASS VELOCITY
   FORCING FUNCTION FOR HEAT FLUX
     TIME     HEAT FLUX
     (SEC)     FACTOR
     .0000     1.0000
     .5000     1.2000
    1.0000     1.5000
    1.5000      .5000
    2.0000      .2300
    3.0000      .0800
    4.0000      .0400
   50.0000      .0200
```

CHANNEL EXIT SUMMARY RESULTS
CASE 1   SAMPLE PROBLEM FOR COBRA-IIIC WITH FUEL PIN MODEL   DATE 01 MAR 73   TIME 17:20:46

MASS BALANCE - -   ENERGY BALANCE - -
  MASS FLOW IN   .37652+01 LB/SEC   FLOW ENERGY IN   .18598+04 BTU/SEC
  MASS FLOW OUT   .37652+01 LB/SEC   ENERGY ADDED   .75066+03 BTU/SEC
  MASS FLOW ERROR -.37253-05 LB/SEC   FLOW ENERGY OUT   .26108+04 BTU/SEC
                                                          ENERGY ERROR   .32362-00 BTU/SEC

CHANNEL (NO.)	ENTHALPY (BTU/LB)	TEMPERATURE (DEG-F)	DENSITY (LB/FT3)	EQUIL QUALITY	VOID FRACTION	FLOW (LB/SEC)	MASS FLUX (MLB/HR-FT2)
1	681.18	544.60	8.92	.213	.349	.3071	1.0690
2	686.50	544.60	9.65	.222	.855	.6126	1.0597
3	690.53	544.60	8.46	.228	.959	.6070	1.0500
4	697.39	544.60	8.61	.223	.356	.3356	.9273
5	692.26	544.60	8.36	.230	.361	.3003	1.0454
6	697.77	544.60	8.13	.239	.366	.5932	1.0347
7	695.28	544.60	8.24	.235	.364	.3300	.9120
8	706.68	544.60	7.77	.253	.875	.2916	1.0151
9	706.25	544.60	7.76	.252	.874	.3829	.8597

D-6

CHANNEL RESULTS
CASE   1   SAMPLE PROBLEM FOR COBRA-IIIC WITH FUEL PIN MODEL

BUNDLE AVERAGED RESULTS

DISTANCE (IN.)	DELTA-P (PSI)	ENTHALPY (BTU/LB)	TEMPERATURE (DEG-F)	DENSITY (LB/CU-FT)	EQUIL QUALITY	VOID FRACTION	FLOW (LB/SEC)	MASS FLUX (MLB/HR-FT2)
.0	6.99	493.93	505.00	48.66	.000	.000	3.7652	1.0000
4.0	6.85	497.01	507.55	48.52	.000	.000	3.7652	1.0000
8.0	6.72	500.94	510.83	48.34	.000	.000	3.7652	1.0000
12.0	6.59	505.70	514.79	48.12	.000	.000	3.7652	1.0000
16.0	6.46	511.16	519.33	47.85	.000	.000	3.7652	1.0000
20.0	6.33	517.18	524.29	47.57	.000	.000	3.7652	1.0000
24.0	6.02	523.75	529.58	47.24	.000	.000	3.7652	1.0000
28.0	5.89	530.72	535.18	46.91	.000	.000	3.7652	1.0000
32.0	5.76	537.93	541.01	46.52	.000	.000	3.7652	1.0000
36.0	5.60	545.33	544.60	42.47	.005	.087	3.7652	1.0000
40.0	5.41	553.08	544.60	35.11	.016	.254	3.7652	1.0000
44.0	5.22	560.92	544.60	29.79	.028	.375	3.7652	1.0000
48.0	4.72	568.92	544.60	25.79	.041	.466	3.7652	1.0000
52.0	4.54	577.09	544.60	22.68	.053	.536	3.7652	1.0000
56.0	4.35	585.33	544.60	20.22	.066	.592	3.7652	1.0000
60.0	4.17	593.66	544.60	18.22	.079	.638	3.7652	1.0000
64.0	3.99	602.00	544.60	16.58	.092	.675	3.7652	1.0000
68.0	3.80	610.24	544.60	15.22	.104	.706	3.7652	1.0000
72.0	3.03	618.38	544.60	14.08	.117	.731	3.7652	1.0000
76.0	2.84	626.42	544.60	13.11	.129	.753	3.7652	1.0000
80.0	2.65	634.26	544.60	12.29	.141	.772	3.7652	1.0000
84.0	2.47	641.93	544.60	11.57	.153	.788	3.7652	1.0000
88.0	2.28	649.39	544.60	10.96	.164	.802	3.7652	1.0000
92.0	2.09	656.60	544.60	10.42	.176	.815	3.7652	1.0000
96.0	1.06	663.58	544.60	9.95	.186	.825	3.7652	1.0000
100.0	.87	670.14	544.60	9.54	.196	.834	3.7652	1.0000
104.0	.69	676.15	544.60	9.19	.206	.842	3.7652	1.0000
108.0	.51	681.62	544.60	8.90	.214	.849	3.7652	1.0000
112.0	.33	686.38	544.60	8.66	.221	.854	3.7652	1.0000
116.0	.16	690.31	544.60	8.47	.227	.859	3.7652	1.0000
120.0	.00	693.39	544.60	8.33	.232	.862	3.7652	1.0000

CHANNEL RESULTS
CASE   1   SAMPLE PROBLEM FOR COBRA-IIIC WITH FUEL PIN MODEL   DATE 01 MAR 73   TIME 17:20:46

TIME = -.00000 SECONDS   DATA FOR CHANNEL 8

DISTANCE	DELTA-P	ENTHALPY	TEMPERATURE	DENSITY	EQUIL	VOID	FLOW	MASS FLUX
(IN.)	(PSI)	(BTU/LB)	(DEG-F)	(LB/CU-FT)	QUALITY	FRACTION	(LB/SEC)	(MLB/HR-FT2)
.0	6.99	493.93	505.00	48.66	.000	.000	.2872	1.0000
4.0	6.85	497.53	507.98	48.49	.000	.000	.2897	1.0085
8.0	6.72	501.99	511.71	48.29	.000	.000	.2917	1.0156
12.0	6.59	507.33	516.15	48.04	.000	.000	.2935	1.0217
16.0	6.46	513.38	521.16	47.75	.000	.000	.2951	1.0273
20.0	6.33	519.98	526.55	47.43	.000	.000	.2965	1.0322
24.0	6.02	527.15	532.31	47.08	.000	.000	.2923	1.0176
28.0	5.89	534.79	538.47	46.70	.000	.000	.2943	1.0245
32.0	5.76	542.63	544.60	46.00	.000	.007	.2931	1.0206
36.0	5.60	551.02	544.60	36.75	.013	.217	.2707	.9426
40.0	5.41	559.96	544.60	30.26	.027	.364	.2747	.9563
44.0	5.22	568.82	544.60	25.76	.041	.466	.2782	.9686
48.0	4.72	577.73	544.60	22.40	.054	.543	.2748	.9568
52.0	4.54	586.81	544.60	19.78	.068	.602	.2776	.9666
56.0	4.35	595.87	544.60	17.71	.082	.649	.2797	.9738
60.0	4.17	604.90	544.60	16.03	.096	.687	.2814	.9796
64.0	3.99	613.33	544.60	14.67	.110	.718	.2828	.9845
68.0	3.80	622.57	544.60	13.53	.123	.744	.2840	.9888
72.0	3.03	631.16	544.60	12.58	.136	.765	.2788	.9706
76.0	2.84	639.65	544.60	11.76	.149	.784	.2808	.9777
80.0	2.65	647.88	544.60	11.06	.162	.800	.2825	.9834
84.0	2.47	655.85	544.60	10.46	.174	.814	.2840	.9886
88.0	2.28	663.52	544.60	9.94	.186	.825	.2853	.9932
92.0	2.09	670.89	544.60	9.43	.198	.836	.2865	.9976
96.0	1.06	677.96	544.60	9.09	.208	.845	.2814	.9797
100.0	.87	684.54	544.60	8.75	.219	.852	.2836	.9874
104.0	.69	690.57	544.60	8.46	.228	.859	.2853	.9933
108.0	.51	695.93	544.60	8.21	.236	.865	.2869	.9990
112.0	.33	700.47	544.60	8.02	.243	.869	.2885	1.0044
116.0	.16	704.05	544.60	7.87	.248	.872	.2900	1.0098
120.0	.00	706.68	544.60	7.77	.253	.875	.2916	1.0151

CASE   1   SAMPLE PROBLEM FOR COBRA-IIIC WITH FUEL PIN MODEL   DATE 01 MAR 73   TIME 17:20:46

TIME = -.00000 SECONDS   TEMPERATURE DATA FOR ROD 10,   FUEL TYPE 1

DISTANCE (IN.)	FLUX (MBTU/HR-FT2)	DNBR	CHANNEL	TEMPERATURE(F) T(1)	T(2)	T(3)	T(4)	T(5)	T(6)	T(7)	T(8)
.0	.0000	.000	0	.0	.0	.0	.0	.0	.0	.0	.0
4.0	.1782	.000	0	1841.3	1812.3	1725.3	1580.5	1377.6	1116.8	798.0	541.9
8.0	.2238	.000	0	2186.0	2149.6	2040.4	1858.4	1603.7	1276.1	875.8	554.1
12.0	.2694	.000	0	2531.5	2487.6	2356.2	2137.2	1830.5	1436.2	954.3	567.1
16.0	.3033	.000	0	2790.0	2740.7	2592.8	2346.2	2000.9	1557.0	1014.5	578.5
20.0	.3333	.000	0	3020.0	2965.8	2803.2	2532.2	2152.8	1665.0	1068.8	589.6
24.0	.3633	.000	0	3250.3	3191.2	3014.0	2718.6	2305.1	1773.4	1123.5	601.2
28.0	.3807	.000	0	3386.6	3324.7	3138.9	2829.4	2396.0	1838.9	1157.9	610.6
32.0	.3939	.000	0	3491.6	3427.5	3235.4	2915.1	2466.7	1890.2	1185.6	619.4
36.0	.4071	.000	0	3594.5	3528.3	3329.7	2998.7	2535.3	1939.5	1211.3	626.0
40.0	.4176	.000	0	3673.1	3605.2	3401.5	3062.0	2586.6	1975.4	1228.4	628.1
44.0	.4272	.000	0	3745.1	3675.6	3467.2	3119.8	2633.6	2008.3	1244.2	630.0
48.0	.4368	.000	0	3817.0	3746.0	3532.9	3177.7	2680.5	2041.2	1259.9	632.0
52.0	.4428	.000	0	3861.9	3789.9	3573.9	3213.9	2709.8	2061.8	1269.7	633.2
56.0	.4476	.000	0	3897.9	3825.1	3606.8	3242.0	2733.3	2078.2	1277.6	634.1
60.0	.4524	.000	0	3933.9	3860.3	3639.6	3271.6	2756.8	2094.7	1285.4	635.1
64.0	.4500	.000	0	3915.9	3842.7	3623.2	3257.3	2745.0	2086.5	1281.5	634.6
68.0	.4452	.000	0	3879.9	3807.5	3590.3	3228.4	2721.6	2070.0	1273.6	633.6
72.0	.4404	.000	0	3844.0	3772.3	3557.5	3199.4	2698.1	2053.6	1265.8	632.7
76.0	.4320	.000	0	3781.0	3710.8	3500.1	3148.8	2657.0	2024.8	1252.0	631.0
80.0	.4224	.000	0	3709.1	3640.4	3434.4	3090.9	2610.1	1991.9	1236.3	629.1
84.0	.4128	.000	0	3637.2	3570.1	3363.7	3033.0	2563.1	1959.0	1220.6	627.2
88.0	.4005	.000	0	3545.0	3479.9	3284.5	2958.9	2503.0	1916.8	1200.4	624.7
92.0	.3873	.000	0	3446.1	3383.2	3194.2	2879.3	2438.5	1871.6	1178.8	622.1
96.0	.3741	.000	0	3347.3	3286.4	3103.9	2799.7	2373.9	1826.4	1157.2	619.4
100.0	.3483	.000	0	3154.0	3097.3	2927.4	2644.2	2247.7	1738.0	1115.0	614.3
104.0	.3183	.000	0	2929.2	2877.5	2722.2	2463.4	2101.0	1635.2	1065.8	608.3
108.0	.2383	.000	0	2704.5	2657.6	2516.9	2282.5	1954.4	1532.4	1016.7	602.3
112.0	.2466	.000	0	2392.1	2352.0	2231.7	2031.2	1750.4	1389.5	948.4	593.9
116.0	.2010	.000	0	2050.4	2017.8	1919.7	1756.3	1527.5	1233.3	873.8	584.8
120.0	.1554	.000	0	1708.8	1683.5	1607.7	1481.4	1304.5	1077.1	799.1	575.7

ITERATIONS =   7

TIME = 1.00000 SECONDS   DATA FOR CHANNEL 8

DISTANCE (IN.)	DELTA-P (PSI)	ENTHALPY (BTU/LB)	TEMPERATURE (DEG-F)	DENSITY (LB/CU-FT)	EQUIL QUALITY	VOID FRACTION	FLOW (LB/SEC)	MASS FLUX (MLB/HR-FT2)
.0	7.42	493.93	505.00	48.66	.000	.000	.2872	1.0000
4.0	7.28	497.74	508.16	48.49	.000	.000	.2897	1.0085
8.0	7.15	502.45	512.09	48.27	.000	.000	.2917	1.0156
12.0	7.02	508.06	516.76	48.00	.000	.000	.2935	1.0217
16.0	6.89	514.40	522.00	47.70	.000	.000	.2951	1.0273
20.0	6.76	521.31	527.61	47.35	.000	.000	.2965	1.0323
24.0	6.45	528.79	533.62	47.01	.000	.000	.2923	1.0178
28.0	6.32	536.73	540.05	46.60	.000	.000	.2943	1.0246
32.0	6.19	544.38	544.60	43.09	.004	.073	.2814	.9796
36.0	6.01	553.85	544.60	34.41	.018	.276	.2715	.9454
40.0	5.81	563.07	544.60	28.51	.032	.404	.2770	.9643
44.0	5.62	572.21	544.60	24.37	.046	.498	.2810	.9783
48.0	5.08	581.41	544.60	21.26	.060	.569	.2780	.9680
52.0	4.89	590.77	544.60	18.82	.074	.624	.2813	.9793
56.0	4.70	600.10	544.60	16.88	.089	.668	.2838	.9879
60.0	4.50	609.39	544.60	15.32	.103	.703	.2858	.9950
64.0	4.31	618.57	544.60	14.03	.117	.733	.2875	1.0009
68.0	4.11	627.56	544.60	12.96	.131	.757	.2890	1.0062
72.0	3.27	636.38	544.60	12.06	.144	.777	.2841	.9889
76.0	3.07	645.09	544.60	11.29	.158	.795	.2863	.9968
80.0	2.87	653.54	544.60	10.63	.171	.810	.2882	1.0033
84.0	2.67	661.71	544.60	10.06	.183	.823	.2898	1.0091
88.0	2.46	669.57	544.60	9.56	.196	.834	.2913	1.0143
92.0	2.26	677.12	544.60	9.13	.207	.844	.2927	1.0192
96.0	1.15	684.34	544.60	8.76	.218	.852	.2877	1.0017
100.0	.94	691.07	544.60	8.43	.229	.860	.2901	1.0099
104.0	.74	697.22	544.60	8.16	.238	.866	.2919	1.0164
108.0	.55	702.67	544.60	7.93	.246	.871	.2937	1.0225
112.0	.36	707.27	544.60	7.74	.253	.875	.2954	1.0284
116.0	.17	710.89	544.60	7.60	.259	.878	.2971	1.0343
120.0	.00	713.51	544.60	7.51	.263	.881	.2987	1.0400

CASE   1   SAMPLE PROBLEM FOR COBRA-IIIC WITH FUEL PIN MODEL   DATE 01 MAR 73   TIME 17:21:51

TIME = 1.00000 SECONDS   TEMPERATURE DATA FOR ROD 10,   FUEL TYPE 1

DISTANCE (IN.)	FLUX (MBTU/HR-FT2)	DNBR	CHANNEL	TEMPERATURE(F) T(1)	T(2)	T(3)	T(4)	T(5)	T(6)	T(7)	T(8)
.0	.0000	.000	0	.0	.0	.0	.0	.0	.0	.0	.0
4.0	.1893	.000	0	1877.4	1848.4	1761.4	1616.1	1412.1	1147.7	817.5	544.2
8.0	.2376	.000	0	2231.4	2195.0	2085.6	1903.2	1647.0	1315.0	900.4	557.1
12.0	.2859	.000	0	2586.1	2542.3	2410.7	2191.1	1882.7	1483.0	984.0	570.8
16.0	.3218	.000	0	2851.6	2802.2	2654.1	2406.9	2059.7	1609.7	1047.9	582.8
20.0	.3536	.000	0	3087.6	3033.4	2870.6	2598.9	2217.4	1722.8	1105.5	594.5
24.0	.3853	.000	0	3324.6	3264.9	3087.4	2791.3	2375.5	1836.5	1163.6	606.6
28.0	.4036	.000	0	3463.8	3401.9	3215.9	2905.6	2469.8	1905.0	1200.0	616.5
32.0	.4175	.000	0	3571.5	3507.4	3315.0	2994.0	2543.1	1958.7	1229.3	625.6
36.0	.4325	.000	0	3677.1	3610.8	3412.0	3080.1	2614.1	2010.0	1255.7	631.1
40.0	.4437	.000	0	3757.9	3689.9	3485.9	3145.5	2667.5	2047.8	1274.1	633.3
44.0	.4539	.000	0	3831.3	3762.2	3553.6	3205.3	2716.3	2082.4	1290.9	635.4
48.0	.4641	.000	0	3905.6	3834.5	3621.2	3265.1	2765.1	2116.9	1307.6	637.4
52.0	.4705	.000	0	3951.0	3879.7	3663.4	3302.5	2795.6	2138.5	1318.1	638.7
56.0	.4756	.000	0	3988.7	3915.9	3697.2	3332.4	2820.0	2155.8	1326.5	639.7
60.0	.4807	.000	0	4025.7	3952.0	3731.0	3362.3	2844.4	2173.1	1334.9	640.7
64.0	.4781	.000	0	4007.2	3934.0	3714.1	3347.3	2832.2	2164.5	1330.7	640.2
68.0	.4730	.000	0	3970.3	3897.8	3680.3	3317.4	2807.8	2147.2	1322.3	639.2
72.0	.4679	.000	0	3933.3	3861.7	3646.5	3287.5	2783.4	2129.9	1313.9	638.2
76.0	.4590	.000	0	3868.7	3798.4	3587.4	3235.2	2740.7	2099.7	1299.2	636.4
80.0	.4488	.000	0	3794.8	3726.1	3519.7	3175.4	2691.9	2065.1	1282.5	634.4
84.0	.4386	.000	0	3721.0	3653.8	3452.1	3115.6	2643.1	2030.5	1265.7	632.3
88.0	.4255	.000	0	3626.3	3561.1	3365.5	3039.0	2580.6	1986.3	1244.2	629.7
92.0	.4115	.000	0	3524.8	3461.7	3272.5	2956.0	2513.5	1938.8	1221.2	626.9
96.0	.3975	.000	0	3423.2	3362.3	3179.5	2874.6	2446.4	1891.2	1198.1	624.1
100.0	.3701	.000	0	3224.7	3168.0	2997.8	2713.9	2315.2	1798.4	1153.0	618.6
104.0	.3382	.000	0	2993.8	2942.0	2786.5	2527.1	2162.7	1690.4	1100.6	612.2
108.0	.3063	.000	0	2763.0	2716.1	2575.2	2340.1	2010.2	1582.4	1048.2	605.9
112.0	.2620	.000	0	2442.1	2402.0	2281.5	2080.5	1798.2	1432.3	975.4	597.0
116.0	.2136	.000	0	2091.2	2058.5	1960.3	1796.5	1566.4	1268.1	895.7	587.3
120.0	.1651	.000	0	1740.4	1715.1	1639.1	1512.5	1334.6	1104.0	816.1	577.6

ITERATIONS =   6

CHANNEL RESULTS
CASE   1   SAMPLE PROBLEM FOR COBRA-IIIC WITH FUEL PIN MODEL   DATE   01 MAR 73   TIME 17:23:05

TIME = 2.00000 SECONDS   DATA FOR CHANNEL 8

DISTANCE (IN.)	DELTA-P (PSI)	ENTHALPY (BTU/LB)	TEMPERATURE (DEG-F)	DENSITY (LB/CU-FT)	EQUIL QUALITY	VOID FRACTION	FLOW (LB/SEC)	MASS FLUX (MLB/HR-FT2)
.0	6.45	493.93	505.00	48.66	.000	.000	.2872	1.0000
4.0	6.32	497.30	507.79	48.50	.000	.000	.2897	1.0085
8.0	6.19	501.51	511.31	48.32	.000	.000	.2917	1.0156
12.0	6.06	506.58	515.52	48.07	.000	.000	.2935	1.0217
16.0	5.93	512.35	520.31	47.80	.000	.000	.2950	1.0271
20.0	5.80	518.69	525.50	47.50	.000	.000	.2964	1.0320
24.0	5.49	525.59	531.06	47.16	.000	.000	.2921	1.0171
28.0	5.36	532.99	537.02	46.79	.000	.000	.2941	1.0240
32.0	5.23	540.62	543.17	46.41	.000	.000	.2950	1.0270
36.0	5.09	548.67	544.60	38.94	.010	.167	.2712	.9440
40.0	4.91	557.42	544.60	31.86	.023	.328	.2711	.9440
44.0	4.73	566.11	544.60	26.98	.036	.439	.2736	.9525
48.0	4.26	574.85	544.60	23.39	.050	.520	.2691	.9370
52.0	4.09	583.78	544.60	20.56	.064	.584	.2710	.9436
56.0	3.93	592.72	544.60	18.38	.077	.634	.2722	.9478
60.0	3.76	601.63	544.60	16.60	.091	.674	.2731	.9510
64.0	3.59	610.45	544.60	15.15	.105	.707	.2739	.9535
68.0	3.42	619.11	544.60	13.96	.118	.734	.2745	.9558
72.0	2.72	627.62	544.60	12.96	.131	.757	.2688	.9360
76.0	2.55	636.07	544.60	12.09	.144	.777	.2704	.9414
80.0	2.38	644.26	544.60	11.36	.157	.793	.2716	.9457
84.0	2.21	652.20	544.60	10.73	.169	.807	.2728	.9496
88.0	2.04	659.66	544.60	10.18	.181	.820	.2738	.9532
92.0	1.87	667.21	544.60	9.71	.192	.831	.2747	.9565
96.0	.95	674.28	544.60	9.29	.203	.840	.2695	.9384
100.0	.78	680.89	544.60	8.93	.213	.846	.2715	.9451
104.0	.62	686.95	544.60	8.63	.222	.855	.2729	.9502
108.0	.45	692.35	544.60	8.37	.231	.861	.2743	.9551
112.0	.30	696.96	544.60	8.17	.238	.866	.2757	.9598
116.0	.14	700.63	544.60	8.01	.243	.869	.2770	.9645
120.0	.00	703.38	544.60	7.90	.247	.872	.2783	.9691

TIME = 2.00000 SECONDS   TEMPERATURE DATA FOR ROD 10,   FUEL TYPE 1

DISTANCE (IN.)	FLUX (MBTU/HR-FT2)	DNBR	CHANNEL	TEMPERATURE(F) T(1)	T(2)	T(3)	T(4)	T(5)	T(6)	T(7)	T(8)
.0	.0000	.000	0	.0	.0	.0	.0	.0	.0	.0	.0
4.0	.1658	.000	0	1811.4	1782.4	1695.1	1549.6	1345.8	1085.3	775.5	539.3
8.0	.2084	.000	0	2148.5	2112.0	2002.4	1819.6	1563.7	1236.6	847.5	550.7
12.0	.2510	.000	0	2486.4	2442.4	2310.5	2090.5	1782.5	1388.6	920.2	562.9
16.0	.2828	.000	0	2739.3	2689.8	2541.3	2293.6	1946.8	1503.4	976.0	573.6
20.0	.3109	.000	0	2964.2	2909.8	2746.6	2474.4	2093.3	1606.1	1026.5	584.2
24.0	.3391	.000	0	3189.5	3130.2	2952.4	2655.6	2240.3	1709.1	1077.4	595.2
28.0	.3555	.000	0	3322.9	3260.7	3074.4	2763.4	2328.2	1771.6	1109.5	604.2
32.0	.3680	.000	0	3425.7	3361.4	3168.6	2846.9	2396.5	1820.7	1135.6	612.7
36.0	.3786	.000	0	3526.3	3459.9	3260.6	2928.1	2462.6	1867.5	1159.9	620.3
40.0	.3884	.000	0	3603.2	3535.1	3330.6	2989.6	2512.1	1901.6	1175.8	622.3
44.0	.3973	.000	0	3673.6	3603.9	3394.7	3045.8	2557.3	1932.8	1190.3	624.1
48.0	.4062	.000	0	3743.9	3672.6	3458.7	3102.0	2602.5	1964.0	1204.8	625.8
52.0	.4118	.000	0	3787.8	3715.6	3498.8	3137.1	2630.8	1983.5	1213.8	627.0
56.0	.4163	.000	0	3823.0	3749.9	3530.8	3165.2	2653.4	1999.1	1221.1	627.9
60.0	.4208	.000	0	3858.1	3784.3	3562.8	3193.3	2676.0	2014.7	1228.4	628.8
64.0	.4185	.000	0	3840.5	3767.1	3546.8	3179.3	2664.7	2006.9	1224.7	628.3
68.0	.4141	.000	0	3805.4	3732.8	3514.8	3151.2	2642.1	1991.3	1217.5	627.4
72.0	.4096	.000	0	3770.2	3698.4	3482.8	3123.1	2619.5	1975.7	1210.2	626.5
76.0	.4018	.000	0	3708.7	3638.2	3426.7	3073.9	2579.9	1948.4	1197.5	625.0
80.0	.3929	.000	0	3638.4	3569.5	3362.7	3017.0	2534.7	1917.2	1183.0	623.2
84.0	.3839	.000	0	3568.1	3500.7	3298.6	2961.5	2489.5	1886.0	1168.5	621.4
88.0	.3725	.000	0	3478.0	3412.7	3216.6	2889.5	2431.5	1846.0	1149.9	619.1
92.0	.3602	.000	0	3381.3	3318.1	3128.5	2812.2	2369.3	1803.2	1130.0	616.6
96.0	.3479	.000	0	3284.6	3223.6	3040.4	2734.9	2307.1	1760.3	1110.0	614.2
100.0	.3239	.000	0	3095.7	3038.8	2868.3	2583.8	2185.6	1676.4	1071.0	609.4
104.0	.2960	.000	0	2875.9	2824.0	2668.2	2408.2	2044.2	1578.9	1025.7	603.8
108.0	.2681	.000	0	2656.2	2609.2	2468.0	2232.5	1902.9	1481.4	980.3	598.2
112.0	.2293	.000	0	2350.8	2310.5	2189.8	1988.4	1706.4	1345.9	917.3	590.5
116.0	.1869	.000	0	2016.8	1984.0	1885.6	1721.4	1491.6	1197.8	848.4	582.0
120.0	.1445	.000	0	1682.8	1657.4	1581.4	1454.4	1276.8	1049.6	779.5	573.5

ITERATIONS =   8

D-13

FLUID PROPERTY TABLE

P	T	VF	VG	HF	HG	VISC.	KF	SIGMA
.0	500.00	.01801	999999.01000	303.76	2204.83	.92350	45.43000	.01238
.0	550.00	.01801	999998.01000	319.44	2212.94	.85910	44.60000	.01219
.0	600.00	.01828	999997.00000	335.01	2220.52	.80380	43.79000	.01200
.0	650.00	.01842	409866.01000	350.49	2227.58	.75580	42.98000	.01181
.0	700.00	.01856	178122.00000	365.88	2234.13	.71380	42.18000	.01162
.0	750.00	.01870	83152.00100	381.19	2240.18	.67670	41.39000	.01143
.0	800.00	.01885	41266.00000	396.43	2245.77	.64370	40.62000	.01124
.0	840.00	.01897	24533.00100	408.58	2249.94	.61980	40.00000	.01109
.0	880.00	.01909	15060.00000	420.69	2253.87	.59800	39.39000	.01094
.1	920.00	.01921	9519.00000	432.77	2257.57	.57780	38.79000	.01078
.1	940.00	.01927	7635.00000	438.80	2259.35	.56830	38.50000	.01071
.1	960.00	.01933	6130.00000	444.83	2261.09	.55920	38.20000	.01063
.1	980.00	.01940	5026.00000	450.85	2262.78	.55040	37.91000	.01056
.2	1000.00	.01946	4111.00000	456.86	2264.44	.54190	37.61000	.01048
.2	1020.00	.01952	3392.00000	462.87	2266.06	.53380	37.42000	.01040
.2	1040.00	.01959	2798.00000	468.88	2267.65	.52590	37.03000	.01033
.3	1060.00	.01965	2326.00000	474.88	2269.22	.51830	36.74000	.01025
.4	1080.00	.01971	1944.00000	480.88	2270.75	.51100	36.46000	.01017
.5	1100.00	.01978	1632.00000	486.88	2272.27	.50040	36.03000	.01006
.5	1120.00	.01985	1376.00000	492.87	2273.76	.49700	35.89000	.01002
.6	1140.00	.01991	1166.00000	498.87	2275.24	.49040	35.61000	.00995
.7	1160.00	.01998	992.00000	504.86	2276.70	.48400	35.33000	.00987
.8	1180.00	.02005	847.50000	510.86	2278.15	.47780	35.05000	.00979
1.0	1200.00	.02011	726.90000	516.85	2279.60	.47170	34.78000	.00972
2.1	1300.00	.02046	356.30000	546.85	2286.72	.44420	33.42000	.00934
4.2	1400.00	.02082	189.10000	576.95	2293.86	.42040	32.11000	.00896
7.8	1500.00	.02119	107.40000	607.21	2301.10	.39950	30.84000	.00857
14.0	1600.00	.02157	64.63000	637.70	2308.47	.38110	29.61000	.00819
15.0	1619.00	.02165	59.34000	643.40	2310.19	.37790	29.38000	.00812
120.0	2145.00	.02388	8.52153	810.92	2351.67	.30940	23.64000	.00612

FRICTION FACTOR CORRELATION
    CHANNEL TYPE 1   FRICT = .316*RE**(-.250) + -.0000
    WALL VISCOSITY CORRECTION TO FRICTION FACTOR IS INCLUDED

TWO-PHASE FLOW CORRELATIONS
    NO SUBCOOLED VOID CORRELATION
    HOMOGENEOUS BULK VOID MODEL
    HOMOGENEOUS MODEL FRICTION MULTIPLIER

HEAT FLUX DISTRIBUTION
   X/L   RELATIVE FLUX
  .000   1.000
 1.000   1.000

ROD INPUT DATA
ROD   TYPE   DIA   RADIAL POWER   FRACTION OF POWER TO ADJACENT CHANNELS (ADJ. CHANNEL NO.)
NO.   NO.   (IN)   FACTOR

ROD NO.	TYPE NO.	DIA (IN)	RADIAL POWER FACTOR					
1	1	.2300	1.0000	.1670(1)	.1670(2)	.1670(3)	.1670(4)	.1670(5)	.1670(6)
2	1	.2300	1.0000	.1670(1)	.1670(6)	.3330(7)	.3330(12)	-.0000(-0)	-.0000(-0)
3	1	.2300	1.0000	.1670(1)	.1670(2)	.3330(8)	.3330(7)	-.0000(-0)	-.0000(-0)
4	1	.2300	1.0000	.1670(2)	.1670(3)	.3330(9)	.3330(8)	-.0000(-0)	-.0000(-0)
5	1	.2300	1.0000	.1670(3)	.1670(4)	.3330(9)	.3330(10)	-.0000(-0)	-.0000(-0)
6	1	.2300	1.0000	.1670(4)	.1670(5)	.3330(10)	.3330(11)	-.0000(-0)	-.0000(-0)
7	1	.2300	1.0000	.1670(5)	.1670(6)	.3330(11)	.3330(12)	-.0000(-0)	-.0000(-0)

CALCULATION PARAMETERS
CROSSFLOW RESISTANCE,KIJ   .500
MOMENTUM TURBULENT FACTOR   -.0000
PARAMETER, (S/L)   .500
CHANNEL LENGTH   36.00 INCHES
CHANNEL ORIENTATION   .0 DEGREES
NUMBER OF AXIAL NODES   36
NODE LENGTH   1.000 INCHES
NUMBER OF TIME STEPS   0
TOTAL TRANSIENT TIME   .000 SECONDS
TIME STEP   .0000 SECONDS
ALLOWABLE ITERATIONS   30
FLOW CONVERGENCE FACTOR   .10000-02

MIXING CORRELATIONS
SUBCOOLED MIXING,   BETA = .0200
BOILING MIXING, BETA IS ASSUMED SAME AS SUBCOOLED

OPERATING CONDITIONS
SYSTEM PRESSURE   =   64.0 PSIA
INLET ENTHALPY   =   395.4 BTU/LB
AVG. MASS VELOCITY   =   3.000 MILLION LB/(HR-SQFT)
INLET TEMPERATURE   =   804.0 DEGREES F
AVG. HEAT FLUX   =   .50000 MILLION BTU/(HR-SQFT)
UNIFORM INLET TEMPERATURE
FLOWS SPLIT TO GIVE EQUAL PRESSURE GRADIENT

CHANNEL EXIT SUMMARY RESULTS
CASE   2   7-PIN WIRE WRAP SAMPLE PROBLEM FOR COBRA-IIIC   DATE 01 MAR 73   TIME 17:26:17

MASS BALANCE - -
MASS FLOW IN   .15903+01 LB/SEC
MASS FLOW OUT   .15903+01 LB/SEC
MASS FLOW ERROR   -.10232-05 LB/SEC

ENERGY BALANCE - -
FLOW ENERGY IN   .63043+03 BTU/SEC
ENERGY ADDED   .17554+03 BTU/SEC
FLOW ENERGY OUT   .80621+03 BTU/SEC
ENERGY ERROR   .23890-00 BTU/SEC

CHANNEL (NO.)	ENTHALPY (BTU/LB)	TEMPERATURE (DEG-F)	DENSITY (LB/FT3)	EQUIL QUALITY	VOID FRACTION	FLOW (LB/SEC)	MASS FLUX (MLB/FR-FT2)
1	509.90	1176.80	49.90	.000	.000	.0983	3.4918
2	507.20	1167.79	49.98	.000	.000	.0791	2.8075
3	509.92	1176.80	49.90	.000	.000	.0949	3.3680
4	510.96	1180.32	49.87	.000	.000	.0834	2.9614
5	511.64	1182.59	49.86	.000	.000	.1023	3.6326
6	509.60	1175.81	49.91	.000	.000	.0838	2.9772
7	503.97	1157.01	50.06	.000	.000	.1761	2.9261
8	503.46	1155.32	50.09	.000	.000	.1902	3.1603
9	505.35	1161.65	50.04	.000	.000	.1840	3.0578
10	507.16	1167.68	49.98	.000	.000	.1799	2.9885
11	507.13	1167.58	49.93	.000	.000	.1631	2.7104
12	505.73	1162.91	50.02	.000	.000	.1551	2.5774

BUNDLE AVERAGED RESULTS

DISTANCE (IN.)	DELTA-P (PSI)	ENTHALPY (BTU/LB)	TEMPERATURE (DEG-F)	DENSITY (LB/CU-FT)	EQUIL QUALITY	VOID FRACTION	FLOW (LB/SEC)	MASS FLUX (MLB/HR-FT2)
.0	11.45	396.43	800.00	53.05	.000	.000	1.5903	3.0000
1.0	11.10	399.49	810.09	52.97	.000	.000	1.5903	3.0000
2.0	10.81	402.58	820.24	52.88	.000	.000	1.5903	3.0000
3.0	10.47	405.62	830.26	52.80	.000	.000	1.5903	3.0000
4.0	10.18	408.75	840.56	52.71	.000	.000	1.5903	3.0000
5.0	9.83	411.76	850.50	52.63	.000	.000	1.5903	3.0000
6.0	9.54	414.87	860.79	52.54	.000	.000	1.5903	3.0000
7.0	9.20	417.90	870.80	52.46	.000	.000	1.5903	3.0000
8.0	8.90	421.03	881.13	52.38	.000	.000	1.5903	3.0000
9.0	8.56	424.04	891.10	52.29	.000	.000	1.5903	3.0000
10.0	8.26	427.16	901.44	52.21	.000	.000	1.5903	3.0000
11.0	7.92	430.19	911.44	52.13	.000	.000	1.5903	3.0000
12.0	7.62	433.33	921.85	52.04	.000	.000	1.5903	3.0000
13.0	7.28	436.33	931.80	51.96	.000	.000	1.5903	3.0000
14.0	6.99	439.45	942.17	51.88	.000	.000	1.5903	3.0000
15.0	6.65	442.46	952.15	51.80	.000	.000	1.5903	3.0000
16.0	6.35	445.60	962.55	51.71	.000	.000	1.5903	3.0000
17.0	6.01	448.60	972.53	51.62	.000	.000	1.5903	3.0000
18.0	5.71	451.73	982.93	51.53	.000	.000	1.5903	3.0000
19.0	5.37	454.74	992.94	51.44	.000	.000	1.5903	3.0000
20.0	5.08	457.87	1003.36	51.36	.000	.000	1.5903	3.0000
21.0	4.74	460.87	1013.36	51.23	.000	.000	1.5903	3.0000
22.0	4.44	464.00	1023.77	51.20	.000	.000	1.5903	3.0000
23.0	4.10	467.01	1033.78	51.11	.000	.000	1.5903	3.0000
24.0	3.80	470.14	1044.21	51.02	.000	.000	1.5903	3.0000
25.0	3.46	473.15	1054.22	50.94	.000	.000	1.5903	3.0000
26.0	3.17	476.28	1064.66	50.86	.000	.000	1.5903	3.0000
27.0	2.83	479.28	1074.68	50.78	.000	.000	1.5903	3.0000
28.0	2.54	482.42	1085.12	50.69	.000	.000	1.5903	3.0000
29.0	2.20	485.42	1095.14	50.60	.000	.000	1.5903	3.0000
30.0	1.90	488.55	1105.59	50.51	.000	.000	1.5903	3.0000
31.0	1.56	491.56	1115.63	50.42	.000	.000	1.5903	3.0000
32.0	1.27	494.69	1126.08	50.34	.000	.000	1.5903	3.0000
33.0	.93	497.70	1136.09	50.25	.000	.000	1.5903	3.0000
34.0	.63	500.83	1146.54	50.17	.000	.000	1.5903	3.0000
35.0	.29	503.83	1156.57	50.08	.000	.000	1.5903	3.0000
36.0	.00	506.96	1167.02	49.99	.000	.000	1.5903	3.0000

CHANNEL RESULTS
CASE 2   7-PIN WIRE WRAP SAMPLE PROBLEM FOR COBRA-IIIC   DATE 01 MAR 73   TIME 17:26:17

TIME = -.00000 SECONDS   DATA FOR CHANNEL 1

DISTANCE (IN.)	DELTA-P (PSI)	ENTHALPY (BTU/LB)	TEMPERATURE (DEG-F)	DENSITY (LB/CU-FT)	EQUIL QUALITY	VOID FRACTION	FLOW (LB/SEC)	MASS FLUX (MLB/HR-FT2)
.0	11.46	396.43	800.00	53.05	.000	.000	.0931	3.3074
1.0	11.27	400.18	812.34	52.95	.000	.000	.0914	3.2466
2.0	10.81	403.90	824.60	52.84	.000	.000	.0763	2.7094
3.0	10.37	408.23	838.84	52.72	.000	.000	.0758	2.6903
4.0	10.18	411.72	850.39	52.63	.000	.000	.0945	3.3564
5.0	9.75	414.24	858.69	52.56	.000	.000	.0986	3.5010
6.0	9.53	417.32	866.86	52.48	.000	.000	.0764	2.7131
7.0	9.09	420.71	880.07	52.38	.000	.000	.0740	2.6287
8.0	8.90	423.06	887.84	52.32	.000	.000	.0884	3.1395
9.0	8.66	424.32	892.01	52.28	.000	.000	.0877	3.1150
10.0	8.27	427.19	901.54	52.21	.000	.000	.0734	2.6051
11.0	8.01	432.00	920.11	52.06	.000	.000	.0694	2.4654
12.0	7.64	436.35	931.89	51.96	.000	.000	.0935	3.3200
13.0	7.41	438.30	938.33	51.91	.000	.000	.0940	3.3372
14.0	6.98	442.12	951.03	51.81	.000	.000	.0811	2.8795
15.0	6.52	446.75	966.39	51.67	.000	.000	.0825	2.9290
16.0	6.35	450.16	977.69	51.57	.000	.000	.1015	3.6035
17.0	6.92	452.59	985.80	51.50	.000	.000	.1049	3.7236
18.0	5.71	455.53	995.57	51.42	.000	.000	.0826	2.9323
19.0	5.26	458.52	1005.52	51.34	.000	.000	.0793	2.8175
20.0	5.06	460.75	1012.94	51.29	.000	.000	.0943	3.3469
21.0	4.84	461.30	1016.44	51.26	.000	.000	.0931	3.3063
22.0	4.44	464.23	1024.69	51.19	.000	.000	.0781	2.7734
23.0	4.19	469.74	1042.87	51.02	.000	.000	.0739	2.6239
24.0	3.82	473.17	1054.31	50.93	.000	.000	.0975	3.4617
25.0	3.62	475.21	1061.09	50.89	.000	.000	.0975	3.4621
26.0	3.17	478.99	1073.70	50.73	.000	.000	.0837	2.9722
27.0	2.70	483.62	1089.12	50.65	.000	.000	.0845	3.0009
28.0	2.54	487.09	1100.70	50.55	.000	.000	.1028	3.6517
29.0	2.11	489.62	1109.15	50.47	.000	.000	.1056	3.7504
30.0	1.90	492.51	1116.78	50.39	.000	.000	.0832	2.9528
31.0	1.44	495.37	1128.39	50.31	.000	.000	.0797	2.8308
32.0	1.27	497.56	1135.63	50.26	.000	.000	.0948	3.3653
33.0	1.03	493.56	1138.97	50.23	.000	.000	.0936	3.3248
34.0	.54	501.03	1147.20	50.16	.000	.000	.0787	2.7957
35.0	.36	506.49	1165.39	50.00	.000	.000	.0746	2.6497
36.0	.00	509.90	1170.80	49.90	.000	.000	.0983	3.4918

CHANNEL RESULTS
CASE   2   7-PIN WIRE WRAP SAMPLE PROBLEM FOR COBRA-IIIC   DATE 01 MAR 73   TIME 17:26:17

TIME = -.00000 SECONDS   DATA FOR CHANNEL   7

DISTANCE (IN.)	DELTA-P (PSI)	ENTHALPY (BTU/LB)	TEMPERATURE (DEG-F)	DENSITY (LB/CU-FT)	EQUIL QUALITY	VOID FRACTION	FLOW (LB/SEC)	MASS FLUX (MLB/HR-FT2)
.0	11.46	396.43	800.00	53.05	.000	.000	.1719	2.8556
1.0	11.28	399.13	808.89	52.98	.000	.000	.1628	2.7049
2.0	10.81	402.02	818.42	52.90	.000	.000	.1513	2.5134
3.0	10.36	405.15	828.70	52.81	.000	.000	.1519	2.5247
4.0	10.17	408.26	838.95	52.72	.000	.000	.1595	2.6506
5.0	9.72	411.24	848.79	52.64	.000	.000	.1668	2.7713
6.0	9.53	414.09	858.19	52.55	.000	.000	.1785	2.9661
7.0	9.13	416.33	865.59	52.50	.000	.000	.1862	3.0942
8.0	8.90	418.78	873.68	52.44	.000	.000	.1859	3.0896
9.0	8.61	421.18	881.63	52.37	.000	.000	.1868	3.1034
10.0	8.27	423.94	890.78	52.29	.000	.000	.1918	3.1873
11.0	8.04	427.16	901.43	52.21	.000	.000	.1888	3.1374
12.0	7.63	430.65	912.99	52.11	.003	.000	.1768	2.9368
13.0	7.42	434.34	926.85	52.00	.000	.000	.1699	2.8229
14.0	6.98	438.43	938.76	51.90	.000	.000	.1552	2.5788
15.0	6.53	442.20	951.28	51.80	.000	.000	.1562	2.5950
16.0	6.35	445.96	963.77	51.70	.000	.000	.1633	2.7128
17.0	5.89	449.11	974.21	51.60	.000	.000	.1701	2.8268
18.0	5.71	452.05	983.98	51.51	.000	.000	.1799	2.9899
19.0	5.30	454.21	991.19	51.46	.000	.000	.1867	3.1016
20.0	5.07	456.36	998.32	51.40	.000	.000	.1843	3.0618
21.0	4.79	458.06	1004.00	51.36	.000	.000	.1842	3.0607
22.0	4.45	460.55	1012.29	51.29	.000	.000	.1897	3.1518
23.0	4.22	463.64	1022.57	51.21	.000	.000	.1870	3.1075
24.0	3.81	467.19	1034.36	51.10	.000	.000	.1758	2.9203
25.0	3.60	471.46	1048.60	50.98	.000	.000	.1695	2.8155
26.0	3.17	475.12	1060.79	50.88	.000	.000	.1553	2.5807
27.0	2.71	478.93	1073.51	50.79	.000	.000	.1566	2.6024
28.0	2.53	482.71	1086.10	50.66	.000	.000	.1637	2.7205
29.0	2.08	485.85	1096.58	50.59	.000	.000	.1706	2.8338
30.0	1.90	488.81	1106.44	50.50	.000	.000	.1802	2.9945
31.0	1.49	490.96	1113.62	50.43	.000	.000	.1869	3.1049
32.0	1.26	493.10	1120.77	50.37	.000	.000	.1843	3.0618
33.0	.98	494.80	1126.44	50.33	.000	.000	.1841	3.0588
34.0	.64	497.30	1134.78	50.27	.000	.000	.1896	3.1501
35.0	.42	500.41	1145.14	50.18	.000	.000	.1870	3.1064
36.0	.00	503.97	1157.01	50.08	.000	.000	.1761	2.9261

DIVERSION CROSSFLOW BETWEEN ADJACENT CHANNELS, W(I,J), (LB/SEC-FT).

CASE   2   7-PIN WIRE WRAP SAMPLE PROBLEM FOR COBRA-IIIC   DATE 01 MAR 73   TIME 17:26:17

X	W(1, 2)	W(1, 6)	W(1, 7)	W(2, 3)	W(2, 8)	W(3, 4)	W(3, 9)	W(4, 5)	W(4,10)	W(5, 6)
.0	.00000	.00000	.00000	.00000	.00000	.00000	.00000	.00000	.00000	.00000
1.0	.00179	.03756	-.01878	.06016	.01089	.03336	.02490	.02563	.03640	-.05719
2.0	.55299	-.32155	-.04994	-.05087	.32947	-.31589	.41824	-.03533	-.46091	.47346
3.0	.33975	-.30116	-.03218	.02067	.32670	-.26226	.30986	.08601	-.32302	.33170
4.0	.28225	-.55495	.04766	.30902	.19044	-.30722	.31021	-.26131	.17161	.06508
5.0	.20096	-.40787	.07814	.12940	.17232	-.19058	.31503	-.22823	.10845	.14588
6.0	.56013	-.08879	-.22503	.31598	.07304	.26300	.24069	-.32384	.30729	-.30398
7.0	.41945	-.17849	-.21242	.30488	.10362	.09451	.21447	-.20592	.30539	-.25594
8.0	.11414	.26392	-.55069	.62290	-.22340	.31692	.09226	.23815	.25257	-.35039
9.0	.18717	.21953	-.39843	.45079	-.21035	.30593	.12427	.07364	.22857	-.22549
10.0	-.28085	.32454	.12863	.11568	-.58340	.62984	-.22804	.31984	.08467	.24677
11.0	-.23170	.20040	.07048	.19059	-.41597	.45680	-.21354	.30947	.12008	.08289
12.0	-.33035	-.23756	.27908	-.28223	.12639	.11855	-.57945	.62138	-.22650	.30741
13.0	-.20865	-.07321	.27598	-.22183	.06171	.20305	-.40833	.46959	-.21710	.29820
14.0	.23579	-.31474	.23353	-.33539	.29297	-.29084	.13142	.11476	-.58675	.61750
15.0	.06278	-.29953	.21985	-.23460	.29867	-.25368	.06751	.17323	-.41228	.44457
16.0	.30286	-.62312	.09222	.22538	.24741	-.35085	.29291	-.27957	.11759	.12641
17.0	.28398	-.45101	.12641	.04299	.23267	-.23964	.28493	-.25105	.06846	.19486
18.0	.61164	-.11747	-.22678	.30632	.06855	.22561	.24860	-.34933	.29542	-.28916
19.0	.43755	-.19180	-.20697	.27694	.12737	.05062	.21908	-.24492	.29976	-.24296
20.0	.10537	.26130	-.56567	.60068	-.22669	.30628	.07794	.22653	.24864	-.34915
21.0	.17557	.23838	-.40129	.42012	-.20322	.28444	.10324	.04502	.23206	-.22972
22.0	-.28295	.32942	.13358	.10344	-.56897	.60098	-.22718	.30829	.07582	.24539
23.0	-.24377	.21401	.08025	.16608	-.39935	.42705	-.21902	.28044	.11503	.07807
24.0	-.33303	-.24112	.29097	-.28198	.12970	.10072	-.56523	.59481	-.22733	.30533
25.0	-.22221	-.07257	.29461	-.25242	.08124	.17009	-.40964	.41572	-.20569	.29365
26.0	.22899	-.30830	.24487	-.34443	.29257	-.28519	.11958	.10405	-.57168	.60017
27.0	.05764	-.29421	.22687	-.24039	.29948	-.24947	.05862	.16488	-.40268	.43305
28.0	.30698	-.61984	.09294	.22615	.24786	-.34701	.29193	-.28102	.11740	.12331
29.0	.28786	-.44826	.12706	.04518	.23328	-.23647	.28446	-.25164	.06869	.19388
30.0	.61590	-.11914	-.22720	.30742	.08983	.22377	.24904	-.34906	.29295	-.28312
31.0	.44110	-.19204	-.20762	.27897	.12870	.04993	.21984	-.24465	.29777	-.23772
32.0	.10640	.28291	-.56992	.60184	-.22735	.30677	.07643	.22662	.24634	-.34502
33.0	.17771	.23983	-.40385	.42176	-.20373	.28565	.10272	.04605	.23029	-.22733
34.0	-.28403	.33006	.13279	.10448	-.56942	.60039	-.22703	.30733	.07504	.24276
35.0	-.24545	.21476	.08000	.16667	-.39974	.42671	-.21850	.28009	.11435	.07643
36.0	-.33557	-.24254	.29354	-.28314	.12522	.09894	-.56405	.59272	-.22675	.30536

DIVERSION CROSSFLOW BETWEEN ADJACENT CHANNELS, W(I,J), (LB/SEC-FT).

CASE   2   7-PIN WIRE WRAP SAMPLE PROBLEM FOR COBRA-IIIC   DATE 01 MAR 73   TIME 17:26:17

X	W(5,11)	W(6,12)	W(7, 8)	W(7,12)	W(8, 9)	W(9,10)	W(10,11)	W(11,12)
.0	.00000	.00000	.00000	.00000	.00000	.00000	.00000	.00000
1.0	.01905	.00023	.03480	.05518	.06403	.05924	-.01914	-.06896
2.0	-.23294	-.04069	.32717	-.23888	.70951	1.02239	.63247	.31056
3.0	-.21476	.01046	.16130	-.20170	.52320	.82457	.51119	.23804
4.0	-.50202	-.23569	.21994	-.26324	.56270	.98828	1.08012	.61671
5.0	-.36076	-.22283	.19629	-.20536	.34416	.71417	.84146	.49173
6.0	.14062	-.59554	.23220	-.59791	.21999	.62203	1.03621	1.13668
7.0	.08712	-.42729	.17250	-.47749	.18954	.38920	.75055	.87940
8.0	.28451	.11632	.56965	-1.11698	.22078	.22701	.63362	1.05859
9.0	.28302	.05817	.45764	-.86605	.15586	.19970	.40096	.76531
10.0	.23410	.30264	1.13249	-1.06445	.56958	.22689	.22450	.62623
11.0	.21242	.29979	.87592	-.76933	.45583	.16379	.19890	.39456
12.0	.08633	.24183	1.05953	-.63555	1.11696	.56718	.22341	.22333
13.0	.13473	.22041	.76687	-.40864	.86117	.45421	.15695	.20506
14.0	-.22559	.07942	.63494	-.22525	1.06231	1.12714	.57393	.22916
15.0	-.22450	.11486	.39975	-.19183	.77442	.87480	.46439	.15837
16.0	-.58083	-.22667	.22504	-.21806	.64287	1.07095	1.11703	.56063
17.0	-.42847	-.21107	.19561	-.15173	.41135	.77367	.87301	.44240
18.0	.11517	-.58903	.21966	-.56436	.22485	.64460	1.07107	1.11758
19.0	.04698	-.42024	.15828	-.44606	.20270	.40783	.78190	.86198
20.0	.29044	.11701	.57530	-1.11235	.23014	.22575	.64369	1.06554
21.0	.27520	.06231	.45893	-.85940	.17428	.19909	.41506	.76577
22.0	.22944	.29565	1.12023	-1.05248	.57990	.23317	.22588	.62690
23.0	.19484	.29410	.86847	-.75617	.46990	.17152	.20673	.38920
24.0	.07049	.23492	1.05610	-.62997	1.12050	.58324	.23762	.22528
25.0	.08825	.21450	.76115	-.39080	.87539	.46701	.18182	.19240
26.0	-.22680	.07510	.63990	-.22545	1.06646	1.12109	.58035	.23300
27.0	-.22582	.10837	.40295	-.19176	.77670	.86940	.46930	.16279
28.0	-.58351	-.22688	.22576	-.21609	.64288	1.06815	1.11961	.56319
29.0	-.43094	-.21180	.19687	-.15168	.41231	.77246	.87432	.44420
30.0	.11218	-.58269	.21979	-.56308	.22592	.64364	1.06908	1.11498
31.0	.04385	-.41665	.15798	-.44548	.20474	.40827	.78075	.85976
32.0	.29043	.11696	.57513	-1.11397	.23169	.22569	.64086	1.06333
33.0	.27549	.06290	.45870	-.86040	.17595	.19993	.41339	.76440
34.0	.22965	.29251	1.11758	-1.05074	.57916	.23394	.22594	.62606
35.0	.19571	.29157	.86686	-.75529	.46852	.17191	.20733	.38988
36.0	.06800	.23222	1.05390	-.63014	1.11042	.57719	.23738	.22494

D-22

No. of
Copies   Offsite

1   <u>AEC Advisory Committee for Reactor Safeguards</u>
    <u>Washington, D.C.</u>

        M. C. Gaskr

1   <u>AEC Chicago Patent Office, Washington, D.C.</u>

        G. H. Lee

7   <u>AEC Directorate of Licensing, Washington, D.C.</u>

        E. G. Case (3)
        V. Stello
        T. Novak
        D. Ross*
        G. M. Lauben

2   <u>AEC Directorate of Reactor Standards, Washington, D.C.</u>

1   <u>AEC Office of Assistant General Counsel for Patents</u>
    <u>Washington, D.C.</u>

        R. A. Anderson

2   <u>AEC Technical Information Center</u>

20   <u>AEC Division of Reactor Development and Technology</u>
    <u>Washington, D.C.</u>

        Assistant Director, Reactor Technology
            Chief, Special Technology Branch
            Chief, Reactor Physics Branch

        Assistant Director, Reactor Engineering
            Chief, Core Design Branch
            Chief, Fuel Engineering Branch

        Assistant Director, Nuclear Safety
            Chief, Fast Reactor Safety Branch
            Chief, Thermal Reactor Safety Branch
            Chief, Analysis and Evaluation Branch

        Assistant Director, Plant Engineering

        Assistant Director, Program Analysis

        Chief, Water Projects Branch

        Chief, LMFBR Projects Branch

        E. Davidson
        F. Goldner
        R. Impara
        T. Speis
        R. M. Scroggins* (2)

* Recipients of COBRA-III card deck.

No. of Copies	Offsite

22   Argonne National Laboratory

      M. Butler (Code Center)* (30)
      H. Fauske*
      R. P. Stein*

1   Atomic Energy Commission

Brussels Office
U.S. Mission to the European Communities
APO, New York, N. Y. 09667

1   Atomic Energy of Canada, Limited
Chalk River, Ontario, Canada

      G. A. Wikhammer

5   Atomics International
P.O. Box 591, Canoga Park, California 91305

      Louis Bernath*
      Donald T. Eggan
      David C. Fulton
      H. Morowitz
      W. B. Wolfe

2   Babcock and Wilcox Company
P.O. Box 1260
Lynchburg, Virginia 24502

      R. E. Willard
      C. Morgan*

2   Babcock and Wilcox
Alliance Research Center
1562 Beeson Street
Alliance, Ohio 44601

      J. S. Gellerstadt
      G. D. Lindstrom

1   Brookhaven National Laboratory

      O. E. Dwyer

2   Chicago Operations Office

      Richard J. Bariboldi

1   Columbia University
Department of Chemical Engineering

      J. E. Casterline*

No. of Copies	Offsite
2	**Combustion Engineering, Inc.** F. Bevilacqua P. Zamola*
1	**duPont Company, Wilmington, Delaware 19898** J. S. Neill
1	**Gulf-General Atomic** P.O. Box 608 San Diego 12, California 92112 R. Katz
1	**General Electric Company, San Jose (Trumbull)** BRDO, Sunnyvale, California P. Magee*
4	**General Electric Company, San Jose** Earl Janssen R. T. Lahey* S. Levy W. Sutherland
1	**Georgia Institute of Technology** Novak Zuber
2	**Idaho Nuclear, Inc.** Idaho Falls, Idaho C. Solbrig* L. Ybarrando
2	**Jersey Nuclear Corp.** Bellevue, Washington L. Bupp G. A. Sofer*
1	**Knolls Atomic Power Laboratory** General Electric Company Schenectady, New York G. H. Halsey
1	**Union Carbide Corporation (ORNL)** Floyd L. Culler

No. of
Copies   Offsite

1   Nuclear Fuel Services
           Rockville, Md.

              R. T. Berringer

1   Union Carbide Corp. (ORNL-Y-12)

              M. Fontana*
              H. W. Hoffman

1   Gulf United Nuclear Fuels Corporation
           Grasslands Road
           Elmsford, New York

              H. S. Chung*

1   University of Minnesota
           Department of Chemical Engineering
           Minneapolis, Minnesota 55455

              H. S. Isbin*

1   Westinghouse Bettis Atomic Power Laboratory

              S. Green

2   Westinghouse Electric Corporation

              H. Chelemer*
              L. S. Tong

2   Westinghouse Electric Corporation
           Waltz Mill Site
           P.O. Box 158
           Madison, Pa.

              E. Novendstern*
              R. Markley*

      Onsite-Hanford

1   AEC Chicago Patent Group

              R. M. Poteat

2   RDT Sr. Site Representative

              F. Standerfer

No. of Copies	Onsite-Hanford
54	Battelle-Northwest

D. T. Aase
R. T. Allemann
N. E. Carter
P. D. Cohn
D. L. Condotta
J. C. Fox
S. Goldsmith
B. M. Johnson
C. W. Lindenmeier
T. I. McSweeney
C. A. Oster
L. T. Pedersen
D. S. Rowe (30)
A. M. Sutey
D. S. Trent
C. L. Wheeler
W. C. Wolkenhauer
F. R. Zaloudek
Technical Information Files (5)
Technical Publications (1)

2	Douglas United Nuclear

R. Shoemaker
R. Baars

10	Westinghouse-Hanford

R. E. Collingham
J. M. Creer
W. M. Gajewski
J. W. Hagan
K. M. Horst
J. Muroaka
R. E. Peterson
J. F. Wett
J. M. Yatabe